

THE  
CRYSTAL AND MOLECULAR STRUCTURES  
OF SOME  
TRANSITION METAL - BARBITURATE COMPLEXES

A thesis submitted to the  
UNIVERSITY OF CAPE TOWN  
in fulfilment of the requirements for the degree of  
DOCTOR OF PHILOSOPHY.

by

ALLEN LAWRENCE RODGERS B.Sc (HONS.) M.Sc.

Department of Physical Chemistry,  
University of Cape Town,  
Rondebosch, Cape,  
Republic of South Africa.

September, 1974.

The copyright of this thesis is held by the  
University of Cape Town.  
Reproduction of the whole or any part  
may be made for study purposes only, and  
not for publication.

The copyright of this thesis vests in the author. No quotation from it or information derived from it is to be published without full acknowledgement of the source. The thesis is to be used for private study or non-commercial research purposes only.

Published by the University of Cape Town (UCT) in terms of the non-exclusive license granted to UCT by the author.

IN MEMORY

OF

MY FATHER

1913 - 1973

A.C.K.N.O.W.L.E.D.G.M.E.N.T.S

The author would like to extend sincere thanks to his supervisor, Dr. L.R. Nassimbeni, for his inspiring guidance and assistance which was enthusiastically given at all times.

Thanks are also due to the author's colleague, Mr. M. Caira, for his general assistance and advice throughout the course of the project and to Dr. G. Percy for his help with the infrared spectra.

The author is indebted to Dr. G. Gafner and Dr. G. Kruger of the South African Council for Scientific and Industrial Research for providing the invaluable service of intensity data collection on the C.S.I.R. automatic diffractometer.

The award of research grants by the C.S.I.R. and the University of Cape Town is gratefully acknowledged.

Finally, the author wishes to thank his wife for her encouragement at all times and Mrs. P. Alexander for her competent typing of this thesis.

C O N T E N T S

	Page
ACKNOWLEDGMENTS .....	(i)
CONTENTS .....	(ii)
PUBLICATIONS .....	(v)
CHAPTER	
I <u>INTRODUCTION</u>	
I.1   General .....	1
I.2   Metals and Life .....	2
I.3   Barbiturates .....	7
I.4   Specificity in metal ion-ligand interactions	20
I.5   Complexes of the type $M(II)(\text{barb})_2L_2$ .....	26
I.6   Objectives of the research project .....	29
II <u>GENERAL EXPERIMENTAL</u>	
II.1   Preparation of the complexes .....	31
II.2   Preliminary work on the crystals .....	35
II.3   The diffractometer data collections .....	36
III <u>THE CRYSTAL AND MOLECULAR STRUCTURE OF THE</u> <u>BIS-(5,5-DIETHYLBARBITURATO)-BIS-(PICOLINE)</u> <u>DIHYDRATE COMPLEX OF COPPER (II)</u>	
III.1   Crystal and intensity data .....	38
III.2   Solution and refinement of the structure ..	40
III.3   Description of the structure .....	45

IV	<u>THE CRYSTAL AND MOLECULAR STRUCTURE OF THE BIS-[5-ALLYL-5-(2-BROMOALLYL) BARBITURATO] BISPYRIDINE DIHYDRATE COMPLEX OF COPPER (II)</u>	
	IV.1 Crystal and intensity data .....	59
	IV.2 Solution and refinement of the structure ...	63
	IV.3 Description of the structure .....	67
V	<u>THE CRYSTAL AND MOLECULAR STRUCTURE OF THE BIS-(5,5-DIETHYLBARBITURATO)-BIS-(PICOLINE) COMPLEX OF Zn(II)</u>	
	V.1 Crystal and intensity data .....	75
	V.2 Solution and refinement of the structure ...	77
	V.3 Description of the structure .....	85
VI	<u>THE CRYSTAL AND MOLECULAR STRUCTURE OF THE BIS-(5-ETHYL-5-ISOAMYLBARBITURATO)-BIS-(IMIDAZOLE) COMPLEX OF Ni(II)</u>	
	VI.1 Crystal and intensity data .....	100
	VI.2 Solution and refinement of the structure ...	102
	VI.3 Description of the structure .....	112
VII	<u>DISCUSSION OF THE CRYSTAL AND MOLECULAR STRUCTURES OF THE COMPLEXES.</u>	
	VII.1 Previous studies on barbiturate complexes ...	125
	VII.2 Proposed formation mechanism of M(II)(barb) <sub>2</sub> L <sub>2</sub> complexes .....	130
	VII.3 Structural features of the complexes .....	133
	VII.4 Hydrogen bonding in the complexes .....	140

VIII	<u>THE INFRARED ABSORPTION SPECTRA OF THE COMPLEXES</u>	
	VIII.1 Introduction .....	154
	VIII.2 Experimental .....	156
	VIII.3 Interpretation of the IR spectra .....	157
IX	<u>CONCLUSION</u> .....	165
	<u>APPENDIX</u>	
	A low temperature device for cooling crystals during x-ray diffraction .....	168
	<u>REFERENCES</u> .....	171

PUBLICATIONS

Parts of this work have been published or are in press as follows:

1. G.V. Fazakerley, P.W. Linder, L.R. Nassimbeni and A.L. Rodgers,  
*Cryst. Struct. Comm.*, 2, 647 (1973).  
"Bis(5,5 -diethylbarbiturato) bis(picoline) copper (II) dihydrate".
2. G.V. Fazakerley, P.W. Linder, L.R. Nassimbeni and A.L. Rodgers,  
*Inorg. Chim. Acta.*, 9, 193 (1974).  
"The Crystal Structure of the bis-(5,5 -diethylbarbiturato)  
-bis-(picoline) dihydrate Complex of Cu(II)".
3. G.V. Fazakerley, P.W. Linder, L.R. Nassimbeni and A.L. Rodgers,  
*Cryst. Struct. Comm.*, in press.  
"Synthesis and Crystal Structure Determination of the  
bis-[5-allyl-5-(2-bromoallyl) barbiturato]- bispicoline dihydrate  
Complex of Cu(II)".
4. Luigi Nassimbeni and Allen Rodgers, *Acta Cryst.*, in press.  
"The Crystal Structure of the bis-(5,5 -diethylbarbiturato)-  
bispicoline Complex of Zinc (II)".
5. Luigi Nassimbeni and Allen Rodgers, *Acta Cryst.*, in press.  
"The Crystal Structure of the bis-(5-ethyl-5-isoamyl barbiturato)  
-bis-(imidazole) Complex of Nickel (II)".
6. G.C. Percy and A.L. Rodgers, *Spectroscopy Letters*, in press.  
"Infrared Spectra of Barbiturate Complexes".

CHAPTER I

INTRODUCTION

## I.1 GENERAL

This thesis describes the synthesis and X-ray structural investigation of four complexes of the type  $M(II)(\text{barb})_2L_2$  where M is a transition metal, barb is the anion of a substituted barbituric acid and L is an organic base. These compounds are of importance in the clinical detection and identification of barbiturate drugs and this aspect is discussed in a later section. An infrared study of these compounds is also described.

The individual components of the complexes, viz. the transition metals and the barbiturate ligands are in themselves of great biological and physiological significance. Although the human body is but 3% metals, life depends upon these elements far more than this figure suggests. For example, the transition series metals, even though some are present in only trace amounts, generally appear in the active centres of enzymes that catalyze substrates to form aggregate molecules. The barbiturates on the other hand are members of a group of widely used drugs known as hypnotics, many of which are medicinally applied today.

It is because of their independent biological interest that sections I.2 and I.3 of this introductory Chapter are devoted to a discussion of their respective properties, functions, structural features and their physiological and chemical activities.

## I.2 METALS AND LIFE<sup>1,2,3</sup>

The elements essential for healthy human life can be divided into three broad classes - main group metals, transition series metals and main group non-metals. In general, these elements occur in our bodies in quantities which follow their abundances in the earth's crust and in sea water<sup>1</sup>. However, there are exceptions where some very abundant metals do not have important roles *in vivo*. For example it appears that the insolubilities of the hydroxides of aluminium and titanium and the extra strong bonding of nickel ions by octahedral coordination with soil silicates have precluded these elements from participating in the evolution of homo-sapiens. Nevertheless, because of modern civilization's pollution of the environment, more and more elements such as boron, germanium and nickel are beginning to traverse the evolution-adaptation scheme of poisons → tolerable impurities → useful elements → essential elements.

The main group metals and the transition series metals are discussed below, the latter in more detail.

### Main-Group Metals

There are four main-group metals essential for life, calcium and sodium being the major cations found outside cell membranes, magnesium and potassium being found within cells. Sodium and potassium keep the osmotic pressure on either side of the cell wall constant and also maintain the sensitivity of the nerves and control of the muscles. For example, sodium ions depress the activity of muscle enzymes and are required for muscle contractions. Potassium permits the heart muscles to relax between beats. Calcium is also involved in coronary activity. Sodium chloride is the source of hydrochloric acid for gastric juices and sodium bicarbonate is a buffer in maintaining the acid-base balance of body fluids and in the transport of CO<sub>2</sub>.

Magnesium ions are found complexed with nucleic acids inside cells and are necessary for nerve impulse transmissions, for muscle contractions and for the metabolism of carbohydrates. Calcium, together with phosphorus and vitamin D are required for the formation of bones and teeth. Calcium is also required in the process of blood clotting.

### Transition series metals

The transition metals are essential to human life and yet are only present in minute amounts. For example in some tissues only one atom in  $10^7$  is copper and, in the body as a whole, the ratio Cu : Mo : Co is 1000 : 100 : 1. The general role of transition metals is one of catalysis, often involving oxidation-reduction processes and this occurs in the active sites of enzymes. In metalloenzymes the metal ion may either be a permanent component of the active site - Fe(II) in haemoglobin - or may "commute" as part of a coenzyme - Co(III) in vitamin B12 coenzyme.

Iron is the most abundant transition metal and is essential for the proper functioning of several organs. Our bodies contain 5-7 g of iron, 65-70 per cent of which is in haemoglobin, 15 per cent in the liver, spleen, marrow and kidneys and the remainder involved in the formation of protein and in redox reactions in the plasma.

Iron deficiencies can occur as a result of bleeding, pregnancy, parturition and menstruation leading to anaemias. This may be remedied by administering ferrous salts which are easily absorbed in the intestine. Alternatively, intravenous injections of iron ascorbates, citrates or colloidal carbohydrate complexes may be used.

The oxidation state of iron depends upon the type of complexing ligand to which it is bonded. In myoglobin and haemoglobin, iron is in the +2 oxidation state. In catalases and oxidases it is in the +3 state while in cytochromes it is oxidized and reduced from one state to the other. Both

oxidation states have octahedral configurations.

In haemoglobin the ferrous ion is located inside a porphyrin ring and is attached to an imidazole nitrogen. The ion is located deep inside a cleft of the enzyme and this combination of bonding and shielding permits the ferrous ion to be reversibly attached to oxygen and not irreversibly oxidized to the ferric state.

During pregnancy, females have an iron deficiency due to foetal requirements. It is interesting to note that the Bantu women of South Africa who cook their food in iron pots do not suffer from this deficiency during pregnancy.

Manganese is the second most abundant heavy metal ion in nature and it is one of the rare elements that can exist in eight different oxidation states. However, just two oxidation states, +2 and +3 are of importance in biological systems. Mn(II) compounds are often pale pink in colour and are stable because of the  $d^5$  configuration. Mn(III) is not stable in aqueous solution unless it is complexed in which case it is usually found in Jahn Teller distorted octahedral configurations. Plants are our bodily source of manganese which is used for enzyme activation (isocitrate dehydrogenase, malic enzyme and pyruvate decarboxylate).

Although cobalt is quite rare on the earth's surface it is found in fertile soil and thus in the plants thereon. We require cobalt for vitamin B12 in which it is in the +3 oxidation state. Animal liver is a very rich source of this vitamin which is necessary for the formation of haemoglobin. Deficiencies cause pernicious anaemia. Vitamin B12 present in our food cannot be absorbed through the intestinal wall unless it encounters hydrochloric acid (from gastric juices) and a protein of molecular weight 50 000 (excreted from the stomach walls) en route to the intestine. Australian sheep used to have a deficiency of B12 due to lack of cobalt salts in the soil but nowadays either the deserts are sprayed with cobalt salts or ceramic slow-release cobalt pellets are placed in the animal's stomachs.

Cobalt (II) is used as an enzyme activator (e.g. in carbonic anhydrase or carboxypeptidase). Co(II) solutions are usually pink and have the ion octahedrally solvated. Tetrahedral configurations are also known and more rarely square or trigonal pyramidal as well. Because of this ability to form 4 different possible configurations, cobalt can enter low symmetry sites in enzymes and this is how the metal is usually found.

Copper is required in the production of haemoglobin and in addition is found in many metalloenzymes such as phenolase or haemocyanin which are capable of carrying oxygen. Cerebrocuprein contains two copper ions and is used in oxygen storage and transport in the brain. Ceruloplasmin contains eight copper ions and is used in oxygen transport in blood plasma. These compounds are usually coloured blue which is characteristic of tetragonal copper (II) and nitrogen donor ligands. Copper is stored in the liver while our main sources of the element are in animal liver and in shellfish. The copper concentrations in various body fluids are sensitive to the presence of a wide range of diseases and there is a current trend towards monitoring the copper concentrations of these fluids in order to detect disease.

In general, copper occurs in two oxidation states, cuprous (+1) and cupric (+2).  $\text{Cu}^+$  complexes can be linear, planar or tetrahedral and are usually colourless. The cupric ion is usually green, brown or blue and can form tetrahedral, trigonal pyramidal, square pyramidal or square complexes. With coordination number 6, Jahn Teller distorted octahedral complexes are formed.

Zinc is an essential constituent of several enzymes as in the activator in carboxypeptidase A where there is one zinc atom per molecule of protein. Carboxypeptidase has both peptidase and esterase activity but when the zinc is replaced by cadmium or mercury the former activity is removed and the latter is enhanced. Our sources of zinc are from plants and animals. At one time zinc deficiencies were believed to have caused dwarf formation amongst some peoples in central Europe.

Zinc occurs in several mineral forms one of which is calamine,  $ZnCO_3$ . In solution, the  $Zn^{2+}$  ion is coordinated with four or six ligands giving rise to tetrahedral (or planar) and octahedral configurations. Zinc (II) has the same ability as Cobalt (II) to occupy low symmetry sites in enzymes. In aqueous solution there is no evidence for zinc (I) or of oxidation states higher than (II).

Molybdenum participates in biochemical redox reactions such as xanthine and purine oxidations in milk and in the liver. It also acts as a cofactor in nitrogen fixation bacteria and as a nitrate reducer in some plants and micro-organisms. During redox reactions Mo (V) and Mo (VI) are attached to oxygen or sulphur containing ligands. These oxidation states can exist only in solution as oxyanions or complexes. In general there is no cationic solution chemistry of molybdenum *in vivo*.

Metal ion dependent processes are thus found throughout our bodies and vary greatly in their function and complexity. Because of the electronic properties of the transition series a variety of powerful instrumental techniques may be brought into play in order to obtain a more intimate understanding of their roles in different biological processes. These processes have already been shown to be quite specific in their metal ion requirements in that only certain metal ions, in specified oxidation states, can fulfil the necessary catalytic or structural requirement. Other processes are much less specific and it is sometimes possible to replace one metal ion by another. Whatever their function however, there can be no doubt that the transition metals are a vital, indispensable part of life. Their true significance is aptly illustrated by D.R. Williams in the last two sentences of his book, 'The Metals of Life'<sup>2</sup>. "Everyone must age and life is finite. Nevertheless the pattern of ageing and the quality of life might well be metal ion controllable".

### I.3. BARBITURATES<sup>4,7</sup>

#### Classification and action of sleep inducing drugs.

The classification of drugs affecting the central nervous system as anaesthetics, hypnotics, sedatives, analgetics, tranquilizers or antidepressants can be misleading since many compounds may behave as members of several of the above classes of drugs depending on the dosage in which they are administered. The effect of different dosages can range from sedation to sleep to anaesthesia to death. Moreover, the actual biochemical mechanisms involved in the functions of the central nervous system are not well understood. However, it is known that there are two primary classes of compound that can modify the activity of the central nervous system. These are:

- 1 drugs that modify biopolymers by interacting with specific receptors (analgetic drugs);
- 2 drugs that modify biopolymers by changing the structure of the surrounding solvent without being attached to specific receptor sites (general anaesthetics).

If the action of drugs is to be attributed to attachment to specific receptors several conditions should be fulfilled:

- (a) The drugs should show structural specificity i.e. common structural features should be shared by all compounds exerting similar effects.
- (b) Stereoisomers should not be equiactive.
- (c) Competitive reversal of drug action should be inducible by structurally related compounds.

These conditions are considered in a later section of this chapter from which it will be apparent that it is extremely unlikely that hypnotics act by being attached to specific "hypnotic receptor sites".

The problem of understanding the action of sleep inducing drugs is complicated by the fact that very little is known about the chemistry and nature of sleep itself. However, two areas in the central nervous system have been implicated in the induction of unconsciousness and of wakefulness. In 1949, Moruzzi and Magoun<sup>5</sup> discovered that stimulation of an area which they called the reticular activating system awakes sleeping animals. In 1952, Hess<sup>6</sup> and his co-workers identified an area in the thalamus where electrical stimulation induced behavioural sleep in experimental animals. This is the sleep inducing centre. It is thus reasonable to theorize that hypnotic agents exert their effect either by stimulating the sleep centre or by inhibiting the function of the arousal centre. It is the latter of these two theories that is generally accepted today. This does not mean however that the reticular formation is accepted uniquely as the site of hypnotic action. A very considerable amount of research work will have to be undertaken in the future before the mysteries surrounding the action of sleep inducing drugs can be solved.

#### Brief History of Hypnotic Drugs

During the nineteenth century, compounds such as ethyl alcohol, belladonna and morphine (in the form of opium) were the only agents capable of inducing lack of consciousness. However, they cannot be classified as hypnotics which, ideally, should induce a state closely resembling natural sleep from which the patient can be readily aroused. In the middle of the nineteenth century, Locock introduced potassium bromide for the treatment of epilepsy and bromides have been used as sedatives ever since. However, when used regularly in hypnotic doses severe states of bromide intoxication (bromism) can occur. For this reason, the use of bromides is not favoured today.

One of the oldest organic sedative and hypnotic agents is chloral hydrate,  $\text{Cl}_3\text{CCH}(\text{OH})_2$ , which was first synthesized by Liebig in 1832 and introduced as a sedative in 1869. Although it is a safe and reliable hypnotic, its

undesirable taste, strong odour and irritation of the gastro-intestinal tract have diminished its general use.

The use of chloral hydrate in medicine was followed in short succession by paraldehyde, sulfonal and urethane leading eventually to the use of barbiturates as hypnotics in 1903 when Emil Fischer and von Mehring discovered the hypnotic action of 5,5 diethylbarbituric acid (fig. I.1 and no. 1, table I.1). Since then, hundreds of barbiturates many of them with medicinally useful hypnotic

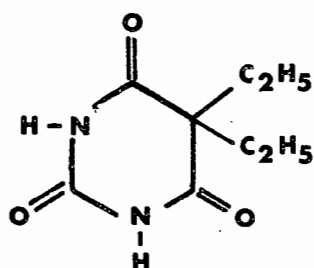


FIG. I. 1

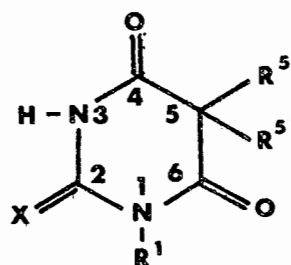


FIG. I. 2

activity have been synthesized. Their basic structure is shown in Fig. I.2 in which X is O or S,  $R^1$  is H or  $CH_3$ ,  $R^5$  is alkyl or aryl and  $R^{5'}$  is alkyl or aryl. The accepted conventional numbering system for barbiturates has been used in Fig. I.2 and will be retained throughout. Table I.1 lists several of the more well known barbiturates as well as all those referred to in this thesis.

### Structure-Activity Relationships

The relationship between chemical structure and drug action of barbiturates has been widely studied. Doran (1959)<sup>7</sup> has reviewed the structures, physical and chemical properties and pharmacological activity of several hundred different barbiturates.

TABLE I.1<sup>4,24</sup>

NO.	BARBITURIC ACID	TRADE NAME	NAME IN STANDARD TEXTS	R'	R <sup>5</sup>	R <sup>5'</sup>
1	5,5 diethyl	Veronal, Barbitone	Barbital	H	C <sub>2</sub> H <sub>5</sub>	C <sub>2</sub> H <sub>5</sub>
2	5,5-Diethyl-1-methyl	Gemonil	Metharbital	CH <sub>3</sub>	C <sub>2</sub> H <sub>5</sub>	C <sub>2</sub> H <sub>5</sub>
3	5-Butyl-5-ethyl	Neonal	Butethal	H	C <sub>2</sub> H <sub>5</sub>	n-C <sub>4</sub> H <sub>9</sub>
4	5-Ethyl-5-phenyl	Luminal	Phenobarbital	H	C <sub>2</sub> H <sub>5</sub>	C <sub>6</sub> H <sub>5</sub>
5	5-Methyl-5-phenyl	Rutonal	Phenylmethyl	H	CH <sub>3</sub>	C <sub>6</sub> H <sub>5</sub>
6	5-Ethyl-5-isopentyl	Amytal	Amobarbital, Amylobarbital	H	C <sub>2</sub> H <sub>5</sub>	(CH <sub>3</sub> ) <sub>2</sub> CHCH <sub>2</sub> CH <sub>2</sub>
7	5,5-Diallyl	Dial	Allobarbital	H	CH <sub>2</sub> =CHCH <sub>2</sub>	CH <sub>2</sub> =CHCH <sub>2</sub>
8	5-(1-Cyclohexen-1-yl)-5-ethyl	Phanodorn	Cyclobarbital	H	C <sub>2</sub> H <sub>5</sub>	(CH <sub>2</sub> ) <sub>4</sub> CH=C-
9	5-(1-Cyclohepten-1-yl)-5-ethyl	Medomin	Heptabarbital	H	C <sub>2</sub> H <sub>5</sub>	(CH <sub>2</sub> ) <sub>5</sub> CH=C-
10	5-Ethyl-5-(1-methyl-1-butenyl)	Delvinal	Vinbarbital	H	C <sub>2</sub> H <sub>5</sub>	CH <sub>3</sub> CH <sub>2</sub> CH=C(CH <sub>3</sub> )
11	5-Ethyl-5-(1-methyl-butyl)	Nembutal	Pentobarbital	H	C <sub>2</sub> H <sub>5</sub>	CH <sub>3</sub> (CH <sub>2</sub> ) <sub>2</sub> CH(CH <sub>3</sub> )
12	5-(1-Cyclohexen-1-yl)- 1,5-dimethyl	Evipal	Hexobarbital	CH <sub>3</sub>	CH <sub>3</sub>	(CH <sub>2</sub> ) <sub>4</sub> CH=C-
13	5-Allyl-5-(1-methylbutyl)	Seconal	Secobarbital, Quinalbarbitone	H	CH <sub>2</sub> =CHCH <sub>2</sub>	CH <sub>3</sub> (CH <sub>2</sub> ) <sub>2</sub> CH(CH <sub>3</sub> )
14	5-Ethyl-5-(1-methylbutyl)- 2-thio	Pentothal	Thiopental	(2-S)H	C <sub>2</sub> H <sub>5</sub>	CH <sub>3</sub> (CH <sub>2</sub> ) <sub>2</sub> CH(CH <sub>3</sub> )
15	5-(2-Bromoallyl)-5-isopropyl	Nostral	Propallylonal	H	CH <sub>2</sub> =CBrCH <sub>2</sub>	(CH <sub>3</sub> ) <sub>2</sub> CH
16	5-(2-Bromoallyl)-5-sec-butyl	Pernoston	Butallylonal	H	CH <sub>2</sub> =CBrCH <sub>2</sub>	CH <sub>3</sub> CH <sub>2</sub> CH(CH <sub>3</sub> )
17	5-ethyl-1-methyl-5-phenyl	Prominal, Nebaral	Mephorbarbital	CH <sub>3</sub>	C <sub>2</sub> H <sub>5</sub>	C <sub>6</sub> H <sub>5</sub>
18	5-(2-Bromoallyl)-5-isopropyl -1-methyl		Pronarcone	CH <sub>3</sub>	CH <sub>2</sub> =C(Br)CH <sub>2</sub> -	(CH <sub>3</sub> ) <sub>2</sub> CH
19	5-ethyl-5-hexyl		Hebaral	H	C <sub>2</sub> H <sub>5</sub>	CH <sub>3</sub> (CH <sub>2</sub> ) <sub>5</sub>
20	5-Allyl-5-(2-bromoallyl)		Brallobarbital	H	CH <sub>2</sub> =CHCH <sub>2</sub>	CH <sub>2</sub> =C(Br)CH <sub>2</sub>

Emil Fischer had observed that the hypnotics, sulfonmethane (Fig.I.3) and amylene hydrate (Fig.I.4) had quaternary carbons and concluded that it was

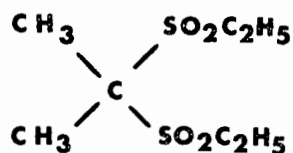


FIG. I.3

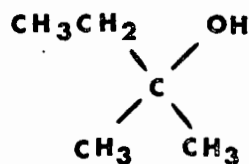


FIG. I.4

this grouping of atoms that causes hypnotic activity. Barbiturates disubstituted at the C(5) position would thus be a convenient source of such compounds.

In agreement with Fischer's original hypothesis it has been shown that in order to possess effective hypnotic activity a barbiturate must be disubstituted at the C(5) ring position by either ethyl or by larger non polar groups eg. allyl, isoamyl, phenyl or cyclohexyl groups. Monosubstituted or unsubstituted barbiturates show a lack of ability to depress the functions of the central nervous system.

It has also been shown that a second requirement for hypnotic action is that the barbiturate ring should have at least a minimum capacity for hydrogen bonding, i.e. no more than one of the two ring imide groups may be methylated and no more than two of the three carbonyl oxygen atoms may be replaced by sulphur<sup>56</sup>.

In general, drug molecules will penetrate cell membranes more effectively when they are in the unionized form than when they are in the ionized form. Introduction of only one alkyl or one aryl group into the 5- position of barbituric acid has little effect on the acidity of this compound, whereas the introduction of two such groups decreases the acidity greatly. (The dissociation constant of barbituric acid is more than  $10^3$  times as great as those of 5,5-

dimethyl and 5,5 deethyl barbituric acids<sup>8</sup>). This may be further illustrated by calculating the percentage dissociation at physiological pH (7,4) occurring in the species unsubstituted, monosubstituted and disubstituted barbituric acid. Application of the Henderson-Hasselbach equation,

$$\text{pH} = \text{pKa} + \log \frac{[\text{A}^-]}{[\text{HA}]}$$

where  $[\text{A}^-]$  is the concentration of the acid anion and  $[\text{HA}]$  is the concentration of the unionized acid, yields the following results (Table I.2).

Compound	pKa	Percentage in undissociated form
Barbituric acid	4,12	0,052
5-phenylbarbituric acid	3,75	0,022
5-phenyl-5-ethylbarbituric acid	7,29	43,0

TABLE I.2

Only the last of these compounds i.e. the disubstituted barbituric acid is likely to penetrate into the extracellular fluid of the central nervous system. No therapeutically useful barbiturates are known that are not disubstituted in the 5- position since monosubstituted barbiturates are almost completely ionized at physiological pH. However, 5 monosubstituted 1,2,4-triazines do exhibit hypnotic activity. This is because these compounds have acid dissociation constants of approximately 7,5 and are thus largely unionized at pH 7,4. Consequently disubstitution is not required to enable them to enter the central nervous system.

Wood<sup>8</sup> postulated that the acidity of unsubstituted and monosubstituted barbiturates was due to the fact that these compounds exist predominantly in the 2,4-diketo-6-hydroxy tautomeric form (Fig. I.5) with the first dissociating hydrogen originating from the 6- hydroxy group. On the other hand 5,5-

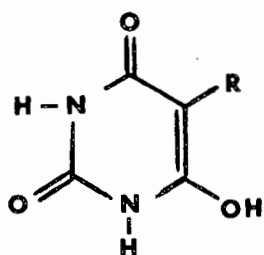


FIG. I.5

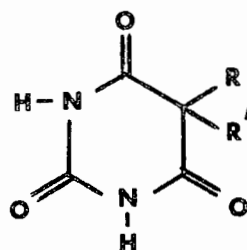


FIG. I.6

disubstituted barbiturates would be forced into the 2,4,6 triketo form (Fig.I.6) with a resulting considerable decrease in acid strength. However the X-ray crystal structure analyses of barbituric acid dihydrate<sup>9</sup> and anhydrous barbituric acid<sup>10</sup> have shown that the unsubstituted acid exists as the triketo tautomer. Nevertheless, the hypnotic activity of disubstituted barbiturates is attributable to their being considerably weaker acids than the monosubstituted or unsubstituted barbiturates (whatever the reason) rather than to an innate structural requirement for disubstitution.

The piperidine derivatives methyprylon (Fig. I.7) and glutethimide (Fig. I.8) are examples of hypnotics which are disubstituted at C(5) while diethylbromoacetylurea (carbromal) is an example of an acyclic hypnotic (Fig. I.9).

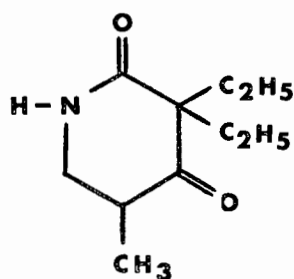


FIG. I.7

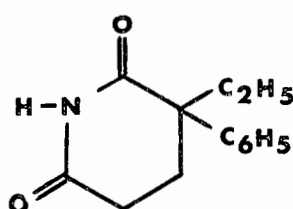


FIG. I.8

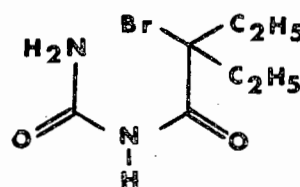


FIG. I.9

Comparison of the structural features of these compounds with those of the barbiturates shows very little structural specificity. In other words, compounds having hypnotic activity do not share a basic common structure. Nor do barbiturates, or hypnotics in general appear to be stereospecific. In several series of N-substituted barbiturates the hypnotic activities of the d- and the l- isomers are equal. The four optically active forms of 1-methyl-5-(1-methyl-2-pentynyl)-5-allyl barbituric acid differ in their hypnotic activity by a factor of only 2 or 3 - a factor very much smaller than is seen in truly stereospecific biologically active molecules.

The absence of structural and stereo-specificity coupled with the fact that no specific antagonist of any hypnotic is known lends doubt to the theory that enzymes provide specific receptor sites for hypnotic attack.

Even though hypnotic action does not appear to be associated with structural properties, modification of the structure of a hypnotic can greatly modify its activity primarily through the alteration of its lipid solubility. In particular, the lipid solubility of barbiturates and related compounds can be altered in the following ways:

- (i) substitution of suitable groups in the 5- position
- (ii) methylation of ring nitrogens
- (iii) substitution of sulphur for oxygen.

Let us consider each of these individually.

(i) Lengthening of the side chain

The lengthening of side chains or introduction of aryl or aralkyl groups increases lipid solubility by increasing the fraction of the molecule that is non polar. Although hypnotic action increases with lipid solubility, a "saturation" point is reached when the total number of carbons of both groups substituted in the 5 position reaches eight. Further lengthening of the side chains yields compounds that tend to be convulsants or inactive.

Hypnotics other than the barbiturates are thought to behave similarly with regard to lengthening of the side chains.

(ii) Methylation of ring nitrogens

As already mentioned, 5,5-disubstituted barbiturates are in the 2,4,6-triketo form with the only protons capable of dissociating originating from the ring nitrogens. Methylation of these groups will thus lead to weaker acids. The pKa of typical 5,5-disubstituted barbiturates<sup>26</sup> is in the neighbourhood of 7,5 while the pKa of the N-methylated barbiturate hexobarbital (Fig. I.10, no. 12 Table I.1) is 8,4. The Henderson-Hasselbach equation shows that 90% of this barbiturate

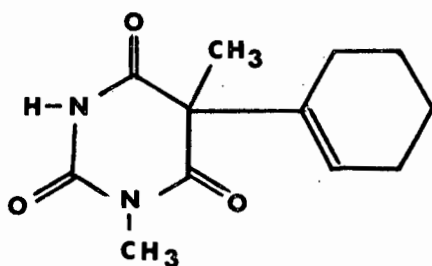


FIG. I. 10

will be in the undissociated form at physiological pH thereby resulting in increased lipid solubility and increased hypnotic ability.

It is interesting to note that if the hydrogen atom of one ring nitrogen is substituted by an alkyl group, the hypnotic action of the barbiturate becomes characterized by rapid onset and short duration. The attachment of alkyl groups to both ring nitrogens yields compounds that tend to be convulsants.

(iii) Replacement of exocyclic oxygen with sulphur

In general the lipid solubility of heterocyclic compounds may be increased by replacing oxygen with sulphur. Thiobarbiturates enter the central nervous system more rapidly than the analogous oxygen compounds because the former are more lipid soluble. Thiobarbiturates thus attain maximum concentration in the brain very rapidly.

In contrast to N-methylated barbiturates, thiobarbiturates are stronger acids than the analogous oxygen containing compounds. Whereas the pKa of phenobarbital is 7,29, that of 2-thiophenobarbital is 6,30. Thus, despite being more highly ionized at physiological pH than oxybarbiturates, thiobarbiturates are much more lipid soluble. The increased acidity is attributable to greater electron withdrawal from the N-H grouping due to the presence of sulphur which has the ability to accommodate electrons by utilization of d-orbitals.

The actual nature of the pharmacological action of barbiturates is greatly affected by the introduction of sulphur into these compounds. For example, pentobarbital (Fig. I.1), no. 11 Table I.1) is a short acting hypnotic while its 2-thio

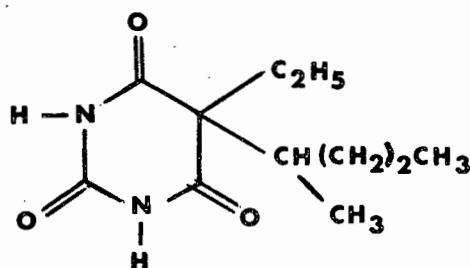


FIG. I. 11

analogue, thiopental is an ultrafast acting anaesthetic. Other examples result in the formation of compounds with predominantly

convulsant activity.

### Metabolism of Barbiturates

The hypnotic effect and activity as well as duration of action and potency of barbiturates are dependent on additional factors other than those mentioned above, eg. rates of absorption, distribution, metabolism and excretion.

The kidney and liver enzyme systems are capable of metabolizing barbiturates through one or more of the following pathways:

- (i) oxidation of groups substituted in the 5,5- position;
- (ii) dealkylation of groups substituted on the ring nitrogens;
- (iii) desulphuration of thiobarbiturates and
- (vi) hydrolysis of the imide linkages.

The metabolic products may be inactive or, in some cases, may be as active as or have a longer duration of action than the parent compound.

The oxidation process yields alcohols, ketones or carboxylic acids. Pentobarbital (Fig. I.11) is enzymatically converted to 5-ethyl-5-(3-hydroxy-1-methylbutyl) barbituric acid and to the carboxylic acid 5-ethyl-5-[2-(4-carboxybutyl)] barbituric acid. Similarly, thiopental (no. 14 Table I.1) is oxidized to the alcohol 5-ethyl-5-(3-hydroxy-1-methylbutyl) thiobarbituric acid. In addition, pentobarbital, which has a longer duration period than the original thiopental, is also detectable in this latter process.

Examples where the metabolic product is a ketone include the oxidation of propallylone (no. 15, Table I.) and butallylone (no. 16, Table I.1) where the bromoallyl group is oxidized to the corresponding ketone. Cyclobarbital (Fig. I.12, no. 8, Table I.1) is oxidized to the conjugated ketone (Fig. I.13)

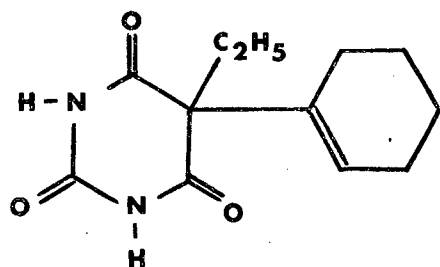


FIG. I.12

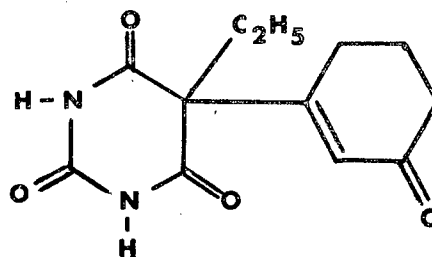


FIG. I.13

Barbiturates that are substituted by a methyl group on a ring nitrogen undergo N- demethylation in addition to oxidation of the groups in the 5- position. An interesting example is the N- demethylation of mephobarbital (no. 17, Table I.1), which has a hypnotic duration of action of 1-4 hours, to produce phenobarbital (no. 4, Table I.1) of hypnotic duration 4-12 hours. The reverse metabolic pathway has been observed, viz. N-methylation. Examples of this are the conversion of cyclobarbital to N- methyl cyclobarbital and the conversion of norhexobarbital to hexobarbital (Fig. I.10, no. 12, Table I.1).

Another minor metabolic pathway is dealkylation of groups in the 5- position, eg. after the administration of cyclobarbital (Fig. I.12), 5 ethyl barbituric acid was found in the urine of rats.

To summarize, all barbiturates and related hypnotics are characterized by alkyl or aryl groups in the vicinity of a carbamoyl grouping. Many major modifications can be carried out on barbiturate structures without loss of hypnotic activity. On the other hand, minor changes of the alkyl or aryl substituents can greatly modify physiological activity. For example pentobarbital (Fig. I.11) and amylobarbital (Fig. I.14, no. 6, Table I.1) are widely used hypnotics. Introduction of a methyl group onto the first carbon of the

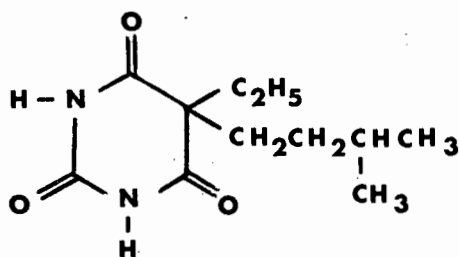


FIG. I.14

isopentyl side chain of amylobarbitone results in a compound which is a powerful convulsant.

Although structural modifications produce different degrees of hypnotic activity, barbiturates and related compounds exhibit almost no structural specificity in their abilities to affect the functions of the central nervous system. Thus, the effect a newly designed hypnotic will have on the central nervous system is difficult to predict. Very slight structural modifications may turn a sedative into a hypnotic, into an anaesthetic or into a convulsant. It does appear however, that it is the physical properties rather than structural geometry which determine in what manner the barbiturates will act.

#### I.4 SPECIFICITY IN METAL ION-LIGAND INTERACTIONS<sup>2,11,12,13.</sup>

Today it is an accepted fact that metal complex formation is deeply involved in normal life processes. Thus before discussing transition metal-barbiturate complexes it would be instructive to consider the modern theories of metal ion-ligand complexation with particular emphasis on those interactions occurring *in vivo*.

Two questions arise:

- 1 Why do some metal ions prefer one type of ligand and others another? Further, is it possible to predict which groups on an enzyme are more likely to be attached to a given metal ion?
- 2 If for medical reasons it is desirable to remove a ligand from a metal ion to which it is complexed or if it is necessary to remove an excess of one particular type of free metal ion from the blood, how must the correct competing ligand be chosen?

In order to produce an answer to these questions it is necessary to focus attention on the nature of the two species concerned - the metal ions and the ligands.

##### a - b Classification of Metal ions

This is based on the chemical behaviour of cations in aqueous solution.

- (i) a-cations form their strongest complexes with first row donor atoms, namely N, O or F. This class contains the majority of elements in aqueous solution and all cations in the gas phase.
- (ii) b-cations form their strongest complexes with second or subsequent row donor atoms:

$P > N$ ;  $S > O$ ;  $I^- > Br^- > Cl^- > F^-$ . This is a small group of metals contained in the Ahrland, Chatt and Davies<sup>14</sup> triangle of the transition series:

			Cu					
[Ru]	Rh	Pd	Ag	Cd				
[Os]	Ir	Pt	Au	Hg	Tl	Pb	[Bi]	

The elements Ru, Os and Bi are borderline cases and can behave as a-cations under certain circumstances.

### Nature of the Ligand

There are many factors which can increase the complexing power of a ligand (eg. the availability of lone pairs) but here it is the comparative specificity of a ligand for a metal ion that must be considered. This specificity arises from:

- (i) a matching of the stereochemistry of the ligand donor groups to the preferred coordination configuration of the metal ion, and
- (ii) the nature of the ligand donor atoms and their immediate neighbours - collectively called the donor groups.

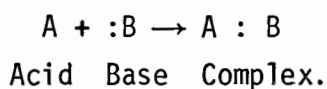
Both the a - b classification of metal ions and the most modern classification of ligand donor groups have been brought together into the "theory" of hard and soft acids and bases (HSAB).

### Hard and Soft Acids and Bases (HSAB)

This approach assumes that:

- (i) if a bond exists between two atoms, one will play the role of an acid and the other a base and
- (ii) that electrons hold the bonded atoms together.

The (Lewis) acid is taken as the species, (atom, molecule or ion), that has vacant accommodation for electron pairs and the base has the tendency to give up electron pairs. A typical acid-base reaction may thus be written:



Thus any species can be considered as comprising an acid and a base fraction. Whether these fractions exist in isolation or not is irrelevant. When A is a metal ion, B may be called a ligand. If A - B is a salt, dissolving it in water results in the cationic portion being associated with the basic end of water molecules  $A(:OH_2)_n$  and the anionic fraction with the acid end  $(HOH)_m:B$ .

### Classification of acids and bases

"Softness" arises from the electron mobility or polarizability of a species. If the electrons are easily moved, the species is soft; if firmly held the species is hard. Thus a soft base would have loosely held valence electrons and would be easily oxidized. Soft bases thus have a low charge density. A hard base has the converse properties. A hard acid is of small size and has a high positive charge density. Hard acids usually do not contain unshared pairs of electrons. These definitions are summarized in Table (I.3). All species can thus be classified into hard or soft acids or bases by consideration of the properties listed in the table.

TABLE I.3

ACID electron acceptor			BASE electron donor		
<u>HARD</u>		<u>SOFT</u>	<u>HARD</u>		<u>SOFT</u>
low	polarizability	high	low	polarizability	high
high	electropositivity	low	high	electronegativity	low
large	+ve oxidation state	small	large	-ve oxidation state	small
small	size	large	small	size	large

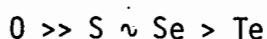
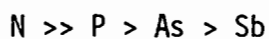
The quantitative approach to softness and hardness is achieved via a parameter called the formation constant, K. For a compound A - B, K is related to two factors. The first is the intrinsic strength (S) and the second is the softness parameter  $\sigma$  of the acid and the base concerned. Then  $\log K =$

$$S_A S_B + \sigma_A \sigma_B.$$

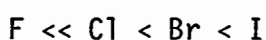
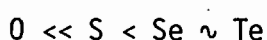
Thus  $\log K$  is measured for a series of compounds with a common acid fraction eg. H - F, H - Cl, H - Br and H - I. Since the common acid  $H^+$  has no electrons, its polarizability  $\sigma_A$  is set at zero while its intrinsic strength factor  $S_A$  is arbitrarily set at a value of 1. Then,

$$\log K (=pK_a) = S_B.$$

In this way  $S_B$  is determined for the halide ions. Similarly a series of metal ions may be classified according to their hardness or softness by determining  $\log K$  for a selection of compounds with a common base. It has been found that typical hard acids are the alkali metal ions, alkaline earth metal ions and ions such as  $Al^{3+}$ ,  $Sc^{3+}$ ,  $Ga^{3+}$ ,  $Cr^{3+}$ ,  $Co^{3+}$ ,  $Fe^{3+}$ ,  $Si^{4+}$ ,  $Ti^{4+}$ ,  $Zr^{4+}$  to mention but a few. These are analogous to the class (a) cations of Ahrlund and Chatt<sup>14</sup> mentioned earlier. They prefer ligand donor atoms in the sequences:



Typical soft acids (class (b)) are  $Cu^+$ ,  $Ag^+$ ,  $Au^+$ ,  $Tl^+$ ,  $Hg^+$ ,  $Pd^{2+}$ ,  $Cd^{2+}$ ,  $Pt^{2+}$ ,  $Hg^{2+}$ . These acids prefer the donor atom sequence:



Thus because  $\log K_{CuI} > \log K_{CuF}$ ,  $Cu^+$  is soft. It is interesting to note that acids like  $Fe^{2+}$ ,  $Co^{2+}$ ,  $Ni^{2+}$ ,  $Cu^{2+}$ ,  $Zn^{2+}$ ,  $Pb^{2+}$ , etc. are borderline cases and are classified as neither soft nor hard. Similarly bases such as  $C_5H_5N$  and  $C_6H_5NH_2$  are intermediate.

### Principle of HSAB

The single principle behind HSAB is : a strong bond is formed by a hard acid combining with a hard base or a soft acid with a soft base. Hard - soft bonds are weak. There are many examples illustrating this. The

distribution of certain complexes in the hydrosphere is one such example. Hard acids such as  $Mg^{2+}$ ,  $Al^{3+}$ ,  $Ca^{2+}$  have formed strong bonds with hard bases such as  $O^{--}$ ,  $CO_3^{--}$ ,  $SO_4^{--}$  while soft acids  $Cu^+$ ,  $Hg_2^{2+}$ ,  $Hg^{2+}$ ,  $Pb^{2+}$ ,  $Ag^+$  form strong bonds with soft bases such as  $S^{--}$ . These compounds readily occur on the earth's surface. However hard acid - soft base or soft acid - hard base combinations have disappeared from the earth's surface because of their weak bonds.

*In vivo* chemistry involves this principle and a process known as symbiosis in which metal ions participate. This is the process whereby a hard base on a metal ion encourages other hard bases to join it. This is of significance for those metal ions which are borderline cases since it means that the metals can behave as either hard or soft acids depending upon whether their environment is one of hard or soft bases. For example, in the cobaltic complexes  $[Co(NH_3)_5X]^{2+}$  where  $X = F^-$  and  $I^-$ , Co(III) can be shown to behave as a hard acid. However, in the complexes  $[Co(CN)_5X]^{3-}$  the stability is reversed and Co(III) behaves as a soft acid. Thus the soft cyanide complexing ligands have symbiotically made Co(III) into a soft acid. Another example occurs in the metalloenzyme carbonic anhydrase which binds halide ions in the order:  $I^- > Br^- > Cl^- > F^-$  thereby allowing the zinc to be classified as soft. In aqueous solution however the order is reversed. The hard sphere of solvation symbiotically renders the zinc hard.

Metal ions in biological systems are often in a state of suspension between two different oxidation states. In Table I.3 it was shown that soft acids have low oxidation states. Thus those metal ions that occur in the lower oxidation states may be symbiotically stabilized by the addition of a soft ligand. Similarly the higher oxidation state metal ions may be stabilized by the addition of hard ligands. Poisoning occurs by the addition of very hard or very soft ligands which result in the metal ions being completely anchored down in one oxidation state thereby preventing the living process of redox reactions

from occurring. Organic mercurials and cadmium ions are examples of soft acid poisons. They bind strongly to sulphur groups and so remove sulphur containing proteins. Very soft base poisons include cyanides, sulphides, trivalent arsenic compounds and carbon monoxide which block the metal sites in metalloporphyrins and copper enzymes.

The principle of HSAB matching of acid and base may be further illustrated in haemoglobin in which iron transports oxygen as a  $\text{Fe(II)}-\text{O}_2$  complex and not  $\text{Fe}^{3+} + \text{O}_2^-$  as occurs in aqueous solution. The reason for this is that the iron in haemoglobin has an environment of soft organic donor groupings which favours the lower oxidation state of iron and discourages the oxidation to ferric as occurs in aqueous solution where the environment is one of a hard solvation sphere.

### Conclusion

HSAB is thus a unifying concept designed to help us remember a vast body of chemical and biochemical facts and it also permits predictions, within limits, to be made. It is not infallible since many apparent discrepancies and exceptions exist.

"As to what the future holds for HSAB, no one can say. It seems inevitable that the entire concept will be replaced by statements that are less ambiguous and more felicitously phrased. Nevertheless, these statements will still have to accomplish the same mission of condensing a maximum amount of chemical information into a minimum number of words"<sup>15</sup>.

### I.5 COMPLEXES OF THE TYPE M(II)(BARB)<sub>2</sub>L<sub>2</sub>

Because barbiturates are so frequently encountered in toxicological examinations a reliable procedure for their detection and identification is essential. Barbiturates are readily detected in tissue extracts by the sensitive Koppanyi<sup>16</sup> reaction. In this procedure a chloroform extract of the sample to be tested (acidulated urine, blood or well ground, liquified tissue) is prepared. One cc of this unknown extract is then treated with 0,05 cm<sup>3</sup> of 1% cobalt acetate solution in absolute methyl alcohol and 0,3 cm<sup>3</sup> of a 5% (by volume) solution of isopropyl amine in absolute methyl alcohol. If barbiturates are present in the extract a reddish violet colour develops which is then compared in a colorimeter with the colour produced under the same conditions by barbiturate solutions of known strength. Using a 0,025% solution of barbiturate in chloroform as a standard, the formula below gives the number of milligrams of barbiturate per cc of chloroform extract.

$$\frac{(\text{colorimeter reading of standard}) \times 0,25}{(\text{colorimeter reading of unknown})} = \text{concentration of unknown.}$$

Other methods for the quantitative determination of barbiturates include gravimetric, ultraviolet spectrophotometric, isotopic and pharmacological procedures<sup>7</sup>.

It is also important to be able to identify the particular barbiturate that has been detected. Doran<sup>7</sup> has listed several methods for the qualitative determination of these compounds. Some of these are based upon the physical properties of the individual barbiturates. For example a precise melting point determination in combination with the measurement of the index of refraction of the melts has been used for differentiation among common barbiturates<sup>17</sup>. The procedure however is laborious and special methods are required to obtain crystals in a state of purity high enough for the reproducibility of melting points on which the identification depends. A microsublimation method, followed

by melting point and mixed melting point determinations, has also been described for identification of the drugs<sup>18</sup>.

An ultraviolet spectrophotometric method has been used for the identification of barbiturates such as amylobarbitol, butallylonal, secobarbital, pentobarbital and phenobarbital<sup>19</sup>.

A number of barbiturates have been characterized by the preparation of such N - substituted derivatives as *o*- and *p* - bromobenzyl and chlorobenzyl, *p* - iodobenzyl, *p* - nitrobenzyl and xanthy<sup>17</sup>.

Methods have recently been described for the separation of barbituric acids by paper chromatography following their extraction from blood and urine<sup>20</sup>. The order of sensitivity is relatively low for this type of procedure, a minimum of 50 micrograms generally being required for identification and quantitative estimation.

Infra red spectra<sup>21</sup> can be used for the detection of barbiturates and their identification. However, because these compounds have closely related chemical structures, the general absorption pattern is typical for the group. Nevertheless, in spite of the similarity in infra red absorption of a number of the members, minor spectral differences can be used to a certain extent to characterize compounds. Today, this process is greatly facilitated by comparison of the infra red absorption spectra of the parent barbituric acid with its transition metal - organic base derivative. These complexes are of the general form  $M(II)(\text{Barb})_2(L)_2$  where M is a transition metal such as Co, Cu, Zn, Cd or Ni; barb is the anion of a substituted barbituric acid and L is an organic base such as ammonia, pyridine or one of the picolines or lutidines.

In general, the spectra of these derivatives show a greater degree of dissimilarity from one another than the spectra of the corresponding barbiturates. This arises from the different structural features displayed by the complexes. Therefore the complexes should prove to be particularly valuable for identification purposes. Furthermore there are greater differences in the physical

properties (such as melting points and decomposition temperatures) of the complexes than in the individual barbiturates thereby providing a further means of distinguishing between them. For example, Levi and Hubley<sup>22</sup> found that the decomposition temperature of a series of  $\text{Cu}(\text{barb})_2(\text{pyridine})_2$  complexes were higher than the corresponding barbituric acids (with one exception - that of Rutonal). In addition, they found that the melting point of the veronal complex differs by about  $35^\circ\text{C}$  from that of its luminal analogue whereas the melting points of the pure drugs lie only  $15^\circ\text{C}$  apart. Similarly the nembutal and neonal complexes were found to decompose at  $160^\circ$  and  $180^\circ\text{C}$  whereas the pure compounds show practically identical melting points ( $\sim 128^\circ\text{C}$ ) and from this aspect the latter are indistinguishable.

Thus complexes of the type described above are providing the toxicologist and forensic chemist with a valuable tool for the identification and characterization of clinically important barbiturates.

## I.6 OBJECTIVES OF THE RESEARCH PROJECT

The clinical importance of complexes of the type  $M(II)(\text{barb})_2L_2$  in the identification of barbiturate drugs has just been discussed. The crystal structure analyses of such complexes had been limited to two isomorphous compounds<sup>23</sup>. The results of this X-ray analysis however do not agree with those predicted from infra red spectral data<sup>22</sup>, specifically with regard to the exact location of the coordination site on the barbiturate ligand. The crystal structures of these compounds are thus relatively unknown and hence the first two objectives of the project are:

- (i) to synthesize several of the above complexes varying the metal and both ligands in as many combinations as possible thereby obtaining a general series characteristic of the  $M(II)(\text{barb})_2L_2$  group of compounds;
- (ii) to determine through X-ray analysis the crystal structures of these complexes and to compare their structural features among themselves and with those of the free barbiturates and barbiturate salts.

Hydrogen bonding has been found to be a prominent feature in the structures of barbiturates, their salts and in the two  $M(II)(\text{barb})_2L_2$  structures reported. Moreover in an earlier section of this introduction it was pointed out that one of the prerequisites for the hypnotic activity of barbiturates is the availability of sites for hydrogen bonding. Thus, a third objective is:

- (iii) to investigate the nature of any intra- and inter-molecular hydrogen bonding that might prevail and to compare this with the hydrogen bonding observed in other members of the series as well as the barbiturates and their salts.

The X-ray crystal structure analyses of (ii) above will establish the exact location of the coordinating site on the barbiturates in these complexes. Nevertheless the contradictory results of the earlier infra red and X-ray studies provides an interesting fourth objective:

- (iv) to measure and interpret the infra red absorption spectra of the new complexes and of their parent barbiturates and to attempt to correlate this data with the observations of the X-ray analyses.

CHAPTER II

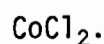
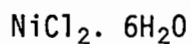
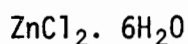
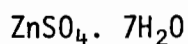
---

GENERAL EXPERIMENTAL

## II.1 PREPARATION OF THE COMPLEXES

### Reagents

Commercially available transition metal salts were used in the preparation of the complexes. These were



The barbiturates and their salts were supplied by Lennon Limited, Port Elizabeth, Republic of South Africa and are listed below. The number in brackets refers to the particular entry in Table I.1.

sodium barbital (no. 1)

phenobarbital (no. 4)

sodium amylobarbital (no. 6)

sodium pentobarbitone (no. 11)

sodium quinalbarbitone (no. 13)

sodium hebaral (no. 19)

calcium brallobarbital (no. 20).

The organic base ligands used were

pyridine

$\alpha$  and  $\beta$  picoline

2,4 2,6 and 3,5 lutidine

2,4,6 collidine

4 propyl pyridine

3 methyl pyridine

ammonia

imidazole.

### Method of Preparation

Dilute aqueous solutions of the metal salt, barbiturate (salt) and organic base were mixed in the molar ratio 1 : 2 : 2. In accordance with objective number (i), a large number of combinations of the three components were mixed together in an attempt to obtain as many different complexes as possible.

All the barbiturates with the exception of calcium brallobarbitol and phenobarbitol dissolved readily in water at room temperature. The latter two however required heating and continual stirring before dissolving.

The rate of evaporation of the resulting solutions was retarded by standard techniques in order to avoid rapid precipitation of the complex. The pH of several of the solutions was carefully altered by the addition of small amounts of 1M NaOH. This follows from the observation already mentioned in chapter I.3 that the  $pK_a$  values of barbiturates<sup>26</sup> are in the vicinity of 7,5. The significance of this is that application of the Henderson-Hasselbach equation shows that in general at  $pH > 7,5$ , barbiturates will be in the ionized form. It was therefore considered that complexation might occur more readily in basic solution. Accordingly solutions with pH values ranging from 7 to 11 were prepared.

Despite these different techniques, the isolation of crystalline complexes proved to be a very tedious and difficult task.

### Results

In most cases, mixing of the metal and ligand solutions resulted in rapid precipitation of complex. Copper complexes had colours ranging from dark to light purple while with nickel, the colour was grey-blue. With  $ZnCl_2 \cdot 6H_2O$  white  $Zn(OH)_2$  precipitated. However,  $ZnSO_4 \cdot 7H_2O$  gave colourless precipitates. Pink precipitates were obtained with cobalt. In general all the precipitates

were in the form of a fine powder but those of cobalt and zinc were often more of an oily, globular nature.

Of the barbiturates, sodium barbital was the most reactive while phenobarbital was the least. The latter did however, form pink oily drops with cobalt as described above.

After much experimentation, two crystalline complexes were finally isolated. The first was obtained from a mixture of  $\text{CuCl}_2$ , sodium barbital and  $\beta$ -picoline and was shown to have the formulation  $\text{Cu}(\text{barbital})_2 (\beta\text{-picoline})_2$ . The second was obtained from a mixture of  $\text{CuCl}_2$ , calcium brallobarbital and pyridine and was  $\text{Cu}(\text{brallobarbital})_2 (\text{pyridine})_2$ . In both cases the crystals were purple monoclinic prisms although, while the former were very well defined, the latter had dull faces and were powder-like in nature. A third complex, which was later shown to be  $\text{Cu}(\text{barbital})_2 (\text{pyridine})_2$ , was also obtained and a study of this compound was undertaken as part of another research project in this department<sup>27</sup>.

After the X-ray crystal structures of the above complexes had been elucidated further attempts at synthesizing similar compounds were made. Metals other than copper were used. Two more crystalline complexes were obtained. The first was from a mixture of  $\text{ZnSO}_4 \cdot 7\text{H}_2\text{O}$ , sodium barbital and  $\beta$ -picoline (later shown to be  $\text{Zn}(\text{barbital})_2 (\beta\text{-picoline})_2$ ) and the second from a mixture of  $\text{NiSO}_4$ , amylobarbital and imidazole (later shown to be  $\text{Ni}(\text{amylobarbital})_2 (\text{imidazole})_2$ ). The crystals of the former were transparent and block-like while those of the latter were small, well defined and blue-grey in colour.

In all, four complexes of the general type  $\text{M}(\text{II})(\text{barb})_2\text{L}_2$  were thus obtained:

- 1  $\text{Cu}(\text{II})(5,5\text{-diethylbarbiturato})_2 (\beta\text{-picoline})_2$
- 2  $\text{Cu}(\text{II})(5\text{-allyl-5-(2-bromoallyl)-barbiturato})_2 (\text{pyridine})_2$
- 3  $\text{Zn}(5,5\text{-diethylbarbiturato})_2 (\beta\text{-picoline})_2$
- 4  $\text{Ni}(5\text{-ethyl-5-isopentyl barbiturato})_2 (\text{imidazole})_2$

The crystal structures of these complexes are described in chapters III, IV, V and VI respectively and they will occasionally be referred to as complex no. 1, complex no. 2, etc.

## II.2 PRELIMINARY WORK ON THE CRYSTALS

### Chemical Analysis

The carbon, hydrogen and nitrogen content of each complex was determined in microanalytical tests in order to verify their composition.

### Density Determination<sup>25</sup>

The density of the crystals of each complex was determined using a density gradient column containing the components m-xylene ( $\rho = 0,86 \text{ g cm}^{-3}$ ) and carbon tetrachloride ( $\rho = 1,60 \text{ g cm}^{-3}$ ) which was precalibrated with aqueous caesium chloride solutions.

### Preliminary X-ray Analysis

Suitable crystals were selected and mounted along their respective crystallographic axes. A two-circle optical goniometer was used to align well formed crystals. In cases where crystals were malformed the alignment technique developed by Weisz and Cole was used<sup>28</sup>.

Rotation and Weissenberg photographs were taken using a Stoe (Heidelberg) and a Stoe (Darmstadt) goniometer in conjunction with a Philips PW 1120 and a Philips PW 1008 generator. The generators were both operated at 20 mA and 40 kV. A copper target was used and  $\text{CuK}\alpha$  ( $\lambda = 1,5418 \text{ \AA}$ ) radiation was obtained with the aid of a nickel filter.

In the collection of the X-ray data, Kodak "Kodirex" film was used. The film was developed in Kodak X-ray developer for 5 minutes, immersed for 5 seconds in a stop bath containing 3% acetic acid and was fixed for 5 minutes by agitation in Kodak X-ray fixer.

From the photographs it was possible to determine the unit cell parameters and space group for each of the complexes.

### II.3 THE DIFFRACTOMETER DATA COLLECTIONS

After the unit cell parameters and space group for a particular complex had been established, several crystals of roughly cubical or spherical shape were mounted at the tips of thin glass rods and were sent to Dr. G. Gafner of the National Physics Research Laboratory, C.S.I.R. (South Africa) where the diffractometer data collection was carried out.

The intensity data for each of the complexes was collected on a Philips PW 1100 computer-controlled, single crystal, four-circle diffractometer operating in the  $\omega$ - $2\theta$  scan mode. In this scanning process<sup>29</sup> the detector of the diffractometer rotates at an angular rate which is twice that of the crystal. In the  $\omega$  scan of a given reflection, the crystal and hence the reciprocal lattice is rotated by the  $\omega$  circle to carry the lattice point from the outside of the sphere of reflection to the inside. The  $\omega$  scan is similar to a photometric trace made parallel to the central line of the film on a zero level Weissenberg photograph while the  $2\theta$  scan corresponds to a similar trace made along the diagonal passing through reflections on a common central lattice row. In this way a given reflection is accurately centred so that a reasonable number of quanta are detected during one traverse through the reflecting position.

A Philips PW 1130 3kW X-ray generator operating at 50 kV and 20 mA provided the source of radiation. Molybdenum  $K_{\alpha}$  radiation ( $\lambda = 0,7107 \text{ \AA}$ ) was obtained with the aid of a graphite monochromator. The take-off angle, source to crystal distance and crystal to counter distance were  $6^{\circ}$ , 24,5 cm and 22cm respectively. The receiving aperture at the counter was 2 degrees in the  $2\theta$  plane and 1 degree in the plane normal to this.

The lattice constants of the respective unit cells were obtained from a least squares analysis of the  $\chi$ ,  $\phi$  and  $2\theta$  angles of 25 reflections accurately centered on the diffractometer.

During the collection of intensity data, three reference reflections were measured periodically to ensure stability of operation and to monitor any crystal decomposition. The variation in intensity of a reference reflection was observed to be less than 3% of its mean value for all the complexes with the exception of  $\text{Cu}(\text{brallobarbital})_2(\text{pyridine})_2$ . The data collection for this latter complex was poor due to the inferior quality of the crystals. This aspect of the complex is discussed in Chapter IV.

Reflections were rejected<sup>30</sup> if  $I_{\text{rel}} < 1,65 \sigma(I_{\text{rel}})$  where

$$\sigma(I) = [(0,02 N_o)^2 + K^2 N_b + N_o]^{\frac{1}{2}}$$

In this equation  $N_o$  is the gross peak count for a particular reflection,  $N_b$  the background count and  $K$  the ratio of scan to background times. The background scan time on each side of the reflection peak was equal to half the scan time over the peak.

Lorentz-Polarization corrections were applied to all the data. However, in all cases, extinction was not regarded as being significant and no corrections were made.

Two different program packages were used in the computation of Patterson and Fourier syntheses and in the solution and refinement of the structures. These were the XRAY67 and XRAY72 systems.

Ball and stick type models were used to interpret the various Fourier maps. In cases where the unit cell was triclinic the construction of such models was facilitated by transforming fractional coordinates to orthogonal coordinates.

All calculations were performed on a Univac 1106 computer system.

CHAPTER III

THE CRYSTAL AND MOLECULAR STRUCTURE OF THE  
BIS-(5,5 -DIETHYLBARBITURATO)-BIS-(PICOLINE)  
DIHYDRATE COMPLEX OF COPPER (II).

### III.1 CRYSTAL AND INTENSITY DATA

#### Chemical Analysis

Table III.1 lists the theoretical and experimentally determined analysis figures. Theoretical values for both the anhydrous and dihydrated complexes are given.

TABLE III.1

	%C	%H	%N	%Cu
Theoretical (anhydrous) :	54,54	6,18	13,63	10,30
Theoretical (dihydrate) :	51,57	6,13	12,89	9,75
Experimentally determined :	50,9	6,1	12,7	10,60

The calculated and experimentally determined figures agreed closely enough to suggest that the complex had the composition  $C_{28}H_{36}CuN_6O_6$  corresponding to the expected formulation  $Cu(II)(5,5\text{-diethylbarbiturato})_2(\beta\text{-picoline})_2$ . During X-ray analysis however, water of crystallization was detected giving the complex the composition  $C_{28}H_{36}CuN_6O_6 \cdot 2H_2O$ .

#### Density of Crystals

The density was determined as  $1,37(2) \text{ g cm}^{-3}$ . This value together with preliminary unit cell parameters was used to calculate the number of molecules per unit cell and this was found to be 2.

#### Space Group

From systematic absences observed on zero and upper layer Weissenberg photographs, the conditions for non extinction were found to be

$h00$     no conditions

$0k0$      $k = 2n$

$00l$      $l = 2n$

$0k\ell$  no conditions

$h0\ell$   $\ell = 2n$

These conditions indicated the unequivocal space group  $P2_1/c$  (second setting).

### Unit Cell Parameters

A single crystal of dimensions 0,15 x 0,30 x 0,25 mm was used for the determination of the unit cell parameters and the diffractometer data collection. The unit cell parameters and other crystal data is given in Table III.2.

TABLE III.2 CRYSTAL DATA

$a = 11,196(5) \text{ \AA}$	$V = 1565,23 \text{ \AA}^3$
$b = 15,124(5) \text{ \AA}$	$D_M = 1,37(2) \text{ g cm}^{-3}$
$c = 9,449(5) \text{ \AA}$	$D_C = 1,381 \text{ g cm}^{-3}$ for $Z = 2$
$\beta = 102,0(2)^\circ$	$\mu = 7,79 \text{ cm}^{-1}$ for $\text{MoK}\alpha$ radiation
$F(000) = 718$	Space group : monoclinic, $P2_1/c$

### Intensity Data

The diffractometer scan width was  $0,8^\circ$  and the scan speed  $0,02^\circ \text{ sec}^{-1}$ . The background and scan times were both 40 seconds. Using graphite monochromated  $\text{MoK}\alpha$  radiation, 1631 reflections up to  $2\theta = 40^\circ$  were measured. Of these, 80 were systematically absent while 106 were redundant due to space group equivalence. A further 312 had  $I_{\text{rel}} < 1,65 \sigma (I_{\text{rel}})$  and were omitted as unobserved.

The linear absorption coefficient<sup>31</sup>,  $\mu$ , for  $\text{MoK}\alpha$  radiation was determined as  $7,79 \text{ cm}^{-1}$ . From the dimensions of the crystal used it can be seen that the variation in  $\mu R$  (where  $R =$  radius of crystal) was between 0,06 and 0,12. The corresponding absorption corrections<sup>32</sup>  $A^*$  varied from 1,10 to 1,20 for the entire  $\theta$  range scanned. This was regarded as being insignificant and no absorption correction was applied.

### III.2 SOLUTION AND REFINEMENT OF THE STRUCTURE

With the number of molecules per unit cell having been determined as 2, symmetry considerations required the copper atoms to occupy special positions 0,0,0 and  $0, \frac{1}{2}, \frac{1}{2}$  with the rest of the centrosymmetric molecule occupying general positions. Since the real space location of the copper atom was 0,0,0 the Patterson synthesis (CENTROSY PROGRAM) with copper at the unit cell origin, yielded a map resembling the electron density map which would have been obtained with copper at 0,0,0. Consequently the 3 dimensional Patterson was interpreted as such, but, because it had P2/m symmetry, a mirror image of the molecule was generated and care had to be exercised in distinguishing real molecule peaks from the mirror image peaks. Nevertheless, the 9 atoms of the trioxypyrimidine ring were located and the resulting Fourier synthesis, phased on the positions of these atoms and the position of the copper atom enabled all the other non-hydrogen atoms of the complex to be located. Least-squares refinement of atomic positions and isotropic temperature factors (ORFLS : X-RAY67)<sup>33</sup> brought the residual index, R, down to a terminal value 0,20 where  $R = \Sigma(|F_o| - |F_c|) / \Sigma|F_o|$ . At this stage a difference Fourier synthesis revealed the presence of a hydrate oxygen atom. Further least-squares refinement of atomic positions and anisotropic temperature factors was followed by difference Fourier syntheses in which all hydrogen atom positions were located.

All atomic parameters were then further refined by full-matrix least-squares methods in which the hydrogen atoms were given the same anisotropic temperature factors as the atoms to which they were attached. The function minimized was  $\Sigma w(|F_o| - |F_c|)^2$ , where w is the weight of a reflection. For the anisotropic refinement the thermal parameters were of the form

$$T = \exp[-(\beta_{11}h^2 + \beta_{22}k^2 + \beta_{33}l^2 + 2\beta_{12}hk + 2\beta_{13}hl + 2\beta_{23}kl)]$$

After the last cycle of refinement R had settled at 0,035 and the average e.s.d. in the positional parameters of all atoms was about five times the average parameter shift. In the structure factor calculations, scattering factors for the copper, carbon, nitrogen, oxygen and hydrogen atoms were those obtained from Hanson et al<sup>34</sup>. The copper was treated as Cu<sup>0</sup> and the anomalous dispersion correction ( $\Delta f' = 0,3$  for MoK $\alpha$  radiation) was applied to the scattering curve<sup>35</sup>.

As a final check of the correctness of the structure a difference electron density map with the structure factors calculated in the last cycle of refinement was computed. This map was practically featureless. The final atomic positional and thermal parameters for the non hydrogen atoms are listed in Table III.3 while the final atomic positional parameters for the hydrogen atoms are given in Table III.4. Table III.5 lists the observed and calculated structure factors.

TABLE III.3  
NON HYDROGEN ATOMS  
FRACTIONAL ATOMIC CO-ORDINATES ( $\times 10^4$ ) AND  
THERMAL PARAMETERS ( $\times 10^4$ ) AND THEIR e.s.ds

Atom	X	Y	Z	$\beta_{11}$	$\beta_{22}$	$\beta_{33}$	$\beta_{12}$	$\beta_{23}$	$\beta_{31}$
Cu	0	0	0	30 (1)	19(1)	52 (1)	-2(1)	-2 (1)	-2(1)
C (2)	1450(4)	280(3)	2754 (5)	42 (6)	20(3)	99 (9)	0(3)	13 (6)	-7(4)
C (4)	3506(4)	844(3)	3606 (5)	37 (6)	40(3)	55 (8)	-10(4)	4 (5)	-7(4)
C (5)	3654(4)	940(3)	2063 (5)	39 (5)	30(3)	45 (8)	-2(4)	4 (5)	-7(4)
C (6)	2535(4)	632(3)	946 (5)	55 (6)	16(3)	51 (8)	7(3)	0 (6)	-2(4)
C (7)	3863(5)	1926(4)	1767 (7)	71 (7)	37(4)	110(10)	-13(4)	2 (6)	-2(5)
C (8)	2863(7)	2531(4)	1996 (9)	119 (9)	38(4)	194(13)	1(5)	18 (8)	-5(6)
C (9)	4768(5)	394(4)	1868 (6)	47 (6)	49(4)	82 (9)	3(4)	3 (6)	-4(5)
C(10)	4604(7)	-598(5)	1982 (7)	95 (8)	57(5)	103(10)	34(5)	19 (7)	8(5)
C(12)	54(5)	1864(4)	-847 (6)	65 (7)	46(4)	130(10)	1(4)	8 (7)	5(5)
C(13)	-281(6)	2741(4)	-951 (7)	128(10)	30(4)	193(13)	-2(5)	1 (9)	17(6)
C(14)	-1240(6)	3018(5)	-352 (7)	136(10)	34(4)	176(13)	22(5)	-9 (9)	-8(6)
C(15)	-1875(5)	2422(4)	332 (6)	90 (7)	40(4)	118(11)	22(5)	-6 (7)	-5(5)
C(16)	-1471(5)	1548(4)	385 (6)	63 (6)	34(4)	97 (9)	8(4)	10 (6)	-1(5)
C(17)	-2917(8)	2690(7)	967(11)	174(14)	85(8)	236(19)	50(8)	68(13)	1(9)
N (1)	1525(3)	345(2)	1354 (4)	45 (5)	25(2)	48 (6)	-7(3)	4 (4)	2(3)
N (3)	2440(4)	512(3)	3842 (4)	50 (5)	46(3)	48 (6)	-15(3)	15 (5)	-9(3)
N(11)	-536(3)	1276(2)	-181 (4)	37 (4)	24(3)	87 (7)	-3(3)	-5 (5)	-7(3)
O (2)	507(3)	19(3)	3090 (4)	68 (4)	59(3)	140 (6)	-16(3)	35 (4)	-10(4)
O (4)	4293(3)	-1079(3)	4617 (3)	74 (4)	80(3)	60 (6)	-26(3)	-11 (4)	-8(3)
O (6)	2591(3)	660(2)	-349 (3)	75 (4)	52(3)	54 (5)	-3(3)	1 (4)	-2(3)
O(18)	1926(3)	4826(3)	1650 (4)	86 (4)	60(3)	85 (6)	19(3)	31 (4)	13(3)

TABLE III.4  
HYDROGEN ATOMS  
FRACTIONAL ATOMIC COORDINATES ( $\times 10^3$ )  
AND THEIR e.s.ds

Atom	X	Y	Z
H (3)	228(4)	53(4)	473(5)
H (7 1)	461(5)	204(4)	234(6)
H (7 2)	411(5)	193(4)	67(6)
H (8 1)	270(6)	257(4)	298(7)
H (8 2)	195(6)	238(4)	156(7)
H (8 3)	294(6)	316(4)	174(7)
H (9 1)	547(5)	60(4)	268(6)
H (9 2)	495(5)	58(4)	87(5)
H(10 1)	389(5)	-82(4)	127(6)
H(10 2)	441(5)	-78(4)	295(6)
H(10 3)	527(5)	-93(4)	175(6)
H(12)	67(5)	162(4)	-134(6)
H(13)	17(6)	314(4)	-132(7)
H(14)	-151(6)	363(4)	-27(7)
H(16)	-187(5)	107(4)	90(6)
H(17 1)	-337(7)	237(5)	110(8)
H(17 2)	-259(7)	310(5)	179(8)
H(17 3)	-337(6)	312(5)	22(8)
H(18 1)	98(5)	488(4)	165(6)
H(18 2)	212(5)	462(4)	238(6)



### III.3 DESCRIPTION OF THE STRUCTURE

The structure of the molecule is shown in Figure III.1 (ORTEP PROGRAM)<sup>36</sup>. The intramolecular bond lengths and angles and their associated e.s.ds are given in Tables III.6 and III.7 respectively. These parameters were calculated using the function and error program ORFFE<sup>33</sup>. (In this program the unit cell parameters  $a$ ,  $b$ ,  $c$ ,  $\alpha$ ,  $\beta$ ,  $\gamma$  and their appropriate errors constitute the input data. The atomic positional parameters  $x$ ,  $y$ ,  $z$  are read from the output of the program ORFLS). The program "L S PLANE" (i.e. least squares plane) was used to calculate the best planes through certain sets of atoms. Table III.8 lists these planes with their equations and the perpendicular distances of various atoms from these planes.

#### The Copper Coordination Sphere

The copper atom is coordinated to the barbital anions via their deprotonated nitrogen atoms N(1) and N(1<sup>i</sup>) and to the  $\beta$ -picoline moieties via their nitrogen atoms N(11) and N(11<sup>i</sup>) in square planar arrangement, the bond angles N(1)-Cu-N(11) and N(1)-Cu-N(11<sup>i</sup>) being 90,3(1)° and 89,7(1)° respectively. The bond lengths for Cu-N(1) and Cu-N(11) are 1,980(5) and 2,018(3) Å respectively. As no similar compounds containing copper bound to a barbiturate through a nitrogen atom were known at this stage, the Cu-N(1) distance was compared, as a first approximation, with the analagous Co-N and Zn-N distances (2,020(3) and 2,009(2) Å respectively) found in the complexes reported by Wang and Craven<sup>23</sup>. However, in a simultaneous study by M.R. Caira<sup>27</sup> in which copper is bound to a barbiturate via a nitrogen atom, the Cu-N bond distance was found to be 1,983(5) Å. The Cu-N(11) distance of the present study compares favourably with the Cu-N (picoline) bond length of 1,989(6) Å reported for the complex *trans*-Bis[(chloroacetato)-( $\alpha$ -picoline)] copper (II)<sup>37</sup> and with the Cu-N (pyridine) distance of 2,032(5) Å reported by Caira<sup>27</sup>.

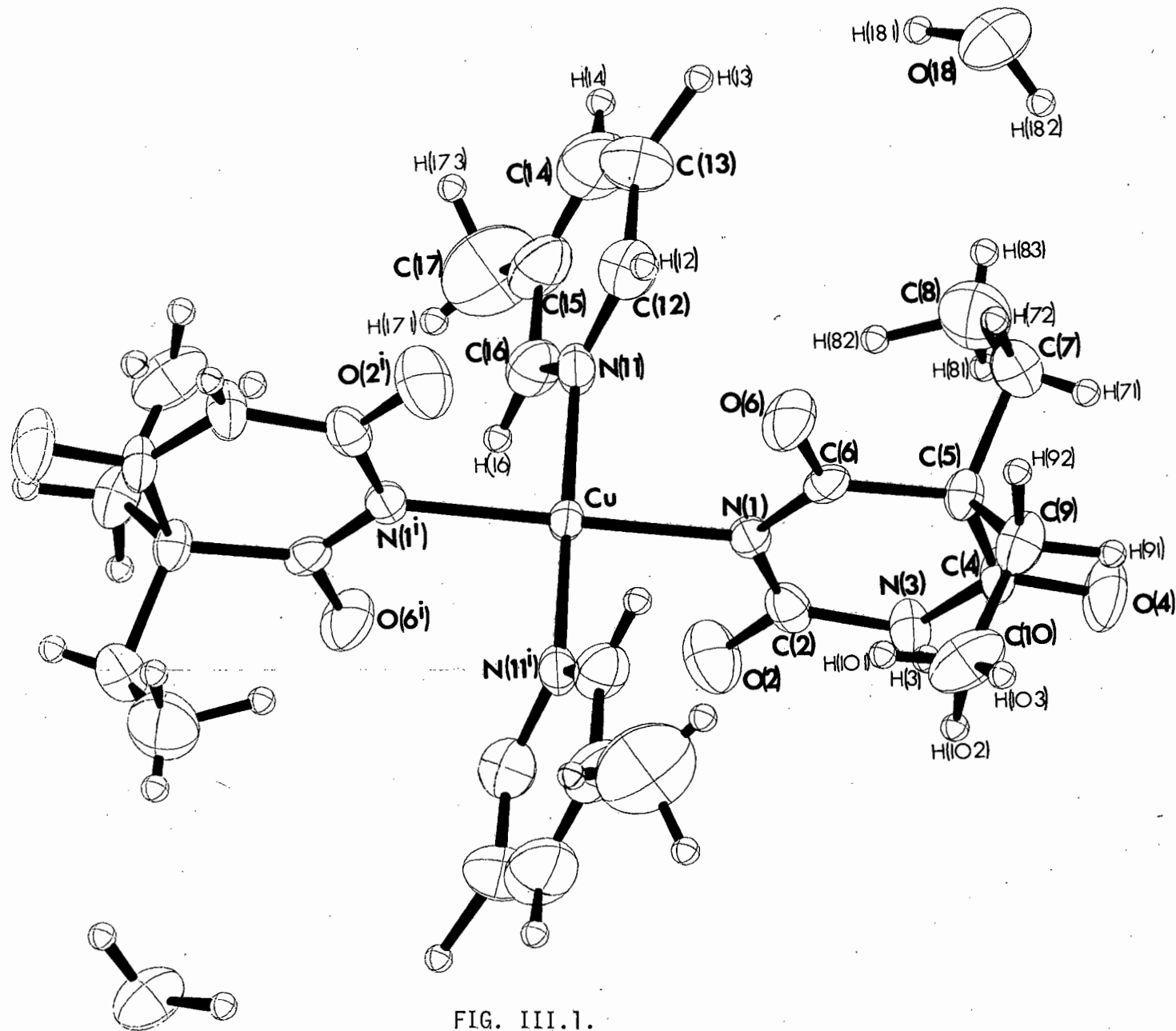


FIG. III.1.

TABLE III.6

INTRAMOLECULAR BOND LENGTHS AND THEIR e.s.ds IN Å

Cu-N(1)	1,980(5)	N(3)-H(3)	0,90(5)
N(1)-C(2)	1,346(6)	C(7)-H(7 1)	0,91(5)
C(2)-N(3)	1,391(6)	C(7)-H(7 2)	1,13(6)
N(3)-C(4)	1,356(7)	C(8)-H(8 1)	0,99(7)
C(4)-C(5)	1,508(7)	C(8)-H(8 2)	1,05(6)
C(5)-C(6)	1,534(6)	C(8)-H(8 3)	0,98(6)
C(6)-N(1)	1,341(6)	C(9)-H(9 1)	1,02(5)
C(2)-O(2)	1,229(6)	C(9)-H(9 2)	1,04(5)
C(4)-O(4)	1,214(6)	C10-H(10 1)	0,99(6)
C(6)-O(6)	1,239(6)	C10-H(10 2)	1,02(6)
C(5)-C(7)	1,544(8)	C10-H(10 3)	0,97(6)
C(7)-C(8)	1,50 (1)	C12-H(12)	0,99(6)
C(5)-C(9)	1,539(8)	C13-H(13)	0,90(6)
C(9)-C(10)	1,52 (1)	C14-H(14)	0,99(6)
Cu-N(11)	2,018(3)	C16-H(16)	1,02(5)
N(11)-C(12)	1,340(7)	C17-H(17 1)	0,74(8)
C(12)-C(13)	1,376(9)	C17-H(17 2)	1,00(8)
C(13)-C(14)	1,38 (1)	C17-H(17 3)	1,01(8)
C(14)-C(15)	1,39 (1)		
C(15)-C(16)	1,396(9)		
C(16)-N(11)	1,335(7)	O(18)-H(18 1)	1,06(6)
C(15)-C(17)	1,48 (1)	O(18)-H(18 2)	0,74(5)

TABLE III.7

INTRAMOLECULAR BOND ANGLES (IN DEGREES)

N(1)-Cu-N(11)	90,3(1)	C(7)-C(5)-C(9)	109,8(4)
N(1)-Cu-N(11 <sup>1</sup> )	89,7(1)	C(6)-C(5)-C(7)	107,5(4)
Cu-N(1)-C(2)	113,4(3)	C(6)-C(5)-C(9)	108,7(4)
Cu-N(1)-C(6)	124,2(3)	C(5)-C(7)-C(8)	114,7(5)
N(1)-C(2)-N(3)	120,4(4)	C(5)-C(9)-C(10)	114,1(5)
C(2)-N(3)-C(4)	124,4(4)	Cu-N(11)-C(12)	120,5(3)
N(3)-C(4)-C(5)	118,2(4)	Cu-N(11)-C(16)	120,3(3)
C(4)-C(5)-C(6)	113,5(4)	N(11)-C(12)-C(13)	121,2(6)
C(5)-C(6)-N(1)	121,1(4)	C(12)-C(13)-C(14)	119,2(6)
C(6)-N(1)-C(2)	122,3(4)	C(13)-C(14)-C(15)	120,7(6)
N(1)-C(2)-O(2)	120,6(4)	C(14)-C(15)-C(16)	116,0(5)
N(3)-C(2)-O(2)	119,0(4)	C(15)-C(16)-N(11)	123,4(5)
N(3)-C(4)-O(4)	120,0(4)	C(16)-N(11)-C(12)	119,2(4)
C(5)-C(4)-O(4)	121,9(4)	C(14)-C(15)-C(17)	122,4(6)
C(5)-C(6)-O(6)	118,0(4)	C(16)-C(15)-C(17)	121,5(6)
N(1)-C(6)-O(6)	120,9(4)		
C(4)-C(5)-C(9)	108,6(4)		
C(4)-C(5)-C(7)	108,6(4)	H(18 1)-O(18)-H(18 2)	97 (5)

TABLE III.8

## LEAST-SQUARES PLANES

The equations of the planes are expressed in  
orthogonalised space as  $lx + my + nz = d$

Plane I	square planar co-ordination around copper atom								
Atoms defining the plane	Cu	N(1)	N(11)	N(1 <sup>i</sup> )	N(11 <sup>i</sup> )				
Atoms not included in the plane						0(2)	0(6)		
Distance from the plane, Å	0,0	0,0	0,0	0,0	0,0	2,221	-2,226		
Equation	$-0,62671x - 0,11646y + 0,77050z = 0,00$								
Plane II	through the 6 atoms of the $\beta$ -picoline ring								
Atoms defining the plane	N(11)	C(12)	C(13)	C(14)	C(15)	C(16)			
Atoms not included in the plane							C(17)		
Distance from the plane, Å	0,003	-0,001	-0,003	0,005	-0,003	-0,001	-0,015		
Equation	$0,46166x + 0,18499y + 0,86755z = -0,05210$								
Plane III	through the 6 pyrimidine ring atoms								
Atoms defining the plane	N(1)	C(2)	N(3)	C(4)	C(5)	C(6)			
Atoms not included in the plane							0(2)	0(4)	0(6)
Distance from the plane, Å	0,008	0,011	-0,017	0,006	0,011	-0,018	0,043	0,060	-0,060
Equation	$-0,36411x + 0,93093y - 0,02822z = -0,08297$								
Plane IV	through the trioxypyrimidine ring atoms								
Atoms defining the plane	N(1)	C(2)	N(3)	C(4)	C(5)	C(6)	0(2)	0(4)	0(6)
Distance from the plane, Å	0,018	-0,003	-0,046	-0,015	0,017	0,003	0,019	0,025	-0,017
Equation	$-0,36090x + 0,93147y - 0,04599z = -0,11030$								
Plane V	through the atoms of the diethyl group and C(5)								
Atoms defining the plane	C(5)	C(7)	C(8)	C(9)	C(10)				
Distance from the plane, Å	0,026	-0,040	0,006	0,044	-0,036				
Equation	$0,20985x + 0,09277y + 0,97332z = 2,73546$								

## INTERSECTION ANGLES

Planes I and II	69,05°	Planes II and III	91,17°
Planes I and III	84,37°	Planes III and IV	1,30°
Planes I and IV	85,28°	Planes III and V	91,00°

The Cu-N (pyridine) bond length of 2,122(9) Å in the structure monopyrindine copper II acetate<sup>38</sup> provides further comparison.

A very interesting feature of the copper coordination sphere arises from the positions of two centrosymmetrically related oxygen atoms O(2) and O(2<sup>i</sup>) which lie above and below the plane through atoms Cu, N(1), N(11), N(1<sup>i</sup>) and N(11<sup>i</sup>) (plane I) at a distance of 2,857(4) Å from the copper atom. This is less than the sum of the van der Waals radii of 3,4 Å for copper and oxygen and it would therefore appear that O(2) and O(2<sup>i</sup>) are involved in "off-the-z-axis coordination" with copper. The z axis is taken as the normal to plane I giving the off-the-z-axis angle as 39,0° (Caira<sup>27</sup>: 35,7°). This type of coordination has also been observed in the structure reported by Davey and Stephens<sup>37</sup>.

A second, similar interaction exists between copper and oxygen atoms O(6) and O(6<sup>i</sup>). Because the separation here is larger (Cu-O : 3,149(4) Å) the interaction is probably much weaker. Caira<sup>27</sup> also observed a second weaker interaction (Cu-O : 3,234(7) Å) in Cu(barbital)<sub>2</sub>(pyridine)<sub>2</sub>.

Figure III.2 is an illustration of the copper coordination sphere while table III.9 lists all relevant bond lengths and angles.

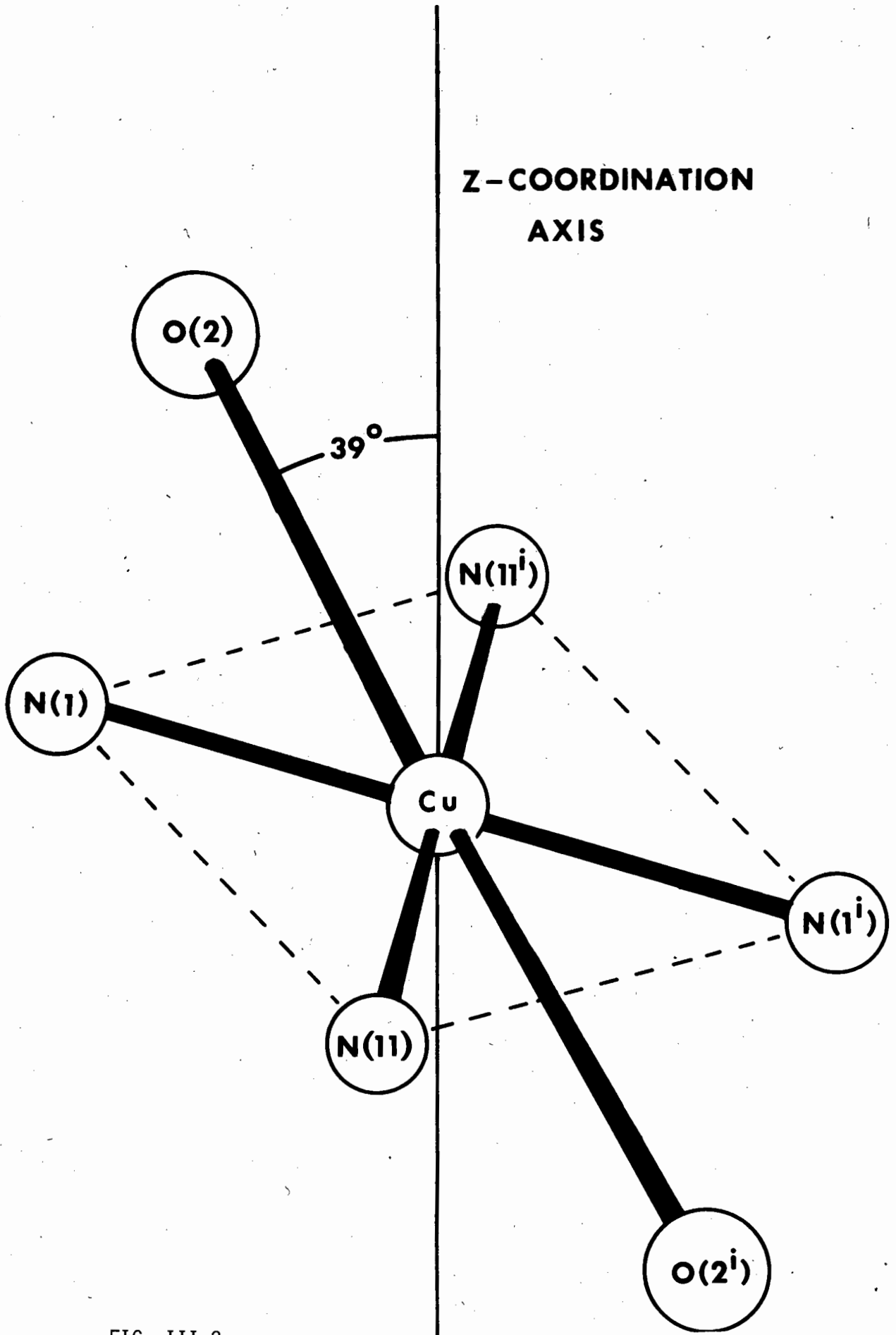


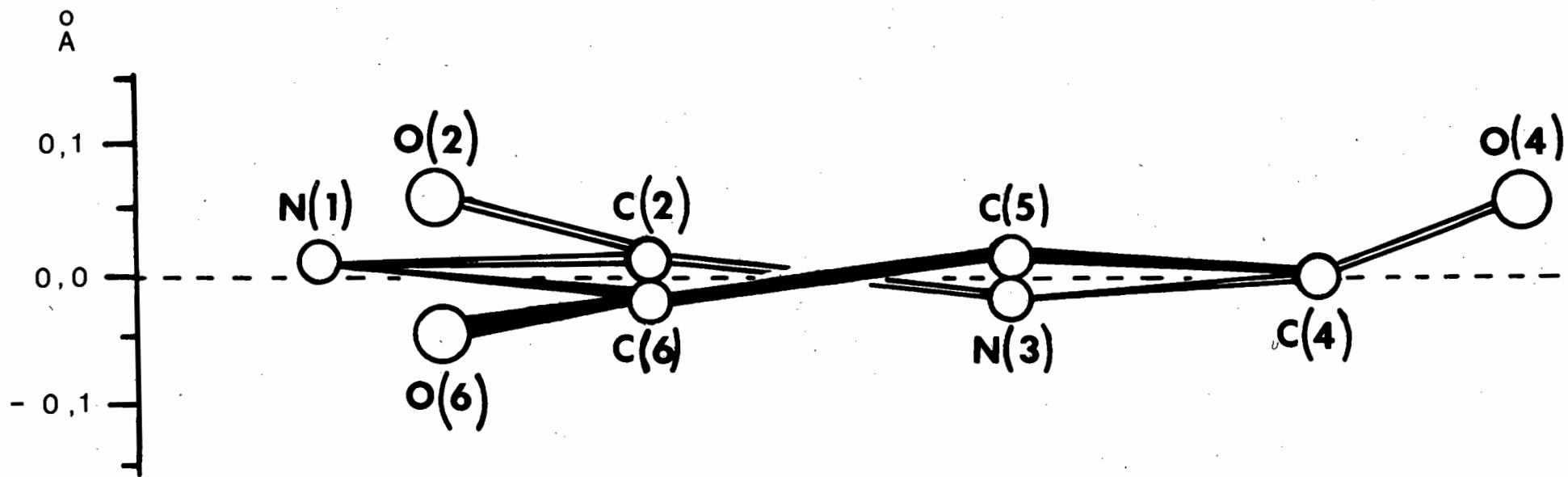
FIG. III.2.

In the  $\beta$ -picoline moiety, the average C-C and C-H bond lengths within the ring are 1,38 Å and 0,98 Å respectively. All bond lengths and angles agree favourably with those reported by Davey and Stephens<sup>37</sup>. The ring is planar, the greatest deviation from the least squares plane through the six atoms (plane II) being that of atom C(14) at a distance of 0,005 Å. The  $\beta$ -methyl group lies at a distance 0,015 Å from this plane. Planes I and II intersect at an angle 69,05°.

#### The barbitol ligand structure

The conformation of the trioxopyrimidine ring is shown in Fig. III.3 in which the dotted line is a trace of the least squares plane through the six ring atoms only (Plane III). The ring is almost planar, the greatest deviation from this plane being that of atom N(3) at a distance of 0,017 Å. However, slight puckering of the ring is evident. In the structure reported by Caira<sup>27</sup> the puckering is more pronounced with the largest deviation from the plane being that of atom C5. Its distance from the plane is 0,1 Å. When the three exocyclic oxygens are included in the least squares plane calculation, it is seen (Plane IV) that the entire trioxopyrimidine moiety is virtually planar, the largest deviation from the plane being that of atom N(3) at a distance of 0,04 Å. Planes III and IV intersect at an angle of 1,30° indicating the coplanarity of the exocyclic oxygen atoms and the pyrimidine ring atoms.

Atoms C(7), C(8), C(9) and C(10) of the two ethyl groups as well as atom C(5) to which they are attached lie in the same plane (Plane V) which is virtually perpendicular (91,0°) to the pyrimidine ring plane (Plane III). The hydrogen atoms of the two ethyl groups are in the staggered configuration. Planes I and III intersect at 84,37°, (Caira 86,7°) i.e. the plane Cu, N(1), N(11) and the pyrimidine ring plane are almost perpendicular. Similarly the planes through the two different moieties of the molecule, i.e. through the picoline ring (Plane II) and the pyrimidine ring plane (Plane III) are normal to each other (91,17°).



(The vertical scale is approximately five times the horizontal scale).

FIG. III.3.

The internal ring angle C(2)-N(1)-C(6) is  $122,3(4)^\circ$  which compares favourably<sup>23</sup> with the  $121,6^\circ$  found in  $\text{Zn(II)(barbital)}_2(\text{imidazole})_2$ . Interest is centred on this angle as N(1) is the site at which deprotonation and subsequent coordination occur. The effects this has on the environment of N(1) are discussed in a later chapter.

### Hydrogen bonding

The intermolecular hydrogen bonding is shown as dotted lines in Figures III.4 and III.5, the [100] and [010] projections of the structure respectively. The [001] projection is shown in Figure III.6. Each discrete molecule of the complex is linked to two other molecules via four bridging water molecules. This gives a sheet-like structure in which the layers comprising the barbiturate anions and the water molecules are orientated approximately parallel to the x-z plane of the crystal lattice.

There are thus 3 crystallographically distinct hydrogen-bonds emanating from each water molecule. The hydrogens of the water molecule H(18.1) and H(18.2) are each hydrogen-bonded to oxygens O(2) and O(6<sup>1</sup>) respectively of the barbiturate moieties of a single molecule of the complex at (x,y,z). The hydrate oxygen is hydrogen-bonded to an N-H group of the molecule at (x,y,z-1).

The geometry of the interactions is shown in Fig. III.7. The hydrogen-bond distances are all in good agreement with those listed by Donohue<sup>39</sup> for an assortment of hydrogen-bonded compounds. Fig. III.7 shows the near linearity of each of the 3 hydrogen-bonds with bond angles well within the maximum allowed deviation from  $180^\circ$ . All bond lengths and angles involved in the hydrogen-bonding are listed in Table III.10.

TABLE III.9  
INTERATOMIC DISTANCES (Å) AND BOND ANGLES (DEGREES) AND  
THEIR e.s.ds INVOLVED IN THE 'OFF-THE-Z-AXIS CO-ORDINATION'

Cu-N(1)	:	1,980(5)	N(1)-Cu-O(2)	:	51,3 (1)
Cu-N(11)	:	2,018(3)	N(11)-Cu-O(2)	:	94,00(5)
Cu-O(2)	:	2,857(4)	N(1 <sup>i</sup> )-Cu-O(2)	:	128,7 (1)
N(1)-O(2)	:	2,237(5)	N(11 <sup>i</sup> )-Cu-O(2)	:	86,00(5)
N(11)-O(2)	:	3,611(3)			
N(1 <sup>i</sup> )-O(2)	:	4,376(7)			
N(11 <sup>i</sup> )-O(2)	:	3,380(4)			
N(1)-N(11)	:	2,833(6)			
N(1)-N(11 <sup>i</sup> )	:	2,820(5)			

TABLE III.10  
BOND-LENGTHS (Å) AND ANGLES (DEGREES) AND  
THEIR e.s.ds INVOLVED IN THE HYDROGEN-BONDING

O(2)-H(18 1)		1,75 (5)			
O(2)-O(18)		2,801(5)			
O(6)-H(18 2)		2,14 (5)			
O(6)-O(18)		2,874(5)			
H(3)-O(18)		2,00 (5)			
N(3)-O(18)		2,875(6)			
	O(2)-H(18 1)-O(18)	:		172(5)	
	O(6)-H(18 2)-O(18)	:		166(5)	
	N(3)-H(3)-O(18)	:		163(5)	

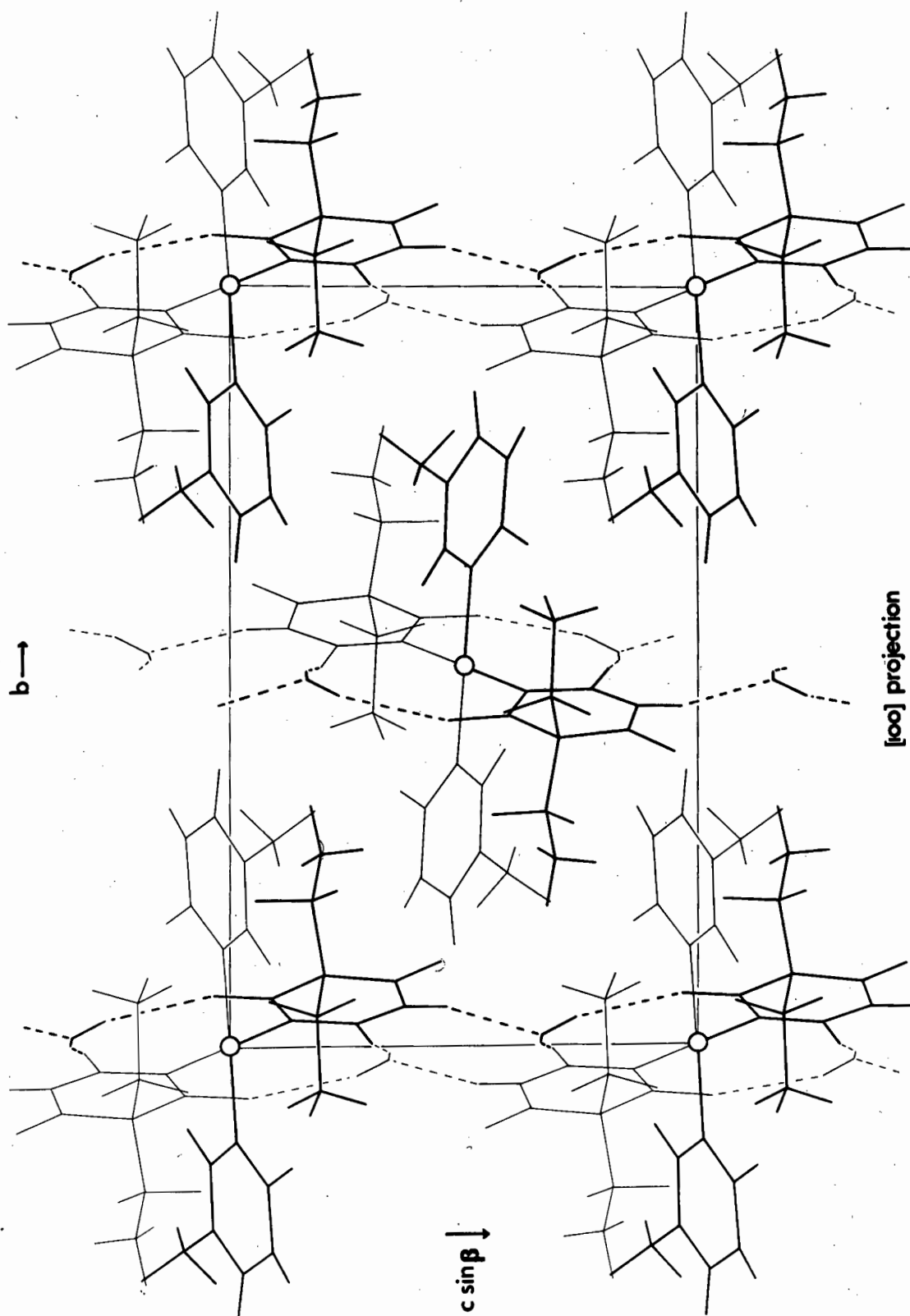
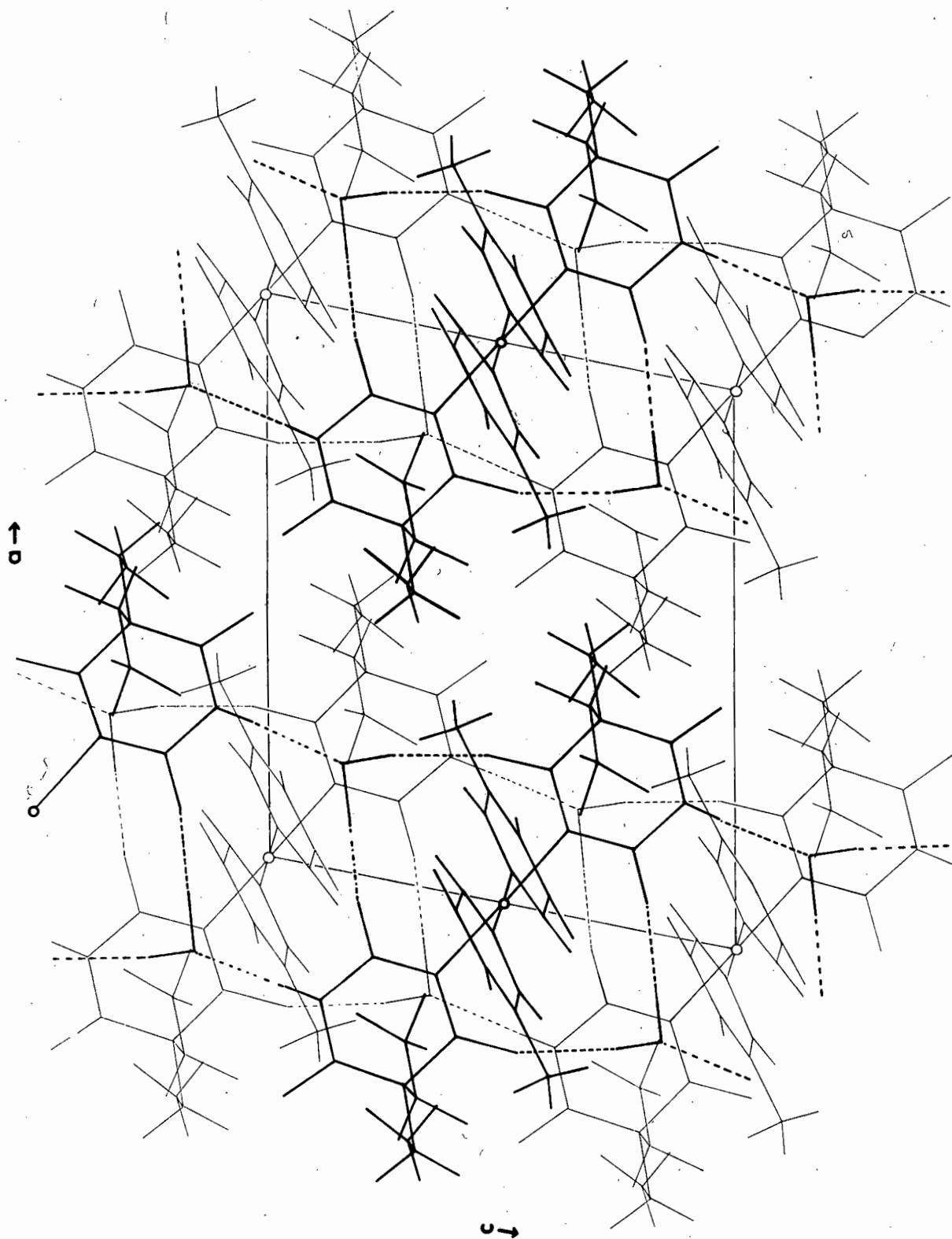
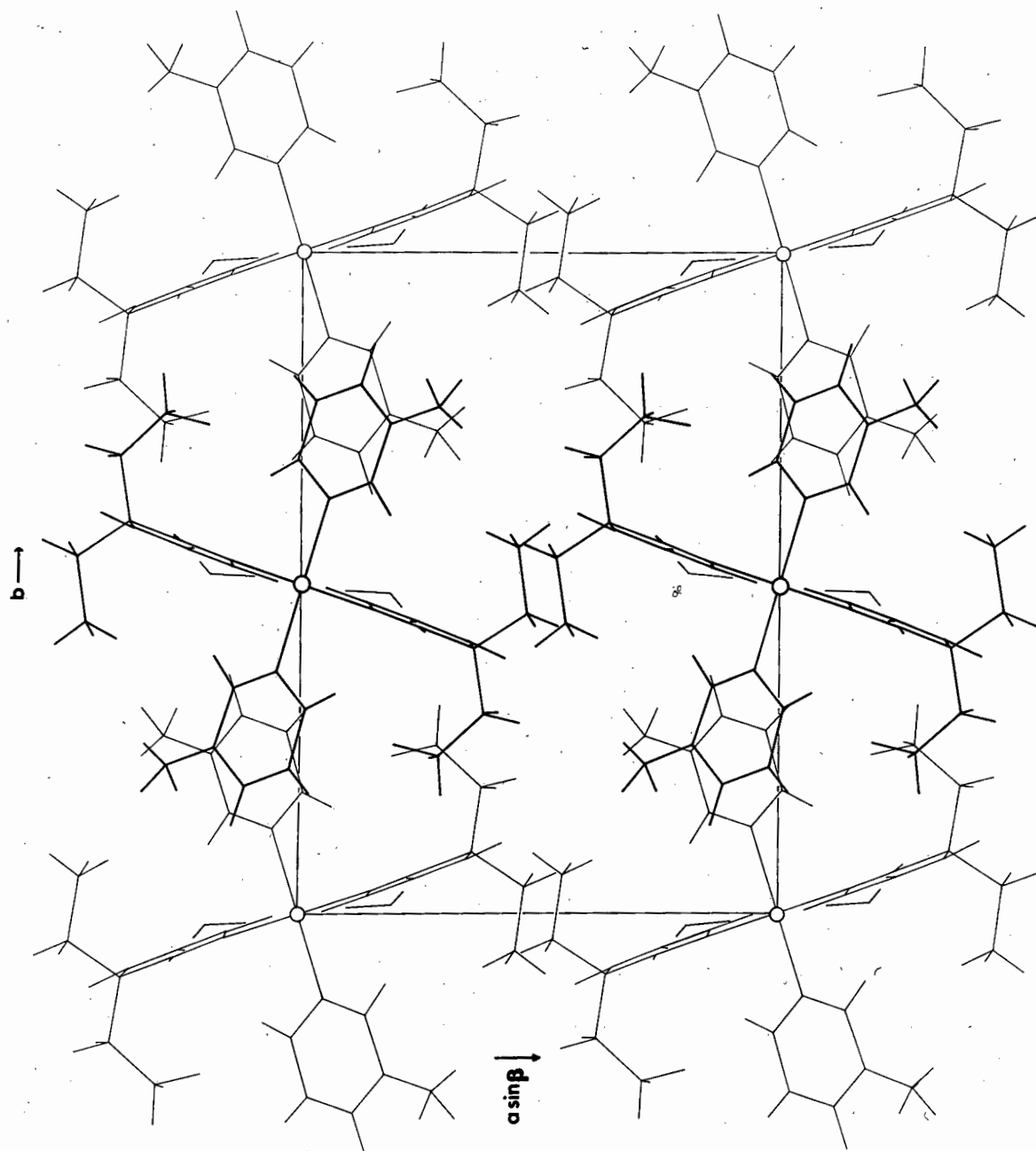


FIG. III.4.



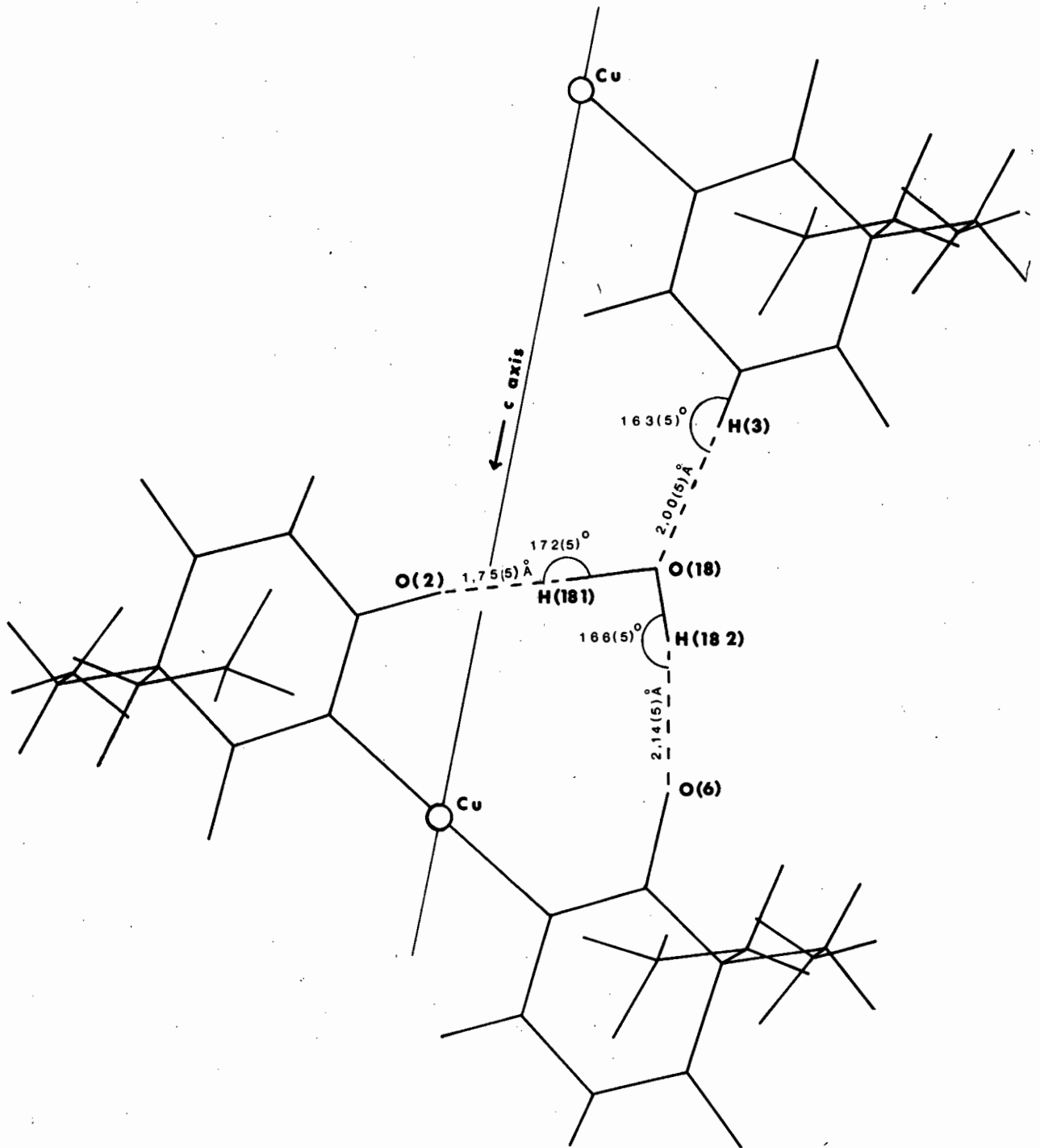
[100] projection

FIG. III.5.



[001] projection

FIG. III.6.



HYDROGEN-BONDING, LENGTHS AND ANGLES

FIG. III.7.

C H A P T E R   I V

THE CRYSTAL AND MOLECULAR STRUCTURE OF THE  
BIS-[5-ALLYL-5-(2-BROMOALLYL) BARBITURATO]-BISPYRIDINE  
DIHYDRATE COMPLEX OF COPPER (II).

## IV.1 CRYSTAL AND INTENSITY DATA

### Chemical Analysis

As with complex no. 1, water of crystallization was detected during the X-ray analysis. Table IV.1 lists the theoretical and experimentally determined analysis figures from which it can be seen that the complex has the composition  $\text{CuC}_{30}\text{H}_{28}\text{Br}_2\text{N}_6\text{O}_6 \cdot 2\text{H}_2\text{O}$  corresponding to the formulation  $\text{Cu(II)(brallobarbital)}_2(\text{pyridine})_2 \cdot 2\text{H}_2\text{O}$ .

TABLE IV.1

	%C	%H	%N
Theoretical (anhydrous) :	45,48	3,53	10,61
Theoretical (dihydrate) :	43,51	3,87	10,15
Experimentally determined :	45,2	3,8	10,3

### Density of Crystals

The density was measured and found to be  $1,54 \text{ g cm}^{-3}$ . This value, together with preliminary unit cell parameters was used to calculate the number of molecules per unit cell as 1.

### Space Group

No systematic absences on zero and upper level Weissenberg photographs indicated that the unit cell was triclinic and that the space group was either  $P1$  or  $P\bar{1}$ .

### Unit Cell Parameters

A crystal of dimensions  $0,18 \times 0,28 \times 0,20 \text{ mm}$  was selected for the determination of the unit cell parameters and the diffractometer data collection. The crystal data is given in Table IV.2.

TABLE IV.2 CRYSTAL DATA

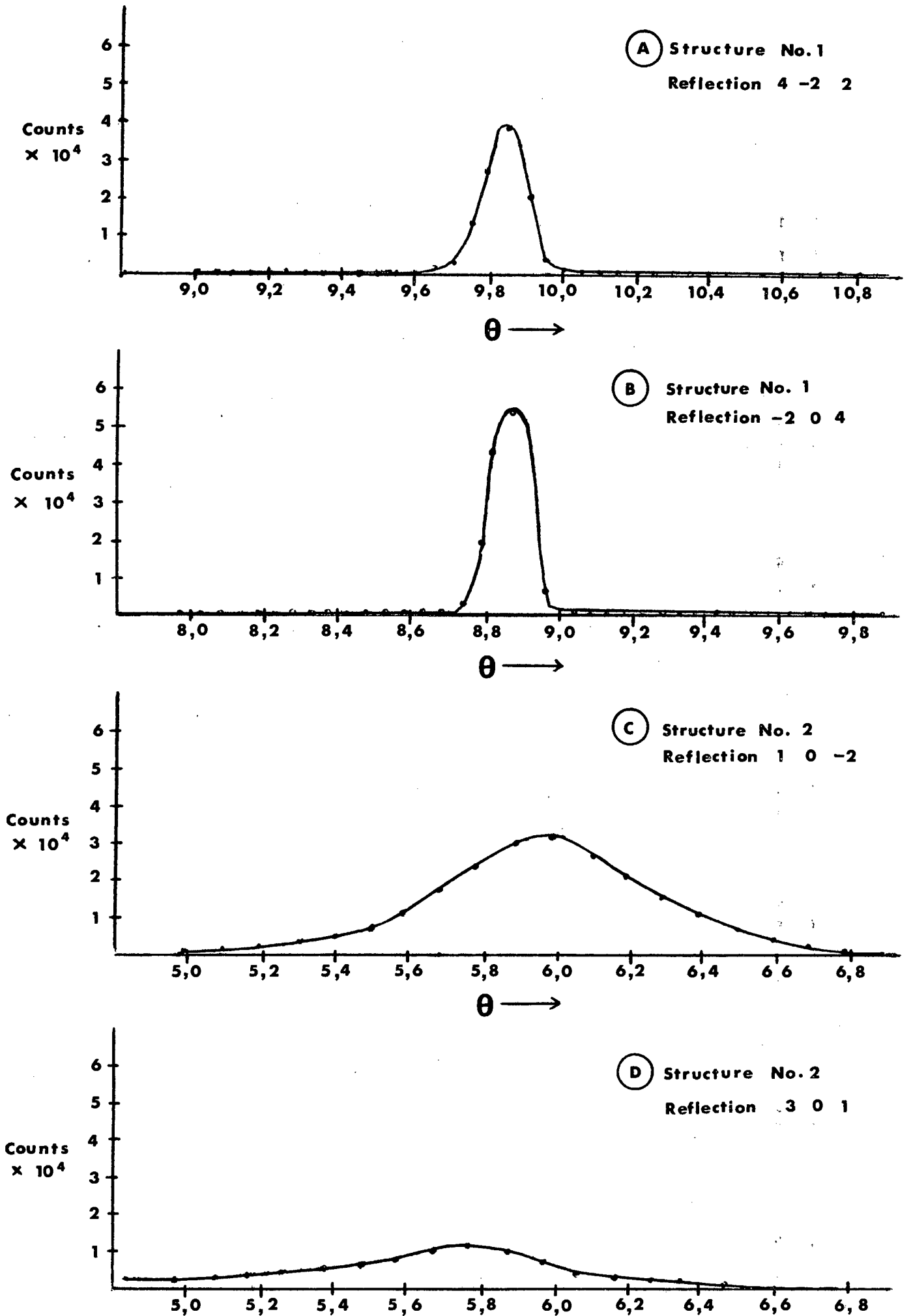
$a = 11,046(16) \text{ \AA}$	$V = 847,30 \text{ \AA}^3$
$b = 9,807(15) \text{ \AA}$	$D_M = 1,54 \text{ g cm}^{-3}$
$c = 8,503(19) \text{ \AA}$	$D_C = 1,62 \text{ g cm}^{-3}$ for $Z=1$
$\alpha = 106,8(2)^\circ$	$\mu = 30,66 \text{ cm}^{-1}$ for $\text{MoK}\alpha$
$\beta = 74,2(3)^\circ$	Space group = triclinic, $P\bar{1}$
$\gamma = 97,3(2)^\circ$	$F(000) = 388.$

### Intensity data

Preliminary measurements on other crystals of this complex as well as the one finally used for the data collection showed that they were of inferior quality as they diffracted poorly. Fig. IV.1 shows the intensity profiles (A and B) for two strong reflections in complex no. 1,  $\text{Cu}(\text{barbital})_2(\beta\text{-pic})_2 \cdot 2\text{H}_2\text{O}$ , as compared with two strong reflections (C and D) in the present complex,  $\text{Cu}(\text{brallobarbital})_2(\text{pyridine})_2 \cdot 2\text{H}_2\text{O}$ . It can be readily seen that the resolution of the latter two intensity peaks is much lower than that of the former two. Despite the obvious poor quality of the crystals it was nevertheless decided to complete the data collection and attempt the structural determination. It was hopefully anticipated that this structure would be of particular interest with regard to the nature of the hydrogen bonding in view of the presence of the electronegative bromine atom in the barbiturate side chain. Moreover, the extreme difficulty experienced in obtaining crystalline complexes of the general type  $\text{M}(\text{II})(\text{barb})_2\text{L}_2$  made it necessary to accept whatever crystals could be successfully grown.

The diffractometer scan width was  $1,40^\circ$  and the scan speed  $0,04^\circ\text{sec}^{-1}$ . The background and scan times were both 60 seconds. A total of 1037 independent reflections were measured up to  $2\theta = 36^\circ$  using graphite monochromated  $\text{MoK}\alpha$  radiation. However, adopting the aforementioned criterion for an observed

# FIG. IV.1 INTENSITY PROFILES



reflection, 383 of the measured reflections were omitted as unobserved. During the data collection process three reference reflections were recorded every hour. The intensities of these standard reflections remained constant to within  $\pm 5\%$  throughout the run. Thus the crystal of this complex was not quite as stable as that used for complex no. 1.

The linear absorption coefficient  $\mu$ , for  $\text{MoK}\alpha$  radiation was determined as  $30,66 \text{ cm}^{-1}$ . The variation in  $\mu R$  for the crystal used in the data collection process was between 0,28 and 0,52 with corresponding absorption corrections 1,60 and 2,27 for the  $\theta$  range scanned. Although this is significant, the absorption corrections were not applied in view of the poor quality of the reflection data.

## IV.2 SOLUTION AND REFINEMENT OF THE STRUCTURE

A Patterson synthesis was calculated and the map was scanned for the Br-Br, Cu-Cu and Br-Cu interactions. The peaks in the map, however, were not well defined and were smeared over large areas. Despite repeated attempts at interpreting the map, the Patterson could not be solved. On the assumption however that the space group was  $P\bar{1}$ , symmetry considerations required the copper atom to be located at the origin. An electron density map phased on copper in this position was accordingly computed and all the non hydrogen atoms of the structure were located therein. The map clearly indicated the position of the bromine atom. The parameters were then refined by a full-matrix least-squares method. After 5 cycles of isotropic refinement (ORFLS : XRAY67)<sup>33</sup>, the residual factor R dropped from 0,50 to a terminal value of 0,22. The isotropic temperature factor for the bromine atom had settled at a significantly high value of  $B = 27 \text{ \AA}^2$ . At this stage a difference electron density map revealed one large unassigned peak as well as other peaks in the vicinity of the heavy atoms. The large peak was attributed to the oxygen atom, O(W), of a water molecule. Refinement was continued with the introduction of anisotropic temperature factors. These were of the same form as those used in the refinement of complex no. 1. It is realised that the relatively small number of observed reflections (654) did not validate the anisotropic refinement in which a total of 217 parameters were varied. For efficient refinement the number of reflections should be approximately five times as large as the number of parameters varied. Thus, for the refinement of the structure of  $\text{Cu}(\text{brallobarbital})_2(\text{pyridine})_2 \cdot 2\text{H}_2\text{O}$ , there should be a minimum of 1100 reflections. The anisotropic refinement was carried out, nevertheless, in order to improve the residual factor and to account for the obviously anisotropic behaviour of the atoms particularly those in the barbiturate side chains.

During the refinement process the atoms of the barbiturate side chains tended to drift by large amounts from their positions as determined in the electron density map. Several attempts were made to locate unequivocally the accurate positions of atoms C(9), C(10), C(11) and C(12) in these chains. Difference electron density maps, computed at various stages of the refinement process however, showed this region to be a smear of electron density with no well defined atom peaks. It was subsequently decided to place these atoms by accurate models and in the final refinement their positional parameters were allowed to vary while their thermal parameters were held constant. The refinement was terminated when the average e.s.d. in the positional and anisotropic temperature factors was about three times the average parameter shift. The final R value was 0,108. No attempt was made to locate the hydrogen atoms of the structure. A final difference electron density map was characterized by several "pockets" of low electron density but no distinct features were discernable.

The final atomic positional and thermal parameters are listed in Table IV.3 while the observed and calculated structure factors are listed in Table IV.4.

TABLE IV.3

FRACTIONAL ATOMIC COORDINATES ( $\times 10^3$ ) AND THERMAL PARAMETERS ( $\times 10^3$ ) AND THEIR RESPECTIVE e.s.d's.

ATOM	X	Y	Z	$\beta_{11}$	$\beta_{22}$	$\beta_{33}$	$\beta_{12}$	$\beta_{23}$	$\beta_{31}$
Cu	0	0	0	8(1)	2(1)	15(1)	0(1)	1(1)	2(1)
N(1)	93(3)	199(3)	34(3)	10(4)	12(5)	17(5)	-4(3)	-1(4)	3(4)
C(2)	48(4)	313(4)	17(4)	15(5)	2(5)	21(6)	1(6)	3(5)	3(6)
N(3)	119(3)	441(3)	42(4)	16(4)	14(5)	31(8)	-4(4)	-7(5)	-1(4)
C(4)	212(5)	440(4)	104(4)	28(6)	7(7)	10(8)	-8(6)	-2(6)	6(6)
C(5)	288(4)	315(3)	123(6)	11(5)	12(5)	51(12)	-5(5)	6(6)	6(7)
C(6)	187(3)	171(4)	92(3)	4(4)	20(7)	12(7)	0(5)	-1(4)	-1(5)
O(2)	-42(3)	319(2)	-36(3)	18(3)	10(3)	35(6)	4(3)	-7(4)	6(4)
O(4)	298(2)	557(3)	133(3)	17(4)	14(4)	54(7)	-1(3)	4(4)	7(4)
O(6)	212(3)	68(2)	123(3)	26(4)	15(4)	37(5)	13(3)	4(3)	8(4)
C(7)	306(7)	338(6)	331(9)	51(12)	-1(13)	110(19)	-6(10)	-48(13)	27(12)
C(8)	161(8)	388(6)	464(8)	51(12)	1(13)	45(19)	16(11)	-11(15)	-34(12)
* C(9)	80(3)	345(3)	506(3)	7	9	13	0	-2	3
* C(10)	416(7)	271(7)	3(8)	35	45	64	2	12	14
* C(11)	466(4)	170(6)	-122(8)	19	36	74	7	12	3
* C(12)	445(4)	40(5)	-235(7)	19	36	74	7	12	3
O(W)	301(3)	436(2)	630(3)	28(5)	17(3)	44(7)	-3(3)	-14(5)	8(4)
N(14)	107(3)	-52(3)	-233(4)	17(4)	12(4)	19(10)	2(4)	1(5)	3(5)
C(15)	96(4)	10(5)	-349(7)	31(7)	31(8)	15(11)	-8(5)	-9(7)	6(7)
C(16)	152(7)	-11(5)	-527(7)	36(11)	10(7)	42(15)	2(8)	8(9)	8(8)
C(17)	231(5)	-115(6)	-575(5)	26(8)	25(8)	45(11)	-3(6)	-7(7)	20(8)
C(18)	256(4)	-203(4)	-476(6)	19(6)	16(7)	57(11)	6(5)	8(8)	-11(7)
C(19)	179(4)	-165(4)	-286(6)	16(5)	14(6)	39(16)	1(5)	7(8)	14(7)
Br	395(1)	308(2)	-299(1)	39(2)	127(5)	85(4)	-8(3)	11(2)	-21(4)

\* The thermal parameters of these atoms were not varied in the final stages of the refinement.

TABLE IV.4  
OBSERVED AND CALCULATED STRUCTURE FACTORS

10FO 10FC	10FO 10FC	10FO 10FC	10FO 10FC	10FO 10FC	10FO 10FC	10FO 10FC	10FO 10FC	10FO 10FC	10FO 10FC	10FO 10FC	10FO 10FC	
M=0-6 0 187 11b 1 173 107 2 232 70c 3 124 119 4 147 159 5 205 196	M=3-4 0 819 31j 1 249 25i 2 232 70c 3 124 119 4 147 159 5 205 196	M=7-5 0 171 16b 1 249 25i 2 232 70c 3 124 119 4 147 159 5 205 196	M=6-1 0 134 12i 1 249 25i 2 232 70c 3 124 119 4 147 159 5 205 196	M=5-1 0 134 12i 1 249 25i 2 232 70c 3 124 119 4 147 159 5 205 196	M=4-1 0 134 12i 1 249 25i 2 232 70c 3 124 119 4 147 159 5 205 196	M=3-1 0 134 12i 1 249 25i 2 232 70c 3 124 119 4 147 159 5 205 196	M=2-1 0 134 12i 1 249 25i 2 232 70c 3 124 119 4 147 159 5 205 196	M=1-1 0 134 12i 1 249 25i 2 232 70c 3 124 119 4 147 159 5 205 196	M=0-1 0 134 12i 1 249 25i 2 232 70c 3 124 119 4 147 159 5 205 196	M=0-2 0 134 12i 1 249 25i 2 232 70c 3 124 119 4 147 159 5 205 196	M=0-3 0 134 12i 1 249 25i 2 232 70c 3 124 119 4 147 159 5 205 196	M=0-4 0 134 12i 1 249 25i 2 232 70c 3 124 119 4 147 159 5 205 196

### IV.3 DESCRIPTION OF THE STRUCTURE

The structure of the molecule is shown in Fig. IV.2 (ORTEP PROGRAM<sup>36</sup>). The intramolecular bond lengths and angles and their associated e.s.d's. are given in Tables IV.5 and IV.6 respectively. These parameters were calculated with the program ORFFE<sup>33</sup>. Table IV.7 lists the equations of several least-squares planes through certain atoms and the perpendicular distances of various atoms from these planes (program : L S PLANE).

#### The Copper Coordination Sphere

As with the previous structure (no. 1), the copper atom is coordinated to the barbiturate anions via their deprotonated nitrogen atoms N(1) and N(1<sup>i</sup>) and to the pyridine moieties via their nitrogen atoms N(14) and N(14<sup>i</sup>) in square planar arrangement (plane I, Table IV.7). The respective Cu-N bond lengths of 2,06(2) and 1,97(3) Å are in reasonable agreement with the 1,980(5) and 2,018(3) Å found in structure no. 1 and the 1,983(5) and 2,032(5) Å reported by Caira *et al*<sup>27</sup>. The bond angles N(1)-Cu-N(14) and N(1)-Cu-N(14<sup>i</sup>) are 88,5(9) and 91,5(9)° respectively, indicating square planar geometry. However, off-the-z-axis coordination between the metal atom and a barbiturate oxygen atom is again evident. This time it is O(6) and O(6<sup>i</sup>) that are involved in the interaction, the Cu-O distance being 2,75(3) Å which agrees favourably with the 2,857(4) Å found in structure no. 1 and the 2,722(5) Å found in Cu(barbital)<sub>2</sub>(pyridine)<sub>2</sub><sup>27</sup>. A second, weaker interaction between Cu and oxygen atoms O(2) and O(2<sup>i</sup>) is again detectable. The Cu-O(2) separation of 3,33(2) Å is slightly larger than the 3,149 Å (structure no. 1) and 3,234(7) Å (Caira<sup>27</sup>) previously observed.

In the pyridine moiety the C-C and C-N bond lengths are within the expected ranges. The average C-C bond length within the ring is 1,44 Å. The ring is planar (plane IV), the greatest deviation from the least-squares plane

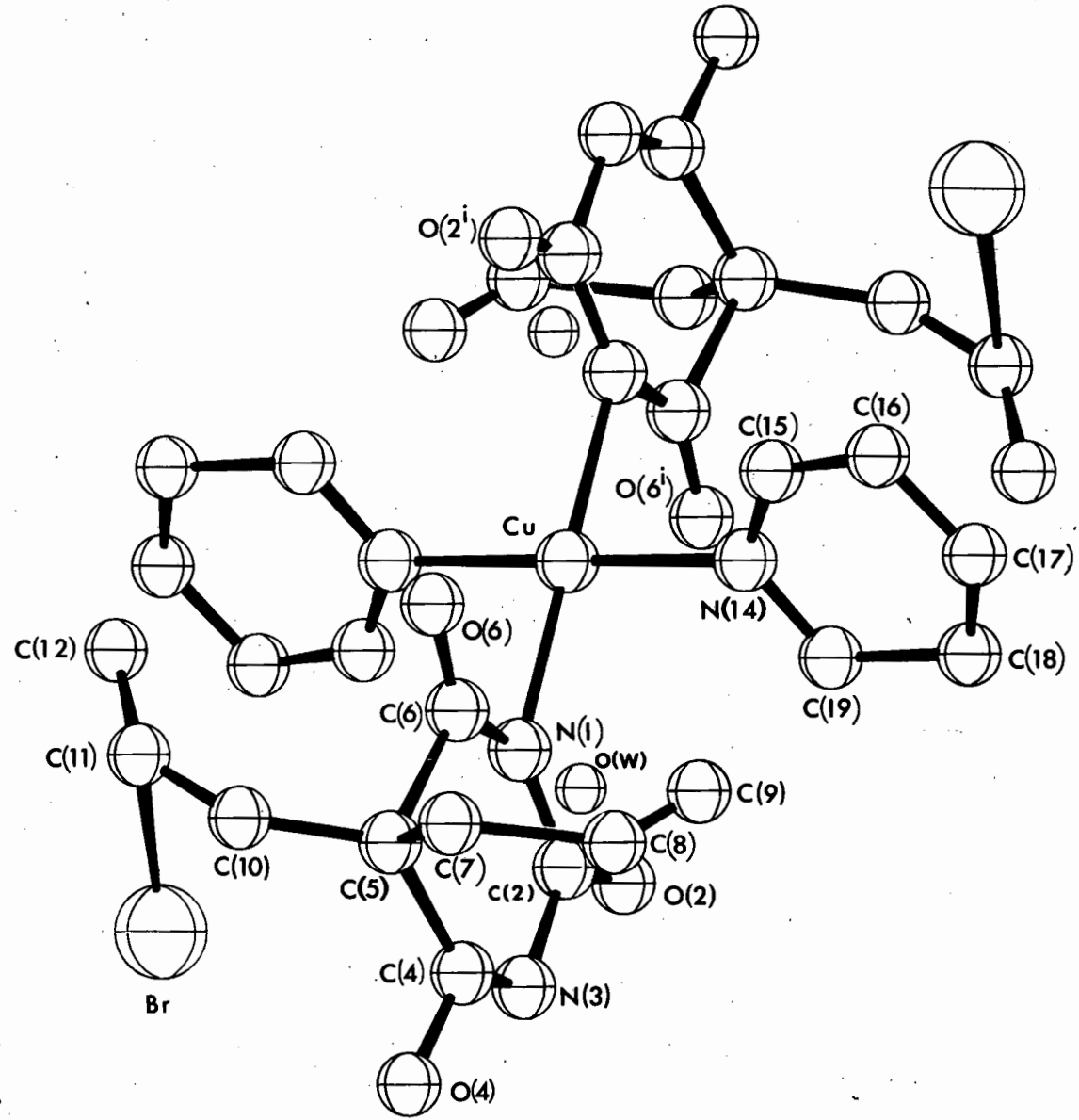


FIG. IV.2.

TABLE IV.5'

INTRAMOLECULAR BOND LENGTHS AND THEIR e.s.d's. in Å

Cu-N(1)	2,06(2)	C(8)-C(9)	0,96(7)
N(1)-C(2)	1,34(4)	C(5)-C(10)	1,53(8)
C(2)-N(3)	1,38(4)	C(10)-C(11)	1,27(7)
N(3)-C(4)	1,27(4)	C(11)-C(12)	1,39(6)
C(4)-C(5)	1,64(5)	C(11)-Br	2,61(6)
C(5)-C(6)	1,68(5)	Cu-N(14)	1,97(3)
C(6)-N(1)	1,35(4)	N(14)-C(15)	1,34(5)
C(2)-O(2)	1,21(4)	C(15)-C(16)	1,43(5)
C(4)-O(4)	1,40(4)	C(16)-C(17)	1,32(6)
C(6)-O(6)	1,19(4)	C(17)-C(18)	1,46(5)
C(5)-C(7)	1,78(7)	C(18)-C(19)	1,56(5)
C(7)-C(8)	1,72(8)	C(19)-N(14)	1,34(4)

TABLE IV.6

INTRAMOLECULAR BOND ANGLES (IN DEGREES)

N(1)-Cu-N(14)	88,5(9)	C(6)-C(5)-C(7)	105(3)
N(1)-Cu-N(14 <sup>1</sup> )	91,5(9)	C(5)-C(7)-C(8)	105(3)
Cu-N(1)-C(2)	123(3)	C(7)-C(8)-C(9)	140(7)
N(1)-C(2)-N(3)	118(4)	C(7)-C(5)-C(10)	106(4)
C(2)-N(3)-C(4)	115(4)	C(6)-C(5)-C(10)	107(3)
N(3)-C(4)-C(5)	134(4)	C(5)-C(10)-C(11)	141(6)
C(4)-C(5)-C(6)	103(3)	C(10)-C(11)-C(12)	146(6)
C(5)-C(6)-N(1)	111(3)	C(10)-C(11)-Br	84(4)
C(6)-N(1)-C(2)	137(3)	C(12)-C(11)-Br	91(4)
Cu-N(1)-C(6)	99(2)	Cu-N(14)-C(15)	121(3)
N(1)-C(2)-O(2)	129(3)	N(14)-C(15)-C(16)	134(5)
O(2)-C(2)-N(3)	113(4)	C(15)-C(16)-C(17)	107(5)
N(3)-C(4)-O(4)	124(3)	C(16)-C(17)-C(18)	129(4)
O(4)-C(4)-C(5)	100(3)	C(17)-C(18)-C(19)	114(3)
C(5)-C(6)-O(6)	116(4)	C(18)-C(19)-N(14)	117(4)
O(6)-C(6)-N(1)	133(3)	C(19)-N(14)-C(15)	118(4)
C(4)-C(5)-C(7)	115(3)	Cu-N(14)-C(19)	121(3)

TABLE IV.7

## LEAST-SQUARES PLANES

The equations of the planes are expressed in  
orthogonalized space as  $PI + QJ + RK = S$

Plane I	square planar coordination around the copper atom								
Atoms defining the plane	Cu	N(1)	N(14)	N(1 <sup>1</sup> )	N(14 <sup>1</sup> )				
Atoms not included in the plane						0(2)	0(6)		
Distance from the plane, Å	0,00	0,00	0,00	0,00	0,00	-2,27	2,28		
Equation	$0,84091I - 0,33226J + 0,42717K = 0,00$								
Plane II	through the six atoms of the pyrimidine ring								
Atoms defining the plane	N(1)	C(2)	N(3)	C(4)	C(5)	C(6)			
Atoms not included in the plane							0(2)	0(4)	0(6)
Distance from the plane, Å	-0,03	0,01	-0,04	0,07	-0,06	0,05	-0,05	-0,01	0,17
Equation	$-0,30375I + 0,22544J + 0,92569K = -0,02911$								
Plane III	through the nine atoms of the trioxypyrimidine ring								
Atoms defining the plane	N(1)	C(2)	N(3)	C(4)	C(5)	C(6)	0(2)	0(4)	0(6)
Distance from the plane, Å	-0,06	0,03	-0,01	0,08	-0,11	-0,01	-0,01	0,01	0,07
Equation	$-0,32033I + 0,24811J + 0,91424K = 0,02807$								
Plane IV	through the six atoms of the pyridine ring								
Atoms defining the plane	N(14)	C(15)	C(16)	C(17)	C(18)	C(19)			
Distance from the plane, Å	0,04	0,00	-0,02	0,02	0,04	-0,04			
Equation	$0,7624I + 0,64514J + 0,05049K = 0,10129$								
Plane V	through some atoms of the barbiturate side chain and C(5)								
Atoms defining the plane	C(5)	C(7)	C(8)	C(10)					
Distance from the plane, Å	0,00	0,00	0,00	0,00					
Equation	$0,18862I + 0,96126J - 0,20099K = 3,38177$								

## INTERSECTION ANGLES

Planes I and II : 86,3°      Planes II and III : 1,7°  
 Planes I and III : 87,8°      Planes II and IV : 87,7°  
 Planes I and IV : 63,4°      Planes III and IV : 89,7°

through the six atoms being that of atom C(19) at a distance of 0,04 Å. This plane and the square plane about the copper atom, plane I, intersect at 63,4°.

#### The barbitol ligand structure

The six atoms of the pyrimidine ring define a plane (plane II) with the largest deviation from this plane being that of atom C(4) at a distance of 0,07 Å. The planarity is retained when the three oxygen atoms are included in the least squares plane calculation (plane III), the largest deviation being that of atom C(5) at a distance of 0,11 Å. The small intersection angle (1,7°) of planes II and III is an indication of their coplanarity.

The bond lengths and angles within the barbiturate ring show only fair agreement with expected figures while in the side chains attached at C(5), the agreement with expected figures is disappointingly poor. This is attributable to the poor quality of the crystal used and the difficulty encountered in anchoring the atoms of the side chains during the refinement process.

The planes through the two different moieties of the molecule, (planes II and IV) are virtually perpendicular to each other (87,7°) as are the planes through the trioxypyrimidine ring (plane III) and the spine of the side chain attached at C(5) (plane V) which intersect at an angle 89,7°. These two features of the structure were also observed in complex no. 1.

Although the hydrogen atoms of the structure were not located in the Fourier syntheses, the structure was examined for possible N ... O and N ... Br interactions (2,9 and 4,0 Å respectively). No such interactions were evident thereby precluding the possibility of a hydrogen bonded network. The bromine atom in the 1:1 complex of 9-ethyladenine with 5-isopropyl-5-bromoallyl barbituric acid does also not participate in any hydrogen bonding<sup>85</sup>. However, hydrogen bonding is nevertheless present in the latter structure.

The [100] and [001] projections of the structure are shown in Figs. IV.3 and IV.4 respectively.

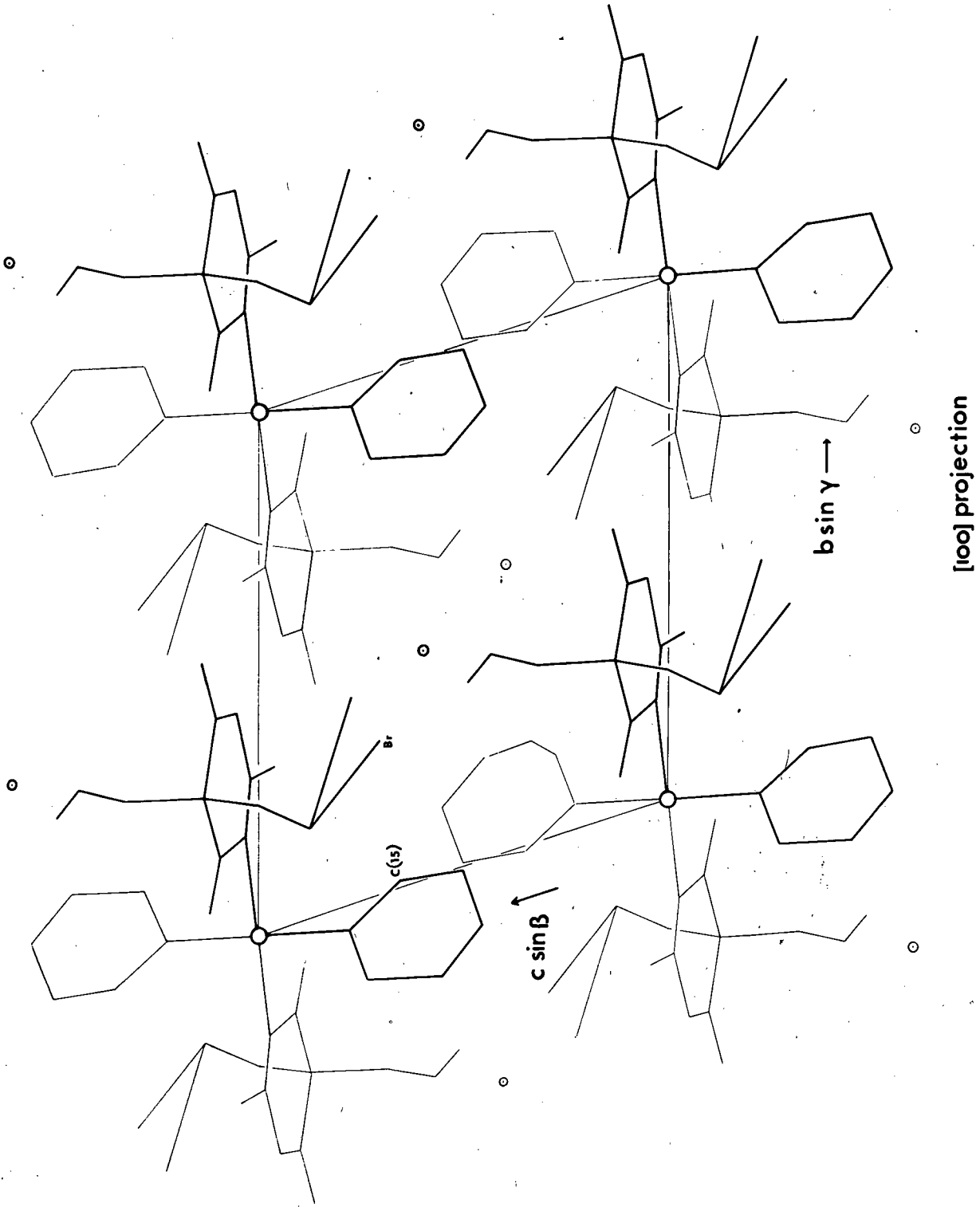


FIG. IV.3.

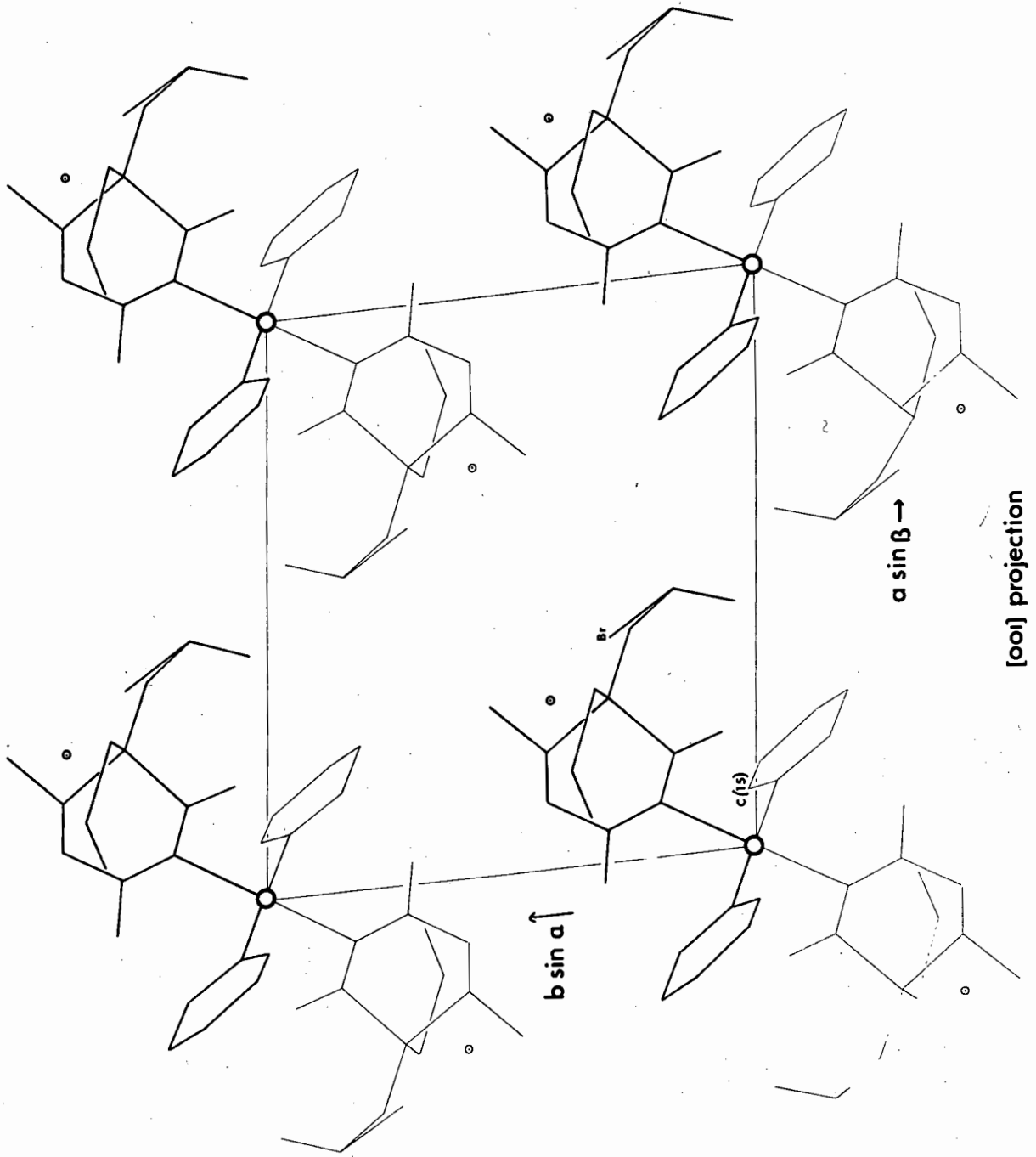


FIG. IV.4.

Comment

Despite the failure of the structure to refine satisfactorily, its elucidation to an R value of 0,108 has yielded several important results with respect to studies of  $M(II)(\text{barb})_2L_2$  complexes. The structure has revealed that coordination of the metal to the barbiturate is again effected via the deprotonated nitrogen atom of the barbiturate ligand. Also, the recurrence of off-the-z-axis coordination in this structure would seem to indicate a tendency for pseudo or distorted octahedral geometry to exist in  $\text{Cu}(\text{barb})_2(\text{pyridine})_2$  complexes. Finally, the orientation of the spine of the barbiturate side chain at right angles to the pyrimidine plane is consistent with that observed in the structures of common barbiturates.

CHAPTER V

THE CRYSTAL AND MOLECULAR STRUCTURE OF THE  
BIS-(5,5 -DIETHYLBARBITURATO)-BIS-(PICOLINE) COMPLEX OF Zn(II).

## V.1 CRYSTAL AND INTENSITY DATA

### Chemical Analysis

The theoretical and experimentally determined analysis figures listed in Table V.1 show that the complex has the composition  $\text{ZnC}_{28}\text{H}_{36}\text{N}_6\text{O}_6$  corresponding to the formulation  $\text{Zn(II)(5,5 -diethylbarbiturato)}_2(\beta\text{-picoline})_2$

TABLE V.1

		%C	%H	%N
Theoretical	:	54,42	5,83	13,60
Experimentally determined	:	54,1	5,8	13,8

### Density of Crystals

The density was measured and found to be  $1,36(2) \text{ g cm}^{-3}$ . From preliminary values for the unit cell parameters, the number of molecules per unit cell was calculated as 2.

### Space Group

Inspection of zero and upper level Weissenberg photographs about the three crystallographic axes revealed no systematic absences from which it was concluded that the unit cell was triclinic and that the space group was  $\text{P}\bar{1}$ .

### Unit Cell Parameters

A single crystal of dimensions  $0,25 \times 0,25 \times 0,38 \text{ mm}$  was used for determining the unit cell dimensions and for the collection of intensity data on the diffractometer. The crystal data is listed in Table V.2 overleaf.

TABLE V.2 CRYSTAL DATA

$a = 13,013(5) \text{ \AA}$	$V = 1509,16 \text{ \AA}^3$
$b = 11,748(5) \text{ \AA}$	$D_M = 1,37(2) \text{ g cm}^{-3}$
$c = 10,842(5) \text{ \AA}$	$D_C = 1,341 \text{ g cm}^{-3}$ for $Z=2$
$\alpha = 114,4 (2)^\circ$	$\mu(\text{MoK}\alpha) = 8,92 \text{ cm}^{-1}$
$\beta = 90,9 (2)^\circ$	$F(000) = 648$
$\gamma = 90,3 (2)^\circ$	space group = triclinic, $P\bar{1}$

Intensity Data

The diffractometer scan width was  $1,20^\circ$  and the scan speed  $0,04^\circ \text{ sec}^{-1}$ . The background and scan times were both 30 seconds. Altogether 3687 reflections up to  $2\theta = 44^\circ$  were measured. Applying the same criterion as before, 344 were omitted as unobserved.

The linear absorption coefficient for  $\text{MoK}\alpha$  radiation was determined as  $8,92 \text{ cm}^{-1}$ . Absorption corrections were not applied to the intensity data as the variation in  $\mu R$  for the particular crystal used was between 0,11 and 0,20 with corresponding  $A^*$  values of 1,18 and 1,40 for the  $\theta$  range scanned<sup>32</sup>. This was regarded as insignificant.

## V.2 SOLUTION AND REFINEMENT OF THE STRUCTURE

The position of the zinc atom was determined from a three dimensional Patterson map (CENTROSY PROGRAM) in which the zinc-zinc interaction at  $2x$ ,  $2y$ ,  $2z$  was easily detectable. From the subsequent Fourier synthesis phased on the position of the zinc atom alone all 41 non hydrogen atoms of the molecule were located. Each reflection was assigned unit weight. Before refinement the conventional R factor was 0,245. After three cycles, the isotropic refinement (CRYLSQ : XRAY72)<sup>40</sup> terminated at an R value of 0,089. Anisotropic temperature factors were then introduced and after 2 cycles of refinement R dropped to 0,054. For the anisotropic refinement the thermal parameters were of the form

$$T = \exp[-2\pi^2(U_{11}h^2a^{*2} + U_{22}k^2b^{*2} + U_{33}l^2c^{*2} + 2U_{12}hka^*b^* + 2U_{13}hla^*c^* + 2U_{23}k\ell b^*c^*)]$$

Before computing difference syntheses to locate the hydrogen atoms of the molecule, the program BONDAT<sup>40</sup> was used to calculate the theoretical positions of these atoms. In the subsequent difference Fourier, 30 of the 36 hydrogen atom peaks were easily found. The 6 atoms not located in this map were those of the  $\beta$ -methyl groups C(17) and C(34). However, these appeared in the following difference synthesis which was phased on 71 atoms. The hydrogens were assigned the isotropic temperature factors of the atoms to which they were bonded. After a further 4 cycles of non-hydrogen refinement, the average e.s.d. in the positional and anisotropic temperature factors was about twelve times the average parameter shift. The hydrogen atom positions were then varied for 3 cycles after which the average e.s.d. in these parameters was about three times the average parameter shift. The last cycle of refinement yielded an R of 0,029. A final difference electron density map was practically featureless.

In the structure factor calculations, scattering factors for the zinc, carbon, nitrogen and oxygen atoms were those obtained from Cromer and Mann<sup>41</sup>. For the hydrogen atoms the scattering factors used were those of Stewart et al<sup>42</sup>. The zinc was treated as Zn<sup>0</sup> and the anomalous dispersion correction ( $\Delta f' = 0,3$  for MoK $\alpha$  radiation)<sup>35</sup> was applied.

The final atomic positional and thermal parameters for the non hydrogen atoms are listed in Table V.3. The final atomic positional parameters for the hydrogen atoms are given in Table V.4. Table V.5 which lists the observed and calculated structure factors was obtained with the aid of the program LISTFC<sup>40</sup>.

TABLE V.3

## NON-HYDROGEN ATOMS

FRACTIONAL ATOMIC COORDINATES AND THEIR E.S.D.'S ( $\times 10^4$ ) ANDANISOTROPIC TEMPERATURE FACTORS AND THEIR E.S.D.'S ( $\times 10^3$ )

Atom	X	Y	Z	$U_{11}$	$U_{22}$	$U_{33}$	$U_{12}$	$U_{13}$	$U_{23}$
Zn	2266(0,3)	2347(0,3)	3761(0,3)	23(0,2)	23(0,2)	25(0,2)	- 3(0,1)	- 2(0,1)	11(0,2)
N (1)	1968 (2)	2109 (2)	5449 (2)	20 (1)	28 (1)	24 (1)	- 9 (1)	- 6 (1)	14 (1)
C (2)	1208 (2)	1269 (3)	5331 (3)	21 (2)	28 (2)	27 (2)	- 3 (1)	- 4 (1)	14 (1)
N (3)	1087 (2)	849 (2)	6340 (3)	29 (1)	43 (2)	35 (2)	-19 (1)	-11 (1)	25 (1)
C (4)	1703 (2)	1168 (3)	7474 (3)	34 (2)	47 (2)	36 (2)	- 8 (2)	- 6 (2)	26 (2)
C (5)	2554 (2)	2126 (3)	7681 (3)	30 (2)	44 (2)	30 (2)	-14 (2)	-14 (1)	20 (2)
C (6)	2581 (2)	2623 (3)	6581 (3)	27 (2)	32 (2)	29 (2)	- 7 (1)	- 2 (1)	13 (1)
C (7)	2405 (3)	3228 (4)	9072 (4)	80 (3)	62 (3)	33 (2)	-23 (2)	-15 (2)	20 (2)
C (8)	1407 (5)	3928 (5)	9192 (5)	134 (5)	83 (4)	56 (3)	29 (3)	23 (3)	14 (3)
C (9)	3594 (3)	1507 (4)	7678 (4)	37 (2)	80 (3)	73 (3)	- 9 (2)	-17 (2)	53 (3)
C(10)	3812 (3)	363 (5)	6412 (6)	58 (3)	103 (4)	106 (4)	33 (3)	17 (3)	66 (4)
O (2)	614 (2)	888 (2)	4349 (2)	32 (1)	53 (1)	35 (1)	-21 (1)	-14 (1)	25 (1)
O (4)	1571 (2)	702 (3)	8269 (3)	64 (2)	97 (2)	61 (2)	-37 (2)	-23 (1)	63 (2)
O (6)	3183 (2)	3471 (2)	6707 (2)	52 (2)	55 (2)	41 (1)	-36 (1)	-16 (1)	25 (1)
N(11)	3715 (2)	3051 (2)	3593 (2)	23 (1)	30 (1)	30 (1)	- 4 (1)	- 1 (1)	12 (1)
C(12)	4571 (2)	2865 (3)	4186 (3)	31 (2)	38 (2)	37 (2)	3 (2)	0 (2)	17 (2)
C(13)	5512 (2)	3326 (3)	4028 (3)	22 (2)	50 (2)	44 (2)	0 (2)	- 6 (2)	16 (2)
C(14)	5586 (2)	3986 (3)	3244 (3)	24 (2)	46 (2)	40 (2)	- 9 (2)	- 1 (1)	12 (2)
C(15)	4715 (2)	4171 (3)	2602 (3)	33 (2)	37 (2)	33 (2)	-11 (1)	- 2 (1)	13 (2)
C(16)	3803 (2)	3687 (3)	2817 (3)	26 (2)	36 (2)	32 (2)	- 7 (1)	- 6 (1)	14 (2)
C(17)	4754 (3)	4871 (4)	1714 (4)	52 (2)	84 (3)	78 (3)	-28 (2)	-13 (2)	57 (3)

TABLE V.3 CONTINUED

Atom	X	Y	Z	U <sub>11</sub>	U <sub>22</sub>	U <sub>33</sub>	U <sub>12</sub>	U <sub>13</sub>	U <sub>23</sub>
N(18)	2124 (2)	734 (2)	2140 (2)	26 (1)	27 (1)	25 (1)	- 2 (1)	- 5 (1)	8 (1)
C(19)	1279 (2)	404 (3)	1302 (3)	31 (2)	31 (2)	28 (2)	- 4 (1)	- 7 (1)	9 (1)
N(20)	1130 (2)	- 836 (2)	417 (3)	45 (2)	27 (2)	44 (2)	- 3 (1)	-24 (1)	2 (1)
C(21)	1770 (3)	-1788 (3)	262 (4)	67 (3)	27 (2)	42 (2)	- 2 (2)	-17 (2)	8 (2)
C(22)	2783 (3)	-1454 (3)	1061 (3)	46 (2)	27 (2)	37 (2)	4 (2)	- 5 (2)	12 (2)
C(23)	2829 (2)	- 117 (3)	2136 (3)	32 (2)	34 (2)	32 (2)	- 2 (1)	- 4 (1)	16 (2)
C(24)	2966 (3)	-2370 (3)	1730 (4)	76 (3)	38 (2)	68 (3)	- 1 (2)	-16 (2)	30 (2)
C(25)	2172 (5)	-2298 (5)	2744 (6)	125 (5)	100 (4)	105 (4)	-20 (3)	3 (4)	77 (4)
C(26)	3672 (3)	-1601 (4)	71 (4)	68 (3)	54 (2)	49 (2)	19 (2)	12 (2)	16 (2)
C(27)	3647 (4)	- 713 (4)	-609 (4)	74 (3)	86 (3)	60 (3)	9 (3)	17 (2)	38 (3)
O(19)	642 (2)	1173 (2)	1323 (2)	37 (1)	33 (1)	45 (1)	4 (1)	-20 (1)	2 (1)
O(21)	1554 (2)	-2860 (2)	-520 (3)	102 (2)	28 (1)	87 (2)	0 (1)	-46 (2)	1 (1)
O(23)	3526 (2)	209 (2)	2993 (2)	43 (1)	43 (1)	52 (2)	0 (1)	-22 (1)	17 (1)
N(28)	1488 (2)	3916 (2)	3870 (2)	26 (1)	28 (1)	33 (1)	0 (1)	4 (1)	15 (1)
C(29)	894 (3)	3960 (3)	2866 (3)	38 (2)	40 (2)	42 (2)	2 (2)	- 3 (2)	22 (2)
C(30)	440 (3)	5047 (4)	2966 (4)	55 (2)	55 (3)	62 (3)	16 (2)	- 4 (2)	34 (2)
C(31)	604 (3)	6126 (3)	4114 (4)	44 (2)	43 (2)	74 (3)	14 (2)	11 (2)	32 (2)
C(32)	1222 (2)	6116 (3)	5163 (4)	32 (2)	28 (2)	54 (2)	- 2 (1)	18 (2)	8 (2)
C(33)	1645 (2)	4976 (3)	4992 (3)	30 (2)	32 (2)	41 (2)	- 1 (1)	5 (1)	13 (2)
C(34)	1444 (4)	7279 (4)	6412 (4)	82 (3)	34 (2)	71 (3)	3 (2)	2 (2)	3 (2)

TABLE V.4  
 HYDROGEN ATOMS  
 FRACTIONAL ATOMIC CO-ORDINATES ( $\times 10^3$ )  
 AND THEIR E.S.D.'S ( $\times 10^3$ )

ATOM	X	Y	Z
H(3)	60(2)	32(3)	620(3)
H(7 1)	243(3)	287(3)	975(4)
H(7 2)	293(3)	382(3)	924(4)
H(8 1)	137(4)	427(4)	859(5)
H(8 2)	82(4)	325(4)	907(5)
H(8 3)	142(4)	460(4)	8(5)
H(9 1)	414(3)	217(3)	782(4)
H(9 2)	359(3)	132(3)	844(4)
H(10 1)	333(3)	-28(4)	627(4)
H(10 2)	379(3)	56(4)	570(4)
H(10 3)	448(3)	4(4)	643(4)
H(12)	449(2)	238(3)	469(3)
H(13)	609(2)	318(3)	445(3)
H(14)	622(2)	434(3)	315(3)
H(16)	318(2)	385(3)	246(3)
H(17 1)	430(3)	550(4)	199(4)
H(17 2)	539(3)	512(3)	161(4)
H(17 3)	456(3)	435(4)	86(4)
H(20)	62(2)	-100(3)	-11(3)
H(24 1)	302(3)	-329(3)	93(4)
H(24 2)	369(3)	-220(3)	215(4)
H(25 1)	205(4)	-140(5)	349(5)
H(25 2)	138(4)	-243(5)	237(5)
H(25 3)	233(4)	-285(5)	306(5)
H(26 1)	434(3)	-145(3)	55(4)
H(26 2)	366(3)	-247(3)	-58(4)
H(27 1)	302(3)	-75(4)	-99(4)
H(27 2)	371(3)	30(4)	17(4)
H(27 3)	427(3)	-89(4)	-113(4)
H(29)	78(2)	315(3)	206(3)
H(30)	-1(3)	515(3)	230(4)
H(31)	29(3)	695(3)	426(4)
H(33)	207(2)	487(3)	572(3)
H(34 1)	65(3)	777(4)	689(4)
H(34 2)	166(3)	704(4)	707(4)
H(34 3)	154(3)	797(4)	627(4)



F <sub>0</sub>		F <sub>1</sub>		F <sub>2</sub>		F <sub>3</sub>		F <sub>4</sub>		F <sub>5</sub>		F <sub>6</sub>		F <sub>7</sub>		F <sub>8</sub>		F <sub>9</sub>		F <sub>10</sub>		F <sub>11</sub>		F <sub>12</sub>		F <sub>13</sub>		F <sub>14</sub>		F <sub>15</sub>		F <sub>16</sub>		F <sub>17</sub>		F <sub>18</sub>		F <sub>19</sub>		F <sub>20</sub>		F <sub>21</sub>		F <sub>22</sub>		F <sub>23</sub>		F <sub>24</sub>		F <sub>25</sub>		F <sub>26</sub>		F <sub>27</sub>		F <sub>28</sub>		F <sub>29</sub>		F <sub>30</sub>		F <sub>31</sub>		F <sub>32</sub>		F <sub>33</sub>		F <sub>34</sub>		F <sub>35</sub>		F <sub>36</sub>		F <sub>37</sub>		F <sub>38</sub>		F <sub>39</sub>		F <sub>40</sub>		F <sub>41</sub>		F <sub>42</sub>		F <sub>43</sub>		F <sub>44</sub>		F <sub>45</sub>		F <sub>46</sub>		F <sub>47</sub>		F <sub>48</sub>		F <sub>49</sub>		F <sub>50</sub>		F <sub>51</sub>		F <sub>52</sub>		F <sub>53</sub>		F <sub>54</sub>		F <sub>55</sub>		F <sub>56</sub>		F <sub>57</sub>		F <sub>58</sub>		F <sub>59</sub>		F <sub>60</sub>		F <sub>61</sub>		F <sub>62</sub>		F <sub>63</sub>		F <sub>64</sub>		F <sub>65</sub>		F <sub>66</sub>		F <sub>67</sub>		F <sub>68</sub>		F <sub>69</sub>		F <sub>70</sub>		F <sub>71</sub>		F <sub>72</sub>		F <sub>73</sub>		F <sub>74</sub>		F <sub>75</sub>		F <sub>76</sub>		F <sub>77</sub>		F <sub>78</sub>		F <sub>79</sub>		F <sub>80</sub>		F <sub>81</sub>		F <sub>82</sub>		F <sub>83</sub>		F <sub>84</sub>		F <sub>85</sub>		F <sub>86</sub>		F <sub>87</sub>		F <sub>88</sub>		F <sub>89</sub>		F <sub>90</sub>		F <sub>91</sub>		F <sub>92</sub>		F <sub>93</sub>		F <sub>94</sub>		F <sub>95</sub>		F <sub>96</sub>		F <sub>97</sub>		F <sub>98</sub>		F <sub>99</sub>		F <sub>100</sub>																																																																																																																																																																																																																																																																																																																																																																																																																																																																																																																																																																																																																																																																																																																																																																																																																																																																																																																																																																																																									
4	422	424	-2	116	-119	10	574	570	-4	1004	1000	-4	1704	1700	-4	2404	2400	-4	3104	3100	-4	3804	3800	-4	4504	4500	-4	5204	5200	-4	5904	5900	-4	6604	6600	-4	7304	7300	-4	8004	8000	-4	8704	8700	-4	9404	9400	-4	10104	10100	-4	10804	10800	-4	11504	11500	-4	12204	12200	-4	12904	12900	-4	13604	13600	-4	14304	14300	-4	15004	15000	-4	15704	15700	-4	16404	16400	-4	17104	17100	-4	17804	17800	-4	18504	18500	-4	19204	19200	-4	19904	19900	-4	20604	20600	-4	21304	21300	-4	22004	22000	-4	22704	22700	-4	23404	23400	-4	24104	24100	-4	24804	24800	-4	25504	25500	-4	26204	26200	-4	26904	26900	-4	27604	27600	-4	28304	28300	-4	29004	29000	-4	29704	29700	-4	30404	30400	-4	31104	31100	-4	31804	31800	-4	32504	32500	-4	33204	33200	-4	33904	33900	-4	34604	34600	-4	35304	35300	-4	36004	36000	-4	36704	36700	-4	37404	37400	-4	38104	38100	-4	38804	38800	-4	39504	39500	-4	40204	40200	-4	40904	40900	-4	41604	41600	-4	42304	42300	-4	43004	43000	-4	43704	43700	-4	44404	44400	-4	45104	45100	-4	45804	45800	-4	46504	46500	-4	47204	47200	-4	47904	47900	-4	48604	48600	-4	49304	49300	-4	50004	50000	-4	50704	50700	-4	51404	51400	-4	52104	52100	-4	52804	52800	-4	53504	53500	-4	54204	54200	-4	54904	54900	-4	55604	55600	-4	56304	56300	-4	57004	57000	-4	57704	57700	-4	58404	58400	-4	59104	59100	-4	59804	59800	-4	60504	60500	-4	61204	61200	-4	61904	61900	-4	62604	62600	-4	63304	63300	-4	64004	64000	-4	64704	64700	-4	65404	65400	-4	66104	66100	-4	66804	66800	-4	67504	67500	-4	68204	68200	-4	68904	68900	-4	69604	69600	-4	70304	70300	-4	71004	71000	-4	71704	71700	-4	72404	72400	-4	73104	73100	-4	73804	73800	-4	74504	74500	-4	75204	75200	-4	75904	75900	-4	76604	76600	-4	77304	77300	-4	78004	78000	-4	78704	78700	-4	79404	79400	-4	80104	80100	-4	80804	80800	-4	81504	81500	-4	82204	82200	-4	82904	82900	-4	83604	83600	-4	84304	84300	-4	85004	85000	-4	85704	85700	-4	86404	86400	-4	87104	87100	-4	87804	87800	-4	88504	88500	-4	89204	89200	-4	89904	89900	-4	90604	90600	-4	91304	91300	-4	92004	92000	-4	92704	92700	-4	93404	93400	-4	94104	94100	-4	94804	94800	-4	95504	95500	-4	96204	96200	-4	96904	96900	-4	97604	97600	-4	98304	98300	-4	99004	99000	-4	99704	99700	-4	100404	100400	-4	101104	101100	-4	101804	101800	-4	102504	102500	-4	103204	103200	-4	103904	103900	-4	104604	104600	-4	105304	105300	-4	106004	106000	-4	106704	106700	-4	107404	107400	-4	108104	108100	-4	108804	108800	-4	109504	109500	-4	110204	110200	-4	110904	110900	-4	111604	111600	-4	112304	112300	-4	113004	113000	-4	113704	113700	-4	114404	114400	-4	115104	115100	-4	115804	115800	-4	116504	116500	-4	117204	117200	-4	117904	117900	-4	118604	118600	-4	119304	119300	-4	120004	120000	-4	120704	120700	-4	121404	121400	-4	122104	122100	-4	122804	122800	-4	123504	123500	-4	124204	124200	-4	124904	124900	-4	125604	125600	-4	126304	126300	-4	127004	127000	-4	127704	127700	-4	128404	128400	-4	129104	129100	-4	129804	129800	-4	130504	130500	-4	131204	131200	-4	131904	131900	-4	132604	132600	-4	133304	133300	-4	134004	134000	-4	134704	134700	-4	135404	135400	-4	136104	136100	-4	136804	136800	-4	137504	137500	-4	138204	138200	-4	138904	138900	-4	139604	139600	-4	140304	140300	-4	141004	141000	-4	141704	141700	-4	142404	142400	-4	143104	143100	-4	143804	143800	-4	144504	144500	-4	145204	145200	-4	145904	145900	-4	146604	146600	-4	147304	147300	-4	148004	148000	-4	148704	148700	-4	149404	149400	-4	150104	150100	-4	150804	150800	-4	151504	151500	-4	152204	152200	-4	152904	152900	-4	153604	153600	-4	154304	154300	-4	155004	155000	-4	155704	155700	-4	156404	156400	-4	157104	157100	-4	157804	157800	-4	158504	158500	-4	159204	159200	-4	159904	159900	-4	160604	160600	-4	161304	161300	-4	162004	162000	-4	162704	162700	-4	163404	163400	-4	164104	164100	-4	164804	164800	-4	165504	165500	-4	166204	166200	-4	166904	166900	-4	167604	167600	-4	168304	168300	-4	169004	169000	-4	169704	169700	-4	170404	170400	-4	171104	171100	-4	171804	171800	-4	172504	172500	-4	173204	173200	-4	173904	173900	-4	174604	174600	-4	175304	175300	-4	176004	176000	-4	176704	176700	-4	177404	177400	-4	178104	178100	-4	178804	178800	-4	179504	179500	-4	180204	180200	-4	180904	180900	-4	181604	181600	-4	182304	182300	-4	183004	183000	-4	183704	183700	-4	184404	184400	-4	185104	185100	-4	185804	185800	-4	186504	186500	-4	187204	187200	-4	187904	187900	-4	188604	188600	-4	189304	189300	-4	190004	190000	-4	190704	190700	-4	191404	191400	-4	192104	192100	-4	192804	192800	-4	193504	193500	-4	194204	194200	-4	194904	194900	-4	195604	195600	-4	196304	196300	-4	197004	197000	-4	197704	197700	-4	198404	198400	-4	199104	199100	-4	199804	199800	-4	200504	200500	-4	201204	201200	-4	201904	201900	-4	202604	202600	-4	203304	203300	-4	204004	204000	-4	204704	204700	-4	205404	205400	-4	206104	206100	-4	206804	206800	-4	207504	207500	-4	208204	208200	-4	208904	208900	-4	209604	209600	-4	210304	210300	-4	211004	211000	-4	211704	211700	-4	212404	212400	-4	213104	213100	-4	213804	213800	-4	214504	214500	-4	215204	215200	-4	215904	215900	-4	216604	216600	-4	217304	217300	-4	218004	218000	-4	218704	218700	-4	219404	219400	-4	220104	220100	-4	220804	220800	-4	221504	221500	-4	222204	222200	-4	222904	222900	-4	223604	223600	-4	224304	224300	-4	225004	225000	-4	225704	225700	-4	226404	226400	-4	227104	227100	-4	227804	227800	-4	228504	228500	-4	229204	229200	-4	229904	229900	-4	230604	230600	-4	231304	231300	-4	232004	232000	-4	232704	232700	-4	233404	233400	-4	234104	234100	-4	234804	234800	-4	235504	235500	-4	236204	236200	-4	236904	236900	-4	237604	237600	-4	238304	238300	-4	239004	239000	-4	239704	239700	-4	240404	240400	-4	241104	241100	-4	241804	241800	-4	242504	242500	-4	243204	243200	-4	243904	243900	-4	244604	244600	-4	245304	245300	-4	246004	246000	-4	246704	246700	-4	247404	247400	-4	248104	248100	-4	248804	248800	-4	249504	249500	-4	250204	250200	-4	250904	250900	-4	251604	251600	-4	252304	252300	-4	253004	253000	-4	253704	253700	-4	254404	254400	-4	255104	255100	-4	255804	255800	-4	256504	256500	-4	257204	257200	-4	257904	257900	-4	258604	258600	-4	259304	259300	-4	260004	260000	-4	260704	260700	-4	261404	261400	-4	262104	262100	-4	262804	262800	-4	263504	263500	-4	264204	264200	-4	264904	264900	-4	265604	265600	-4	266304	266300	-4	267004	267000	-4	267704	267700	-4	268404	268400	-4	269104	269100	-4	269804	269800	-4	270504	270500	-4	271204	



### V.3 DESCRIPTION OF THE STRUCTURE

The structure of the molecule<sup>36</sup> is shown in Figure V.1. The intramolecular bond lengths and angles and their associated e.s.ds. are given in Tables V.6 and V.7 respectively. In both tables the values for the two independent barbiturate and picoline fractions of the molecule have been written side by side thereby making quick comparisons possible. These parameters were calculated with the program BONDLA<sup>40</sup>. Table V.8 lists computed least squares planes with their equations and the distances of various atoms from these planes as well as their intersection angles. These were calculated with the program LSQPL<sup>40</sup>. In Table V.8 the four independent moieties of the molecule have been numbered 1 to 4.

#### The Zinc Coordination Sphere

The zinc atom is tetrahedrally coordinated to the barbital anions via their deprotonated nitrogen atoms N(1) and N(18) and to the  $\beta$  picoline moieties via their nitrogen atoms N(11) and N(28). The respective bond lengths are 2,006(3) and 1,987(3) Å for Zn-N(barb) and 2,095(3) and 2,069(3) Å for Zn-N(picoline). These are in good agreement with Zn-N bond lengths listed by Baenziger and Schultz<sup>43</sup> for a number of tetrahedrally coordinated zinc complexes whose mean distance is 2,04(4) Å. Good agreement is also obtained with the analagous Zn-N(barb) distance of 2,009(2) and Zn-N(imidazole) distance of 2,023(2) Å reported by Wang and Craven<sup>23</sup> while the tetrahedral bond angles in the present complex lie within the same range as those found by the latter authors. Figure V.2 illustrates the bond lengths and angles in the zinc coordination sphere.

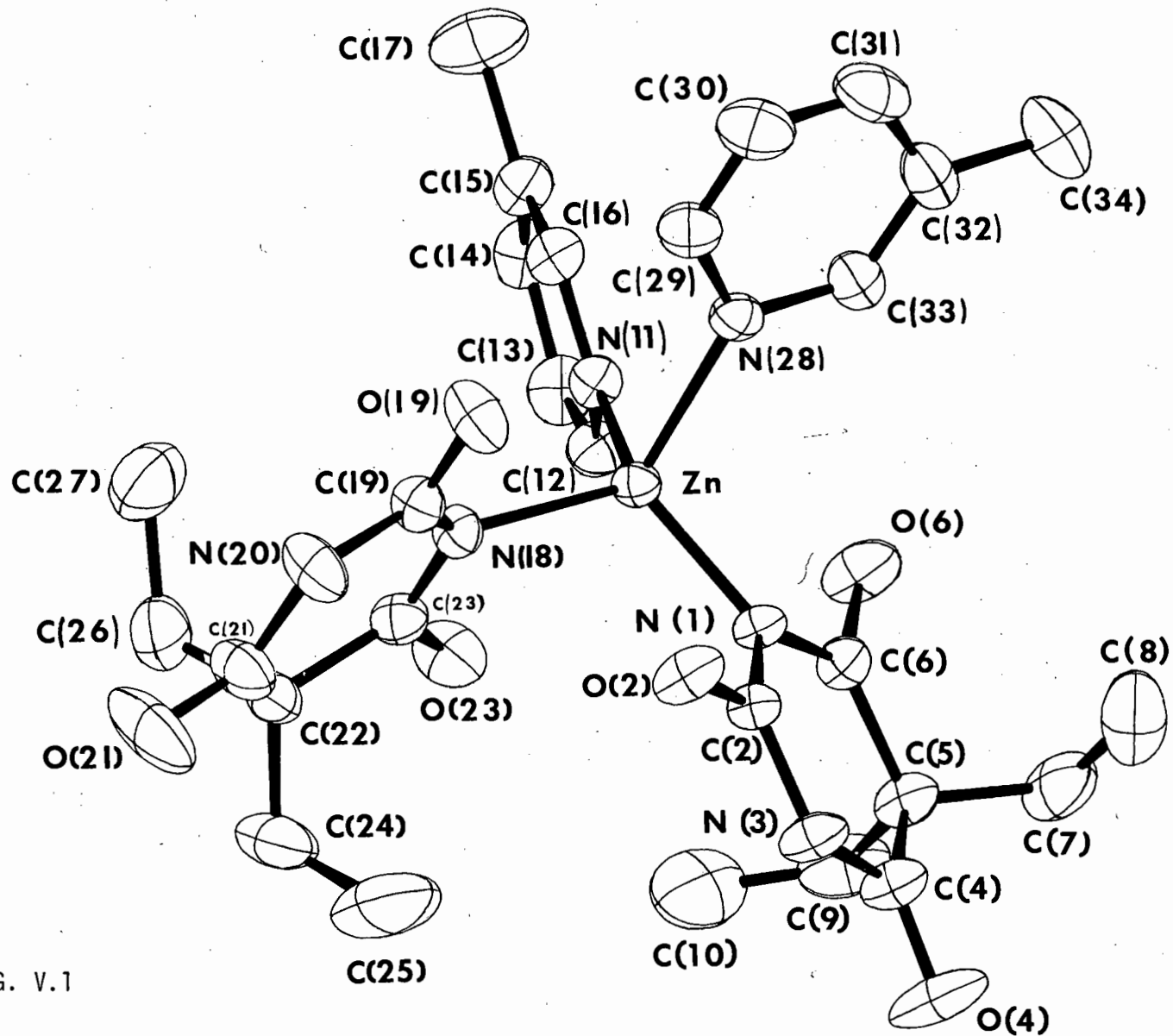


FIG. V.1

TABLE V.6

INTRAMOLECULAR BOND-LENGTHS, AND THEIR E.S.D'S IN Å

Zn-N(1)	2,006(3)	Zn-N(18)	1,987(3)
N(1)-C(2)	1,359(4)	N(18)-C(19)	1,361(4)
C(2)-N(3)	1,383(5)	C(19)-N(20)	1,384(4)
N(3)-C(4)	1,371(4)	N(20)-C(21)	1,353(5)
C(4)-C(5)	1,521(5)	C(21)-C(22)	1,521(5)
C(5)-C(6)	1,530(6)	C(22)-C(23)	1,520(4)
C(6)-N(1)	1,362(4)	C(23)-N(18)	1,359(4)
C(2)-O(2)	1,227(4)	C(19)-O(19)	1,223(4)
C(4)-O(4)	1,211(6)	C(21)-O(21)	1,220(4)
C(6)-O(6)	1,225(4)	C(23)-O(23)	1,228(4)
C(5)-C(7)	1,545(4)	C(22)-C(24)	1,545(7)
C(7)-C(8)	1,520(8)	C(24)-C(25)	1,499(8)
C(5)-C(9)	1,540(5)	C(22)-C(26)	1,554(6)
C(9)-C(10)	1,504(6)	C(26)-C(27)	1,505(8)
Zn-N(11)	2,095(3)	Zn-N(28)	2,069(3)
N(11)-C(12)	1,341(4)	N(28)-C(29)	1,343(5)
C(12)-C(13)	1,378(5)	C(29)-C(30)	1,375(6)
C(13)-C(14)	1,371(6)	C(30)-C(31)	1,373(5)
C(14)-C(15)	1,384(5)	C(31)-C(32)	1,386(6)
C(15)-C(16)	1,378(5)	C(32)-C(33)	1,392(5)
C(16)-N(11)	1,343(5)	C(33)-N(28)	1,344(4)
C(15)-C(17)	1,504(7)	C(32)-C(34)	1,495(5)
N(3)-H(3)	0,85 (3)	N(20)-H(20)	0,84 (3)
C(7)-H(7 1)	0,98 (5)	C(24)-H(24 1)	1,07 (3)
C(7)-H(7 2)	0,93 (4)	C(24)-H(24 2)	1,02 (4)
C(8)-H(8 1)	0,90 (6)	C(25)-H(25 1)	1,04 (4)
C(8)-H(8 2)	1,06 (5)	C(25)-H(25 2)	1,08 (5)
C(8)-H(8 3)	0,96 (4)	C(25)-H(25 3)	0,87 (6)
C(9)-H(9 1)	1,01 (4)	C(26)-H(26 1)	0,98 (4)
C(9)-H(9 2)	0,94 (5)	C(26)-H(26 2)	0,97 (3)
C(10)-H(10 1)	0,94 (5)	C(27)-H(27 1)	0,90 (4)
C(10)-H(10 2)	0,89 (6)	C(27)-H(27 2)	1,14 (4)
C(10)-H(10 3)	0,95 (5)	C(27)-H(27 3)	0,97 (4)
C(12)-H(12)	0,95 (4)	C(29)-H(29)	1,00 (3)
C(13)-H(13)	0,93 (3)	C(30)-H(30)	0,97 (4)
C(14)-H(14)	0,95 (3)	C(31)-H(31)	1,00 (4)
C(16)-H(16)	0,95 (3)	C(33)-H(33)	1,01 (3)
C(17)-H(17 1)	0,90 (4)	C(34)-H(34 1)	1,20 (4)
C(17)-H(17 2)	0,90 (4)	C(34)-H(34 2)	0,91 (5)
C(17)-H(17 3)	0,91 (3)	C(34)-H(34 3)	0,89 (5)

TABLE V.7  
INTRAMOLECULAR BOND ANGLES (IN DEGREES)

N(1)-Zn-N(11)	118,4(1)	N(11)-Zn-N(28)	94,4(1)
N(1)-Zn-N(18)	110,5(1)	N(11)-Zn-N(18)	104,7(1)
N(1)-Zn-N(28)	107,5(1)	N(18)-Zn-N(28)	121,1(1)
Zn-N(1)-C(2)	115,8(2)	Zn-N(18)-C(19)	123,5(2)
N(1)-C(2)-N(3)	119,9(3)	N(18)-C(19)-N(20)	119,1(3)
C(2)-N(3)-C(4)	125,7(3)	C(19)-N(20)-C(21)	126,1(3)
N(3)-C(4)-C(5)	116,9(3)	N(20)-C(21)-C(22)	117,1(3)
C(4)-C(5)-C(6)	114,1(3)	C(21)-C(22)-C(23)	113,3(3)
C(5)-C(6)-N(1)	120,9(3)	C(22)-C(23)-N(18)	120,9(3)
C(6)-N(1)-C(2)	121,9(3)	C(23)-N(18)-C(19)	122,1(2)
C(6)-N(1)-Zn	121,7(2)	C(23)-N(18)-Zn	112,6(2)
N(1)-C(2)-O(2)	120,9(3)	N(18)-C(19)-O(19)	121,7(2)
N(3)-C(2)-O(2)	119,2(3)	N(20)-C(19)-O(19)	119,2(3)
N(3)-C(4)-O(4)	121,1(3)	N(20)-C(21)-O(21)	121,1(4)
C(5)-C(4)-O(4)	122,0(3)	C(22)-C(21)-O(21)	121,8(4)
C(5)-C(6)-O(6)	119,3(3)	C(22)-C(23)-O(23)	119,7(3)
N(1)-C(6)-O(6)	119,8(3)	N(18)-C(23)-O(23)	119,4(3)
C(4)-C(5)-C(7)	107,9(3)	C(21)-C(22)-C(24)	109,3(3)
C(6)-C(5)-C(7)	109,3(3)	C(23)-C(22)-C(24)	109,7(3)
C(5)-C(7)-C(8)	114,5(3)	C(22)-C(24)-C(25)	113,6(4)
C(4)-C(5)-C(9)	108,4(3)	C(21)-C(22)-C(26)	109,0(3)
C(6)-C(5)-C(9)	107,5(3)	C(23)-C(22)-C(26)	107,4(3)
C(7)-C(5)-C(9)	109,6(3)	C(24)-C(22)-C(26)	108,1(3)
C(5)-C(9)-C(10)	115,4(3)	C(22)-C(26)-C(27)	115,0(3)
Zn-N(11)-C(12)	123,4(3)	Zn-N(28)-C(29)	124,3(2)
N(11)-C(12)-C(13)	121,4(4)	N(28)-C(29)-C(30)	121,8(3)
C(12)-C(13)-C(14)	119,9(3)	C(29)-C(30)-C(31)	119,5(4)
C(13)-C(14)-C(15)	119,6(3)	C(30)-C(31)-C(32)	120,2(4)
C(14)-C(15)-C(16)	117,0(4)	C(31)-C(32)-C(33)	116,9(3)
C(15)-C(16)-N(11)	124,2(3)	C(32)-C(33)-N(28)	123,2(3)
C(16)-N(11)-C(12)	117,9(3)	C(33)-N(28)-C(29)	118,4(3)
C(16)-N(11)-Zn	118,7(2)	C(33)-N(28)-Zn	117,2(2)
C(14)-C(15)-C(17)	121,9(3)	C(31)-C(32)-C(34)	121,7(4)
C(16)-C(15)-C(17)	121,1(3)	C(33)-C(32)-C(34)	121,4(4)

TABLE V.8

## LEAST SQUARES PLANES

The equations of the planes are expressed in  
orthogonalised space as  $PI + QJ + RK = S$

Plane I	through the 6 atoms of pyrimidine ring no. 1								
Atoms defining the plane	N(1)	C(2)	N(3)	C(4)	C(5)	C(6)			
Atoms not included in the plane							O(2)	O(4)	O(6)
Distance from the plane, Å	0,039	0,005	-0,032	0,015	0,024	-0,052	-0,013	0,047	-0,158
Equation	$0,65107I - 0,73344J - 0,19539K = -1,05638$								
Plane II	through the 6 atoms of pyrimidine ring no. 2								
Atoms defining the plane	N(18)	C(19)	N(20)	C(21)	C(22)	C(23)			
Atoms not included in the plane							O(19)	O(21)	O(23)
Distance from the plane, Å	-0,007	-0,033	0,011	0,044	-0,076	0,062	-0,080	0,123	0,204
Equation	$-0,49553I - 0,19789J + 0,84575K = 0,16436$								
Plane III	through the 9 atoms of the trioxypyrimidine ring (1)								
Atoms defining the plane	N(1)	C(2)	N(3)	C(4)	C(5)	C(6)	O(2)	O(4)	O(6)
Distance from the plane, Å	0,082	0,011	-0,056	-0,003	0,048	0,002	-0,017	0,002	-0,070
Equation	$0,66810I - 0,71424J - 0,20856K = -1,07862$								
Plane IV	through the 9 atoms of the trioxypyrimidine ring (2)								
Atoms defining the plane	N(18)	C(19)	N(20)	C(21)	C(22)	C(23)	O(19)	O(21)	O(23)
Distance from the plane, Å	-0,021	-0,008	0,022	0,004	-0,162	-0,006	-0,006	0,075	0,102
Equation	$-0,52778I - 0,17888J + 0,83033K = 0,07560$								
Plane V	through the 6 atoms of the $\beta$ -picoline ring no. 3								
Atoms defining the plane	N(11)	C(12)	C(13)	C(14)	C(15)	C(16)			
Atoms not included in the plane							C(17)		
Distance from the plane, Å	0,006	-0,005	-0,002	0,007	-0,005	-0,001	-0,018		
Equation	$-0,18200I + 0,85223J + 0,49049K = 3,09456$								

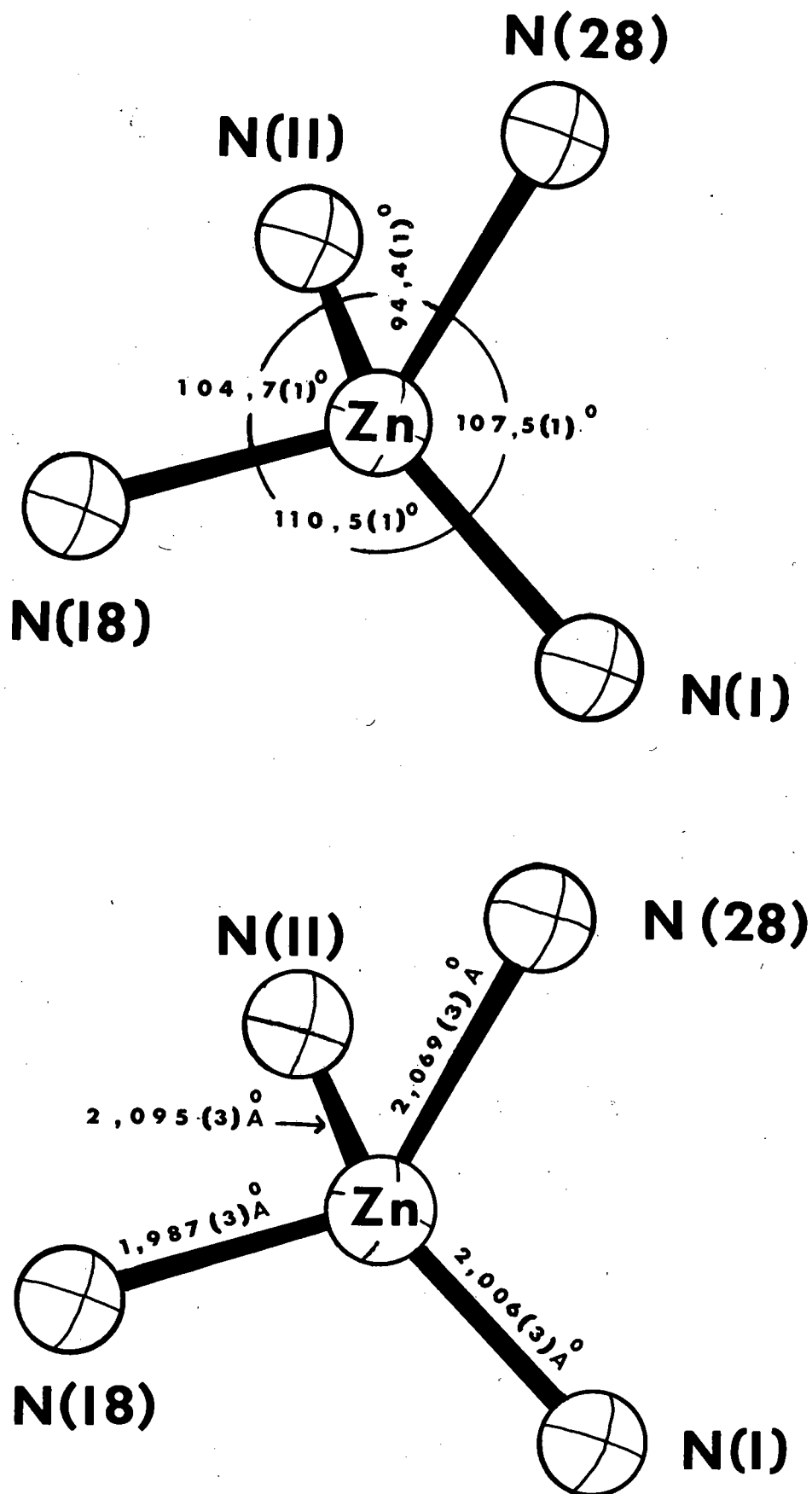
TABLE V.8 - CONTINUED

Plane VI	through the 6 atoms of the $\beta$ -picoline ring no. 4							
Atoms defining the plane	N(28)	C(29)	C(30)	C(31)	C(32)	C(33)		
Atoms not included in the plane							C(34)	
Distance from the plane, Å	-0,002	0,005	-0,003	-0,003	0,005	-0,003	0,046	
Equation	$0,80921I + 0,21277J - 0,54763K = 1,12472$							
Plane VII	through the 4 atoms of the diethyl group and C(5) to which it is attached.							
Atoms defining the plane	C(5)	C(7)	C(8)	C(9)	C(10)			
Distance from the plane, Å	-0,024	0,019	0,004	-0,024	0,025			
Equation	$-0,43932I - 0,59964J + 0,66890K = 2,14875$							
Plane VIII	through the 4 atoms of the diethyl group and C(22) to which it is attached							
Atoms defining the plane	C(22)	C(24)	C(25)	C(26)	C(27)			
Distance from the plane, Å	-0,042	0,005	0,021	-0,014	0,030			
Equation	$0,54010I + 0,67677J + 0,50028K = 1,86887$							

## INTERSECTION ANGLES

Planes I and II	69,96°	Planes II and IV	2,32°
Planes I and III	1,65°	Planes II and V	70,34°
Planes I and V	32,92°	Planes II and VI	25,01°
Planes I and VI	61,46°	Planes II and VIII	88,77°
Planes I and VII	88,68°	Planes V and VI	76,43°

FIG. V.2



In the  $\beta$ -picoline moieties the average C-C and C-H bond lengths are 1,380 and 0,97 Å respectively, in good agreement with the values obtained in complex no. 1 i.e.  $\text{Cu}(\text{barbital})_2(\beta\text{-picoline})_2 \cdot 2\text{H}_2\text{O}$  described in Chapter III. Both picoline rings are planar (planes V and VI) with the greatest deviations from the planes being those of atoms C(14) and C(29) at distances of 0,007 and 0,005 Å respectively. The two planes, i.e. V and VI intersect at an angle of 76,43°.

#### The barbital ligand structure

The analagous bond lengths and angles for the two barbital fractions of the molecule listed in Tables V.6 and V.7 show excellent agreement with one another and with the values listed by Wang and Craven<sup>23</sup>. The conformations of the two trioxypyrimidine rings are shown in Fig. V.3. In both cases the dotted line is a trace of the least-squares plane through the six ring atoms only (planes I and II). Each pyrimidine ring is almost planar but slight puckering is evident. This is a little more pronounced than that observed in the complexes  $\text{Cu}(\text{barbital})_2(\text{pyridine})_2$  (reported by Caira<sup>27</sup>) and  $\text{Cu}(\text{barbital})_2(\beta\text{-picoline})_2 \cdot 2\text{H}_2\text{O}$  (complex no. 1). Planes I and II intersect at 69,96°. The exocyclic oxygen atoms and the pyrimidine ring atoms are virtually coplanar as can be gauged by the small intersection angles (1,65° and 2,32°) of planes I and III and II and IV. (Planes III and IV are those calculated for the atoms of the trioxypyrimidine rings).

Atoms C(7), C(8), C(9) and C(10) of the two ethyl groups as well as atom C(5) to which they are attached lie in the same plane (plane VII) which is virtually perpendicular (88,68°) to the pyrimidine ring plane (plane I) with which it is associated. Similarly, atoms C(24), C(25), C(26) and C(27) as well as C(22) lie in the same plane (plane VIII) which is at 88,77° to the pyrimidine ring plane (plane II) with which it is associated. These results are consistent with those found in complexes no. 1 and 2 (Chapters III and IV). The hydrogen

FIG. V.3

The vertical scale is approximately six times the horizontal scale.

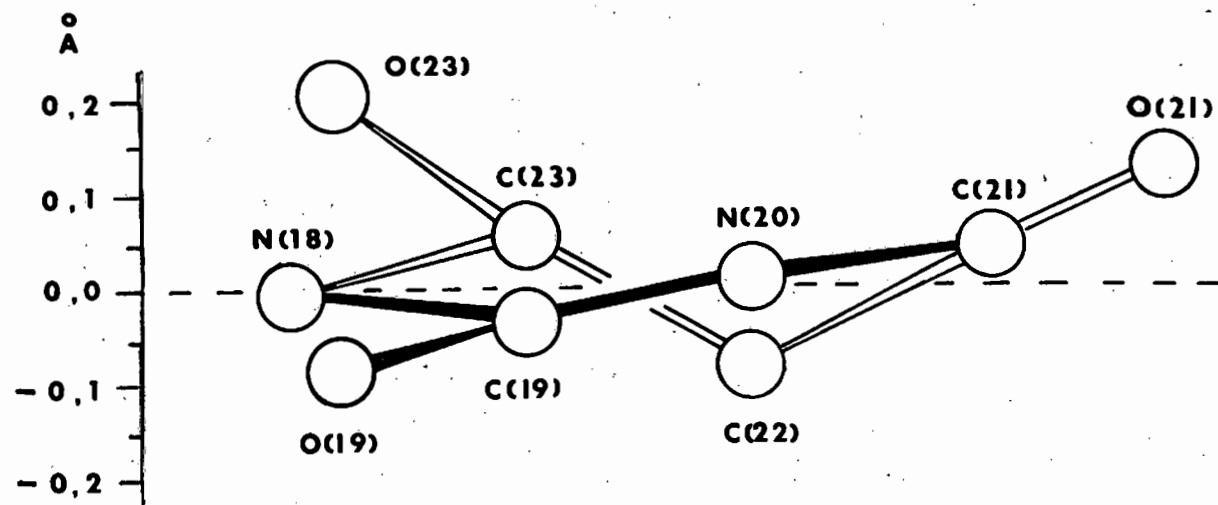
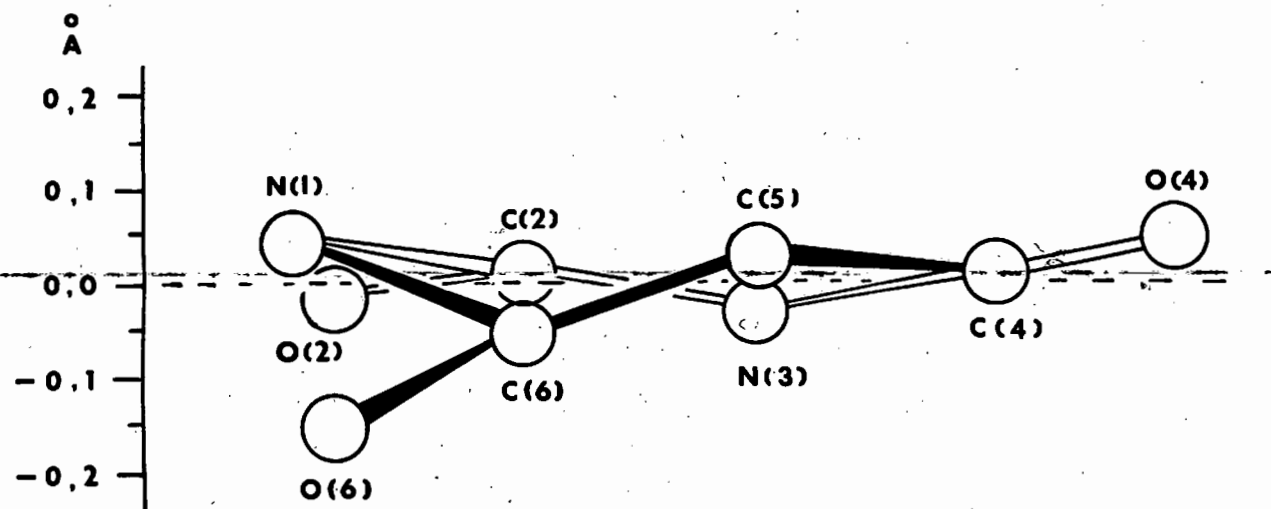
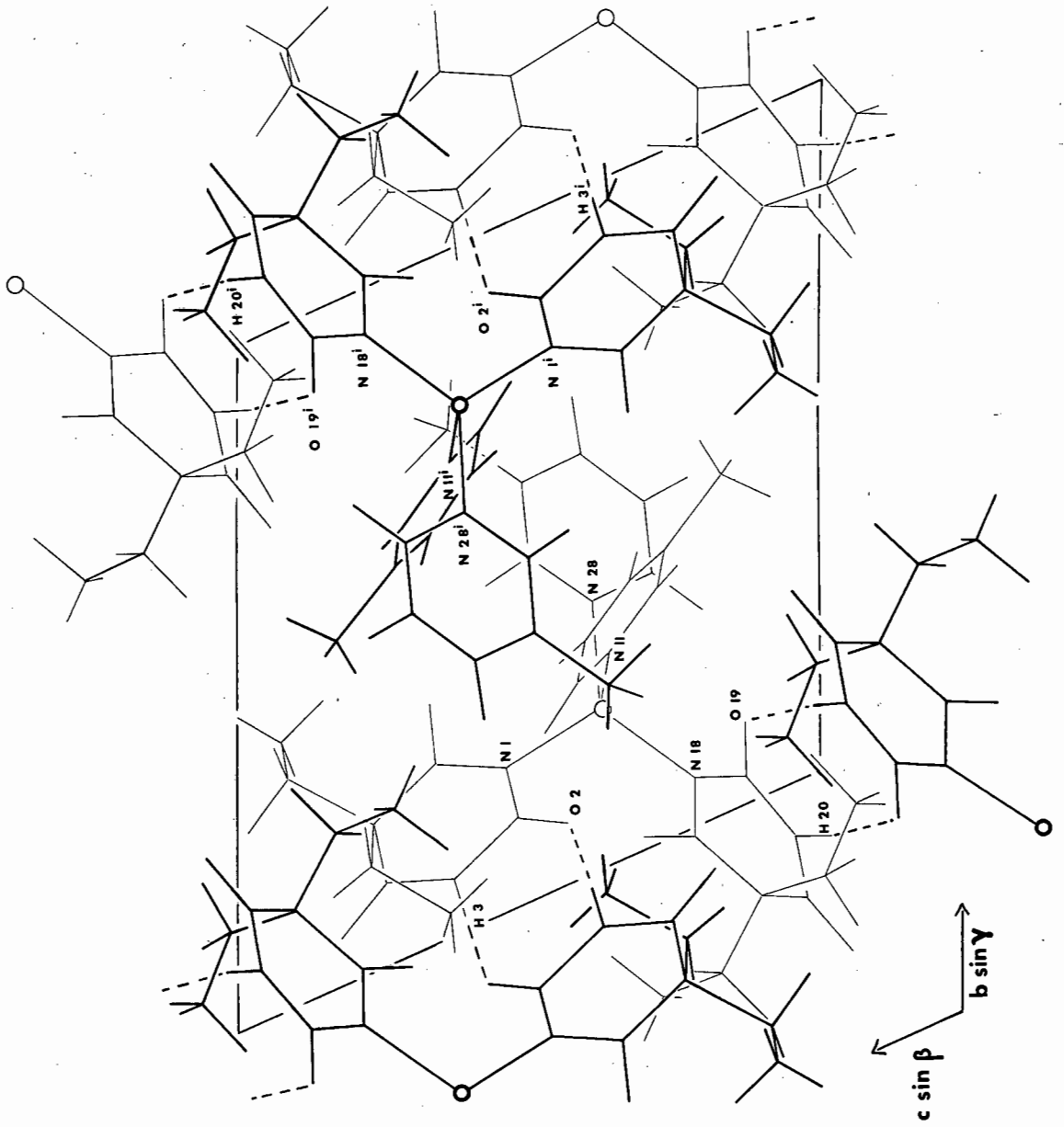


FIG. V.4



[100] projection

FIG. V.5

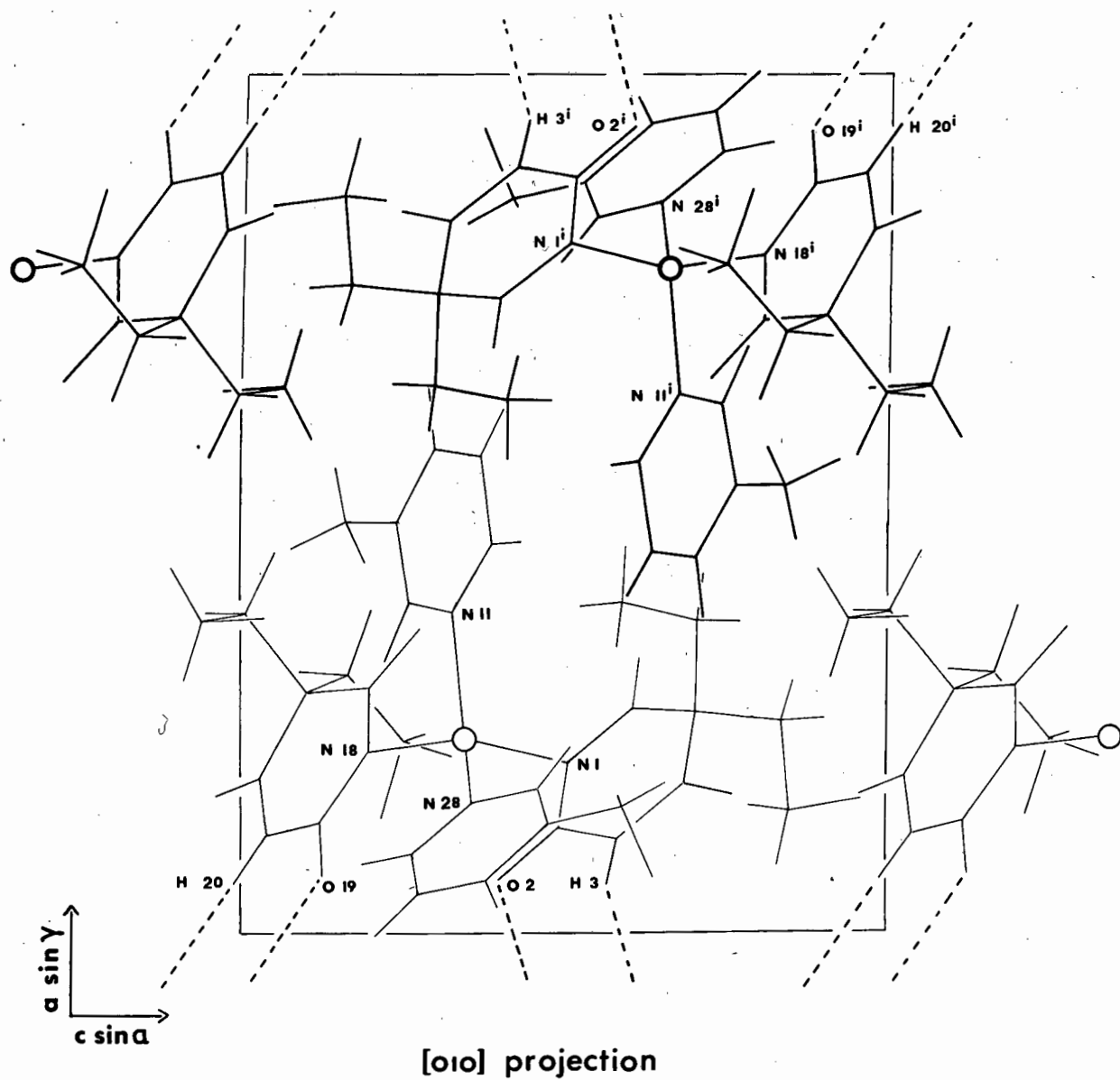


FIG. V.6

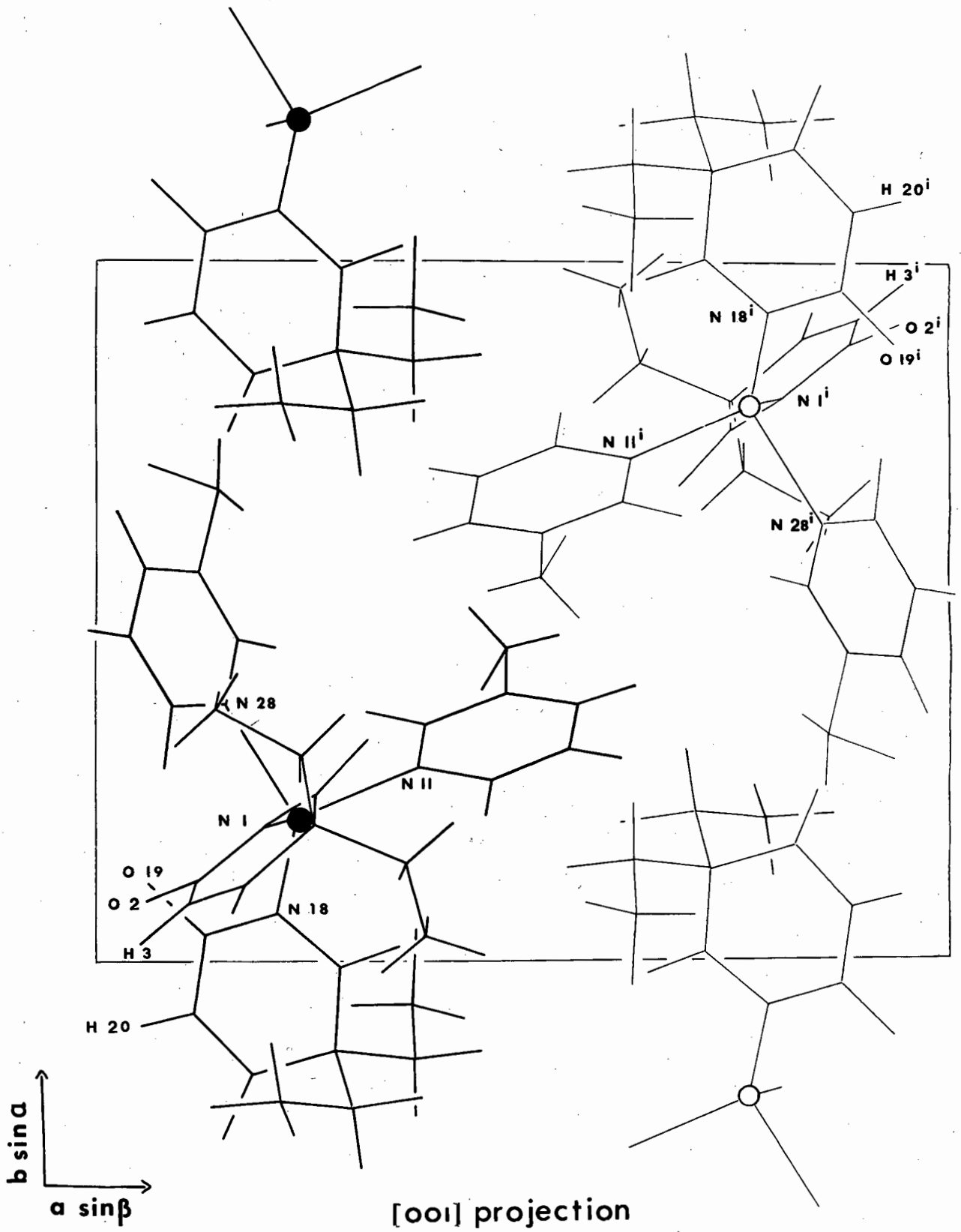
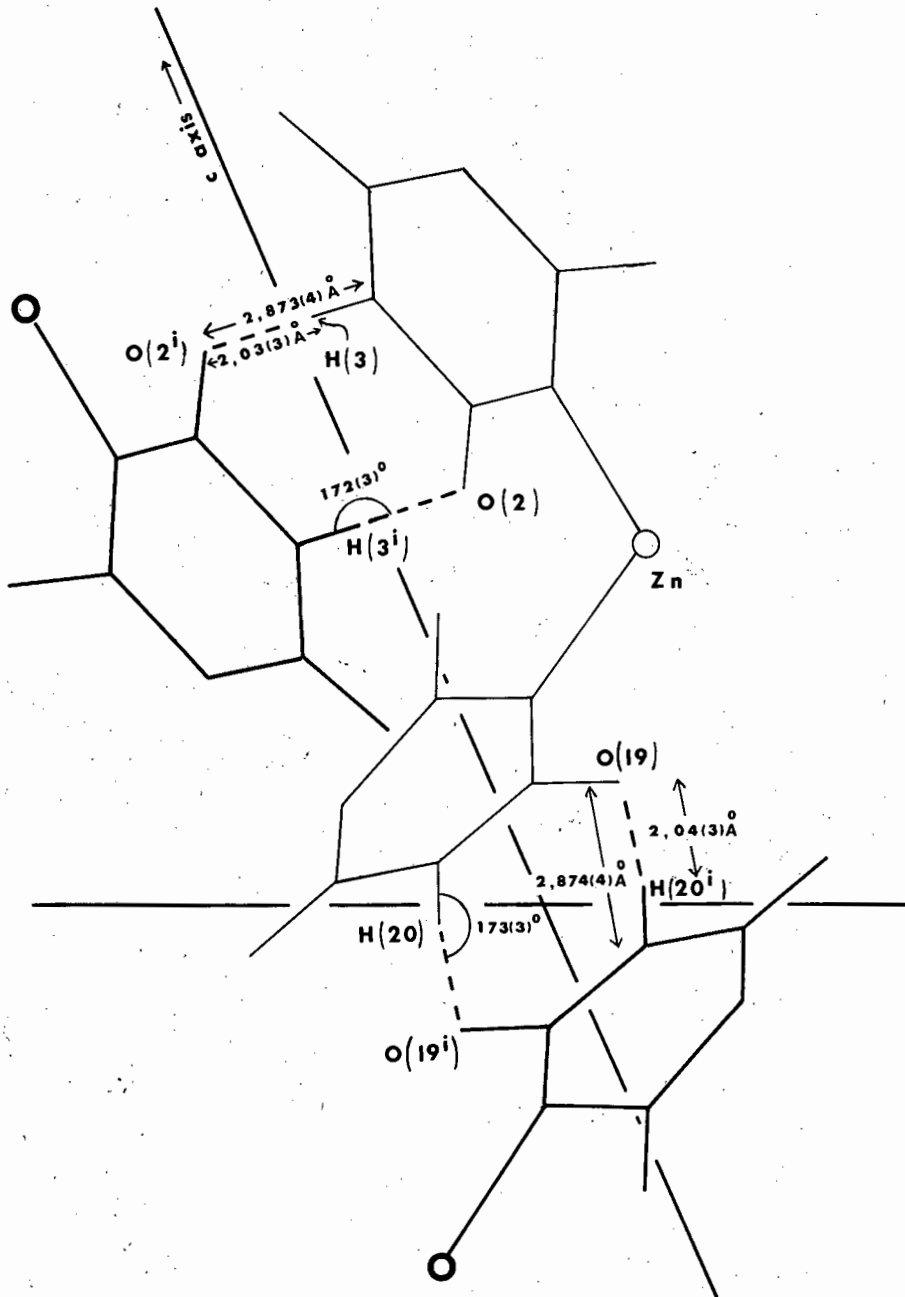


FIG. V.7



HYDROGEN - BOND INTERACTIONS

and that this configuration is stabilised by C-H  $\cdots$  O intra-molecular interactions involving carbon atoms of imidazole and carbonyl oxygen atoms of barbital. In the structure being described here neither of these two effects were observed.

CHAPTER VI

THE CRYSTAL AND MOLECULAR STRUCTURE OF THE  
BIS-(5-ETHYL-5-ISOAMYL BARBITURATO)-BIS-(IMIDAZOLE)  
COMPLEX OF Ni(II).

## VI.1 CRYSTAL AND INTENSITY DATA

### Chemical Analysis

The theoretical and experimentally determined analysis figures are shown in Table VI.1. These figures show that the complex has the composition  $\text{NiC}_{28}\text{H}_{42}\text{N}_8\text{O}_6$  corresponding to the formulation  $\text{Ni(II)(5-ethyl-5-isoamylbarbiturato)}_2(\text{imidazole})_2$ .

TABLE VI.1

	%C	%H	%N
Theoretical	52,11	6,51	17,37
Experimentally determined	51,8	6,7	17,8

### Density of crystals

The density was determined as  $1,38(2) \text{ g cm}^{-3}$  corresponding to 1 molecule per unit cell.

### Space Group

As with  $\text{Cu(brallobarbita)}_2(\text{pyridine})_2 \cdot 2\text{H}_2\text{O}$  and  $\text{Zn(barbita)}_2(\beta\text{-picoline})_2$ , the unit cell was determined as triclinic. Because the molecule itself is centrosymmetric it seemed likely that the space group was  $\text{P}\bar{1}$  requiring the nickel atom to be located at the origin. This was later confirmed in the solution of the structure.

### Unit cell parameters

A single crystal of dimensions  $0,325 \times 0,225 \times 0,100 \text{ mm}$  was used for the determination of the unit cell parameters and for the diffractometer data collection. The crystal data is listed in Table VI.2 overleaf.

TABLE VI.2 CRYSTAL DATA

$a = 10,615(5) \text{ \AA}$	$V = 768,97 \text{ \AA}^3$
$b = 10,544(5) \text{ \AA}$	$D_M = 1,38(2) \text{ g cm}^{-3}$
$c = 7,457(5) \text{ \AA}$	$D_C = 1,392 \text{ g cm}^{-3}$ for $Z=1$
$\alpha = 111,156(2)^\circ$	$\mu = 6,86 \text{ cm}^{-1}$ for $\text{MoK}\alpha$ radiation
$\beta = 97,360(2)^\circ$	$F(000) = 342,0$
$\gamma = 82,675(2)^\circ$	space group = $P\bar{1}$ triclinic

Intensity Data

The diffractometer scan width was  $1,20^\circ$  and the scan speed  $0,04^\circ\text{sec}^{-1}$ . The background and scan times were both 30 seconds. Of the 4469 reflections which were measured up to  $2\theta = 60^\circ$ , 728 were omitted as unobserved.

The linear absorption coefficient for  $\text{MoK}\alpha$  radiation was determined as  $6,86 \text{ cm}^{-1}$ . The variation in  $\mu R$  for the crystal used was between 0,03 and 0,14 with corresponding absorption correction<sup>32</sup> values  $A^*$  of 1,00 and 1,18 for the  $\theta$  range  $0^\circ$  to  $30^\circ$ . This was regarded as insignificant and absorption corrections were consequently ignored.

## VI.2 SOLUTION AND REFINEMENT OF THE STRUCTURE

Assuming the space group to be  $P\bar{1}$ , the symmetry of the molecule required the nickel atom to be located at the origin with the rest of the atoms occupying general positions. A Fourier synthesis (CENTROSY PROGRAM) phased on nickel at (0,0,0) was thus computed. From this map all 22 non hydrogen atoms of the structure were located. While the peaks defining the barbiturate anion could be uniquely assigned to their respective atoms, the identity of the five peaks forming the imidazole ring presented a problem with regard to distinguishing between nitrogen and carbon atoms. Since one of the nitrogens is coordinated to the nickel atom the problem reduced to identifying the second nitrogen atom. Initially atoms 16 and 17 (Figure VI.1) in the imidazole ring were arbitrarily assigned as nitrogen and carbon respectively.

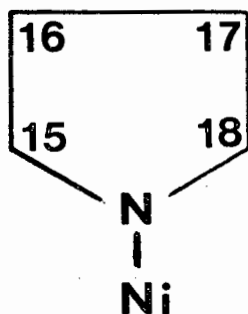


Fig.VI.1

After four cycles of isotropic refinement (CRYLSQ: XRAY72)<sup>40</sup> the conventional R factor dropped from an initial value of 0,371 to a terminal value of 0,112. At this stage the bond lengths and angles within the imidazole ring were calculated (BONDLA: XRAY72)<sup>40</sup>. These are shown in Figure VI.2 (upper numbers). In an effort to verify that the bond distances were not themselves dependent upon the tentative assignment of atoms 16 and 17, a refinement was undertaken

with these atoms interchanged, i.e. atom 16 was assigned as carbon and atom 17 as nitrogen. After two cycles, R terminated at 0,111. The bond lengths were again calculated (lower numbers, Figure VI.2) and, as expected these show no significant differences with the first set of values. Thus since the bond lengths obtained are constant, these may be used to identify atoms 16 and 17 absolutely by comparison with bond lengths obtained for imidazole and some of its complexes. Figures VI.3 to VI.6 show the bond lengths obtained in such compounds.

To facilitate comparison, the atoms have been numbered in a similar fashion to that in VI.2. It can be readily seen that:

- (i) the C(15)-C(16) double bond is flanked on either side by two relatively longer carbon-nitrogen pure single bonds (N(14)-C(15) and C(16)-N(17));
- (ii) C(18) which is situated between the two nitrogen atoms forms C-N bonds, both of which are smaller than C(15)-C(16). (This indicates that these C-N bonds do possess double bond character).

In the present study either atom 16 or 17 is nitrogen. If atom 16 is nitrogen, then, on the basis of the above evidence, we would expect:

- (i)  $d_{17-18} < d_{14-18}$  and  $d_{16-17}$
- (ii)  $d_{17-8} > d_{14-15}$  and  $d_{15-16}$

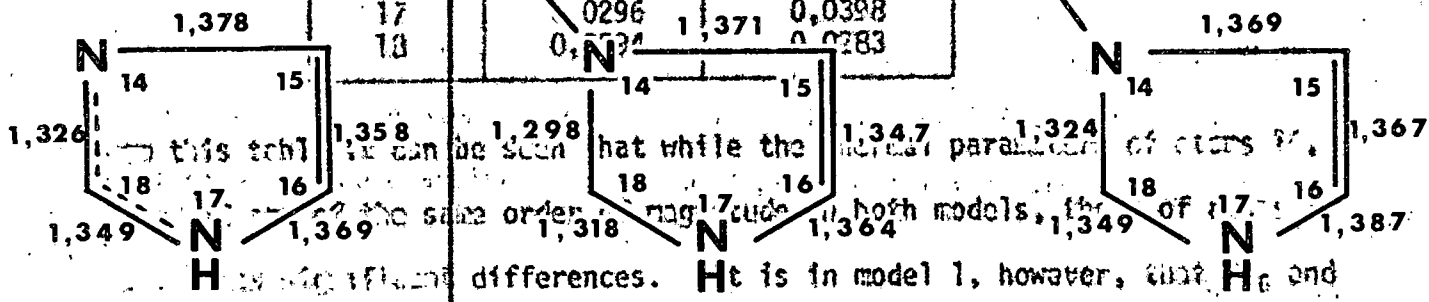
However, neither of these two is true for the complex. Interchanging atoms 16 and 17 resulted in a set of conditions suggesting that atom 16 was carbon and atom 17 nitrogen. Moreover, inspection of the original Fourier showed the peak density corresponding to atom 17 (density = 75) to be greater than that of atom 16 (density = 62).

A further test as to the identity of atoms 16 and 17 was carried out by comparing the isotropic temperature factors indicated in the two refinements. These values are given in Table VI.3 below.

TABLE VI.3

Present study		
	MODEL 1	MODEL 2
ATOM 16:	N	C
ATOM 17:	C	N
ATOM	U	U
14	0,0244	0,0235
15	0,0352	0,0337
16	0,0557	0,0381
17	0,0296	0,0398
18	0,0371	0,0283

Fig. VI.2



U<sub>17</sub> show the standard deviations from the mean value indicating this imidazole Zn (barbital)<sub>2</sub>(imidazole)<sub>2</sub> Zn (imidazole)<sub>2</sub>Cl<sub>2</sub>

Fig. VI.3 Fig. VI.4 Fig. VI.5

... of atom 16 as nitrogen and atom 17 as carbon was incorrect. The ... interchanged and anisotropic temperature factors were ... into the refinement. These parameters were of the same form as

those used in the refinement of complex no. 3 (page 40). After two cycles it dropped to 0.0371. Theoretical coordination number was compared by the program ... on the position of the ... in an attempt to locate the hydrogen atom.

... hydrogen atoms were thus located and they were given the isotropic temperature factors of the atoms to which they were bonded. (In the crystal ... as in the ... hydrazide complex, the hydrogen atoms bonded to the three

Fig. VI.6

terminal isoamyl atoms could not be found in electron density difference maps)<sup>60,74</sup>. After the final cycle of refinement the average e.s.d. in the positional and anisotropic temperature factors of the non-hydrogen atoms was more than fifty times the average parameter shift. The average e.s.d. in the hydrogen atomic positions was about five times the average parameter shift. The final R value was 0,056. As a final check of the correctness of the structure, a difference electron density map with the structure factors calculated in the last cycle of refinement was computed. This map was practically featureless.

In the structure factor calculations, scattering factors for the nickel, carbon, nitrogen and oxygen atoms were again those obtained from Cromer and Mann<sup>41</sup> while the scattering factors for the hydrogen atoms were those of Stewart et al<sup>42</sup>. The nickel atom was treated as Ni<sup>0</sup> and the anomalous dispersion correction<sup>35</sup> ( $\Delta f' = 0,4$  for MoK $\alpha$  radiation) was applied. Each reflection was assigned unit weight.

The final atomic positional and thermal parameters for the non hydrogen atoms are given in Table VI.4 while the atomic positional parameters of the hydrogen atoms are given in Table VI.5. The observed and calculated structure factors (LISTFC)<sup>40</sup> are given in Table VI.6

TABLE VI.4

## NON-HYDROGEN ATOMS.

FRACTIONAL ATOMIC CO-ORDINATES AND THEIR E.S.D's ( $\times 10^4$ ) AND  
ANISOTROPIC TEMPERATURE FACTORS AND THEIR E.S.D's ( $\times 10^4$ ).

Atom	x	y	z	$U_{11}$	$U_{22}$	$U_{33}$	$U_{12}$	$U_{13}$	$U_{23}$
Ni	0	0	0	193(2)	84(2)	164(2)	3(1)	62(2)	17(2)
N(1)	657(2)	-2042(2)	-1231(2)	198(9)	94(8)	196(10)	-2(7)	51(8)	4(7)
C(2)	427(2)	-3229(2)	-2709(3)	219(11)	109(10)	172(11)	-17(8)	65(9)	12(8)
N(3)	1285(2)	-4369(2)	-2858(3)	256(11)	93(9)	260(11)	-6(8)	11(9)	-26(8)
C(4)	2368(3)	-4415(3)	-1681(4)	252(13)	138(11)	267(13)	-13(9)	68(10)	33(9)
C(5)	2669(2)	-3105(2)	-3(4)	204(11)	14(10)	204(11)	2(8)	37(9)	45(9)
C(6)	1667(2)	-1938(2)	54(4)	206(11)	113(9)	201(11)	-18(8)	76(9)	50(8)
C(7)	2730(3)	-3398(3)	1896(4)	398(17)	298(15)	276(14)	22(12)	23(12)	157(12)
C(8)	1528(4)	-3893(4)	2215(6)	569(24)	539(23)	472(21)	10(18)	191(18)	326(19)
C(9)	3975(3)	-2712(3)	-230(5)	196(12)	268(13)	366(16)	-18(10)	32(11)	117(12)
C(10)	3995(3)	-2256(4)	-1942(5)	201(13)	451(18)	451(18)	-54(12)	44(12)	255(15)
C(11)	5304(3)	-1935(4)	-2213(5)	234(14)	465(19)	443(19)	-87(13)	76(13)	163(15)
C(12)	6203(5)	-3221(6)	-2899(9)	420(24)	718(33)	1076(44)	160(22)	356(26)	329(31)
C(13)	5198(4)	-1137(6)	-3559(8)	456(23)	851(35)	832(34)	-201(23)	111(23)	508(30)
O(2)	-501(2)	-3314(2)	-3884(3)	308(11)	205(10)	303(11)	-2(8)	-45(9)	-27(8)
O(4)	3057(2)	-5462(2)	-1947(4)	405(13)	167(10)	530(15)	111(9)	0(11)	15(10)
O(6)	1771(2)	-786(2)	1351(3)	279(10)	137(8)	211(9)	-30(7)	37(7)	2(7)
N(14)	1041(2)	468(2)	-1783(3)	248(11)	185(10)	258(11)	5(8)	78(9)	89(9)
C(15)	1597(3)	1648(3)	-1423(5)	362(16)	220(13)	452(18)	-65(12)	137(14)	82(13)
C(16)	2071(3)	1625(4)	-3014(6)	362(17)	387(18)	622(24)	-86(14)	154(16)	300(17)
N(17)	1814(3)	389(3)	-4427(4)	392(16)	518(18)	333(15)	5(13)	138(12)	203(13)
C(18)	1199(3)	-259(3)	-3621(4)	310(14)	293(14)	239(13)	-8(11)	83(11)	92(11)

TABLE VI.5  
 HYDROGEN ATOMS.  
 FRACTIONAL ATOMIC CO-ORDINATES ( $\times 10^3$ )  
 AND THEIR E.S.D.'s ( $\times 10^3$ )

	X	Y	Z
H(3)	110(3)	-501(3)	-376(5)
H(7 1)	344(3)	-407(4)	189(5)
H(7 2)	297(3)	-264(4)	290(5)
H(8 1)	82(4)	-330(4)	216(6)
H(8 2)	129(4)	-469(4)	116(6)
H(8 3)	165(4)	-402(4)	338(6)
H(9 1)	425(3)	-199(3)	96(5)
H(9 2)	456(3)	-348(3)	-27(5)
H(10 1)	366(3)	-286(4)	-306(5)
H(10 2)	339(3)	-145(4)	-181(5)
H(11)	570(4)	-136(4)	-92(5)
H(12 1)	635(5)	-359(5)	-187(7)
H(12 2)	579(5)	-370(5)	-418(7)
H(12 3)	703(5)	-297(5)	-305(7)
H(13 1)	482(4)	-163(5)	-491(7)
H(13 2)	455(4)	-29(5)	-321(7)
H(13 3)	597(4)	-92(5)	-348(7)
H(15)	167(3)	226(4)	-22(5)
H(16)	239(4)	216(4)	-319(5)
H(17)	194(4)	12(4)	-578(5)
H(18)	91(3)	-112(3)	-430(5)







### VI.3 DESCRIPTION OF THE STRUCTURE

The structure of the molecule is shown in Fig. VI.7 (PLUTO : Motherwell)<sup>47</sup>. The intramolecular bond lengths and angles and their associated e.s.d's are given in Tables VI.6 and VI.7 respectively (BONDLA : XRAY72)<sup>40</sup>. Table VI.8 lists computed least squares planes with their equations and the distances of various atoms from these planes.

#### The nickel coordination sphere

The nickel atom is involved in distorted octahedral coordination and is situated in the centre of a plane defined by the deprotonated donor nitrogen atoms N(1) and N(1<sup>i</sup>) of the barbiturate anions and the donor nitrogens N(14) and N(14<sup>i</sup>) of the imidazole moieties (plane I). The octahedron is completed by two centrosymmetric barbiturato oxygen atoms O(6) and O(6<sup>i</sup>) which lie above and below this plane.

The Ni-N bond lengths are 2,078(2) and 2,055(3)Å for the barbiturate and imidazole ligands respectively. These may be compared with the Ni-N distances of 2,107(3) and 2,082(3)Å reported for the structure diaquobis(2,2'-biimidazole)nickel II dinitrate<sup>46</sup>. Further comparison is afforded in the structure of tetrakis pyrazole-nickel chloride<sup>48</sup> in which the Ni-N bond lengths are 2,097(3) and 2,087(3)Å.

The Ni-O bond length is 2,226(2)Å. In the nickel dinitrate structure mentioned above<sup>46</sup> the water oxygens occupy the octahedral positions at a distance of 2,103(3)Å while in the structure diaquobis-glycinatonickel (II)<sup>49</sup> the Ni-O bond distance is 2,10(1)Å.

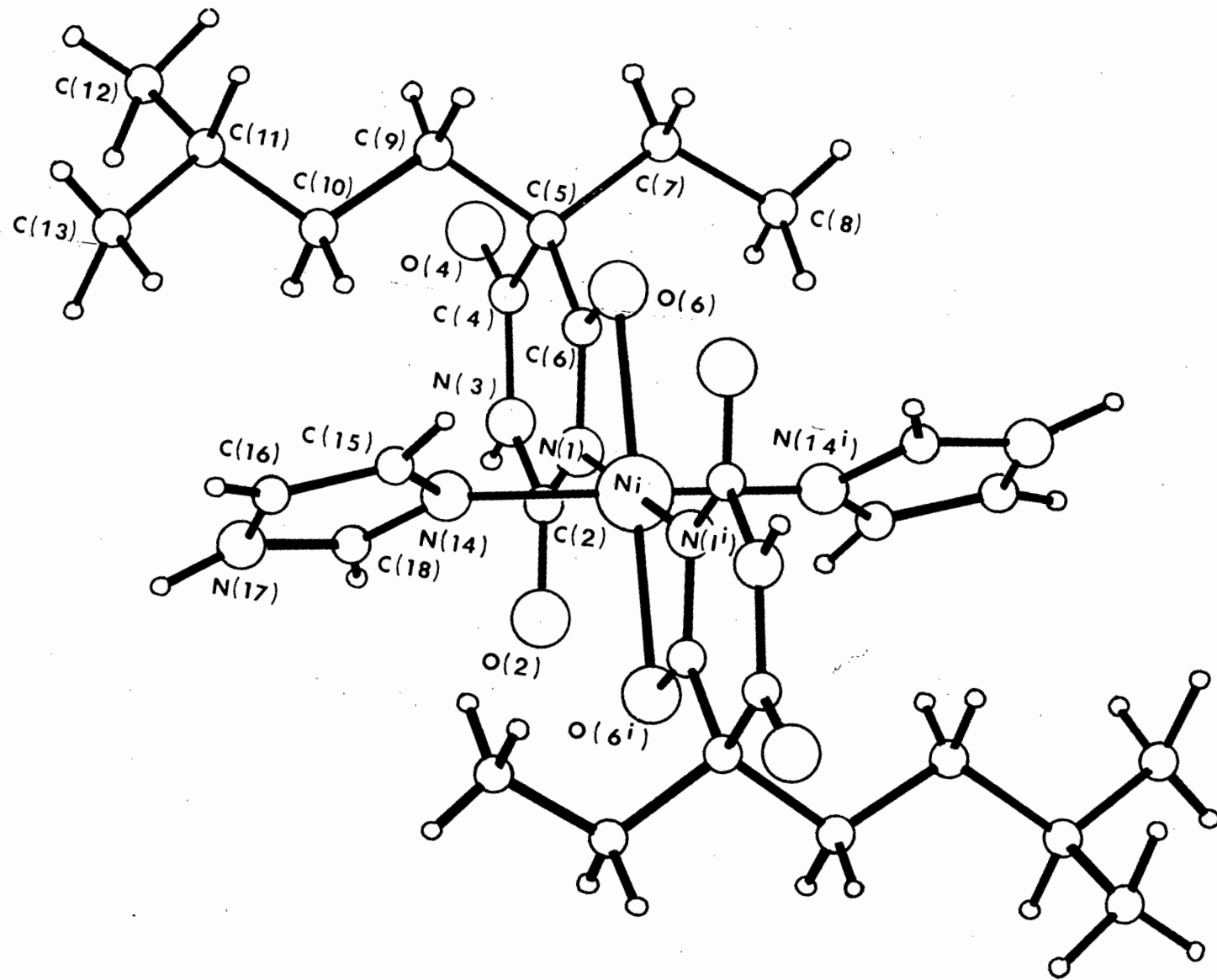


FIG. VI.7

TABLE VI.6

## INTRAMOLECULAR BOND LENGTHS AND THEIR E.S.D'S IN Å

Ni	- N(1)	2,078(2)	N(3)	- H(3)	0,78(3)
N(1)	- C(2)	1,362(3)	C(7)	- H(7 1)	0,97(4)
C(2)	- N(3)	1,392(3)	C(7)	- H(7 2)	0,92(3)
N(3)	- C(4)	1,361(4)	C(8)	- H(8 1)	0,92(4)
C(4)	- C(5)	1,529(4)	C(8)	- H(8 2)	0,96(4)
C(5)	- C(6)	1,513(4)	C(8)	- H(8 3)	0,91(5)
C(6)	- N(1)	1,331(3)	C(9)	- H(9 1)	0,98(3)
C(2)	- O(2)	1,221(3)	C(9)	- H(9 2)	0,95(3)
C(4)	- O(4)	1,210(4)	C(10)	- H(10 1)	0,91(3)
C(6)	- O(6)	1,258(3)	C(10)	- H(10 2)	0,98(4)
C(5)	- C(7)	1,546(5)	C(11)	- H(11)	1,00(3)
C(7)	- C(8)	1,515(6)	C(12)	- H(12 1)	0,97(6)
C(5)	- C(9)	1,543(4)	C(12)	- H(12 2)	0,98(4)
C(9)	- C(10)	1,522(6)	C(12)	- H(12 3)	0,98(5)
C(10)	- C(11)	1,526(5)	C(13)	- H(13 1)	1,01(4)
C(11)	- C(12)	1,518(6)	C(13)	- H(13 2)	1,03(4)
C(11)	- C(13)	1,511(8)	C(13)	- H(13 3)	0,87(5)
Ni	- N(14)	2,055(3)	C(15)	- H(15)	0,89(3)
N(14)	- C(15)	1,369(4)	C(16)	- H(16)	0,75(5)
C(15)	- C(16)	1,338(6)	N(17)	- H(17)	0,97(4)
C(16)	- N(17)	1,382(5)	C(18)	- H(18)	0,93(3)
N(17)	- C(18)	1,328(6)			
C(18)	- N(14)	1,327(4)			
Ni	- O(6)	2,226(2)			

TABLE VI.7

## INTRAMOLECULAR BOND ANGLES AND THEIR E.S.D's IN DEGREES

N(1)	- Ni	- N(1 <sup>i</sup> )	180,0(1)	C(4)	- C(5)	- C(7)	108,0(3)
N(1)	- Ni	- N(14)	89,3(1)	C(6)	- C(5)	- C(7)	109,2(2)
N(1)	- Ni	- N(14 <sup>i</sup> )	90,7(1)	C(5)	- C(7)	- C(8)	114,8(3)
N(14)	- Ni	- N(14 <sup>i</sup> )	180,0(1)	C(4)	- C(5)	- C(9)	108,5(2)
Ni	- N(1)	- C(2)	144,1(2)	C(6)	- C(5)	- C(9)	109,3(2)
N(1)	- C(2)	- N(3)	118,1(2)	C(7)	- C(5)	- C(9)	109,8(2)
C(2)	- N(3)	- C(4)	126,2(2)	C(5)	- C(9)	- C(10)	114,6(2)
N(3)	- C(4)	- C(5)	117,6(2)	C(9)	- C(10)	- C(11)	114,3(3)
C(4)	- C(5)	- C(6)	112,0(2)	C(10)	- C(11)	- C(12)	111,5(4)
C(5)	- C(6)	- N(1)	123,6(2)	C(10)	- C(11)	- C(13)	111,2(3)
C(6)	- N(1)	- C(2)	122,4(2)	C(12)	- C(11)	- C(13)	111,3(4)
C(6)	- N(1)	- Ni	93,5(1)	Ni	- N(14)	- C(15)	128,0(2)
N(1)	- C(2)	- O(2)	122,0(2)	N(14)	- C(15)	- C(16)	110,3(3)
N(3)	- C(2)	- O(2)	119,9(2)	C(15)	- C(16)	- N(17)	106,3(4)
N(3)	- C(4)	- O(4)	120,9(2)	C(16)	- N(17)	- C(18)	106,6(3)
C(5)	- C(4)	- O(4)	121,5(3)	N(17)	- C(18)	- N(14)	112,0(3)
C(5)	- C(6)	- O(6)	120,1(2)	C(18)	- N(14)	- Ni	126,7(2)
N(1)	- C(6)	- O(6)	116,3(2)	C(18)	- N(14)	- C(15)	104,9(3)

TABLE VI.8

## LEAST-SQUARES PLANES

The equations of the planes are expressed in  
orthogonalised space as  $PI + QJ + RK = S$

Plane I	square planar configuration involving the nickel and nitrogen atoms								
Atoms defining the plane	Ni	N(1)	N(14)	N(1 <sup>†</sup> )	N(14 <sup>†</sup> )				
Atoms not included in the plane						0(2)	0(6)		
Distance from the plane, Å	0,0	0,0	0,0	0,0	0,0	-2,016	1,952		
Equation	$0,71545I + 0,13755J + 0,68499K = 0,00$								
Plane II	through the 5 atoms of the imidazole ring								
Atoms defining the plane	N(14)	C(15)	C(16)	N(17)	C(18)				
Distance from the plane, Å	-0,001	0,001	-0,002	0,001	0,000				
Equation	$0,78785I - 0,42039J + 0,45007K = 0,19227$								
Plane III	through the 6 pyrimidine ring atoms								
Atoms defining the plane	N(1)	C(2)	N(3)	C(4)	C(5)	C(6)			
Atoms not included in the plane							0(2)	0(4)	0(6)
Distance from the plane, Å	0,003	0,006	-0,009	0,003	0,005	-0,008	0,019	-0,001	-0,011
Equation	$0,64340I + 0,25957J - 0,72018K = -0,05739$								
Plane IV	through the 9 atoms of the trioxypyrimidine ring								
Atoms defining the plane	N(1)	C(2)	N(3)	C(4)	C(5)	C(6)	0(2)	0(4)	0(6)
Distance from the plane, Å	0,001	0,000	-0,014	0,003	0,010	-0,004	0,008	0,000	-0,004
Equation	$0,64601I + 0,26122J - 0,71724K = -0,05807$								
Plane V	through the atoms of the hydrocarbon chain attached at C(5)								
Atoms defining the plane	C(5)	C(7)	C(8)	C(9)	C(10)	C(11)			
Atoms not included in the plane							C(12)	C(13)	
Distance from the plane, Å	-0,020	0,055	-0,030	-0,027	0,049	-0,026	-1,147	0,426	
Equation	$-0,21224I + 0,95481J + 0,20809K = -3,16104$								

## INTERSECTION ANGLES

Planes I and II	35,50°	Planes II and III	85,78°
Planes I and III	89,85°	Planes III and IV	0,25°
Planes I and IV	89,61°	Planes III and V	87,79°

The bond angles N(1)-Ni-N(14) and N(1)-Ni-N(14<sup>i</sup>) with values 89,3(1) and 90,7(1)° respectively indicate regular geometry. However the distorted octahedral configuration arises from the positions of O(6) and O(6<sup>i</sup>) which lie off the normal to plane I (i.e. "off-the-z-axis"). This may be seen from the angles N(1)-Ni-O(6) and N(14)-Ni-O(6) which are 61,33(8) and 89,14(9)° respectively while the "off-the-z-axis angle" is 28,73°. This type of bonding is similar to, but much stronger than the off-the-z-axis interactions occurring in complexes 1 and 2 (chapters III and IV) and is discussed more fully in a later section.

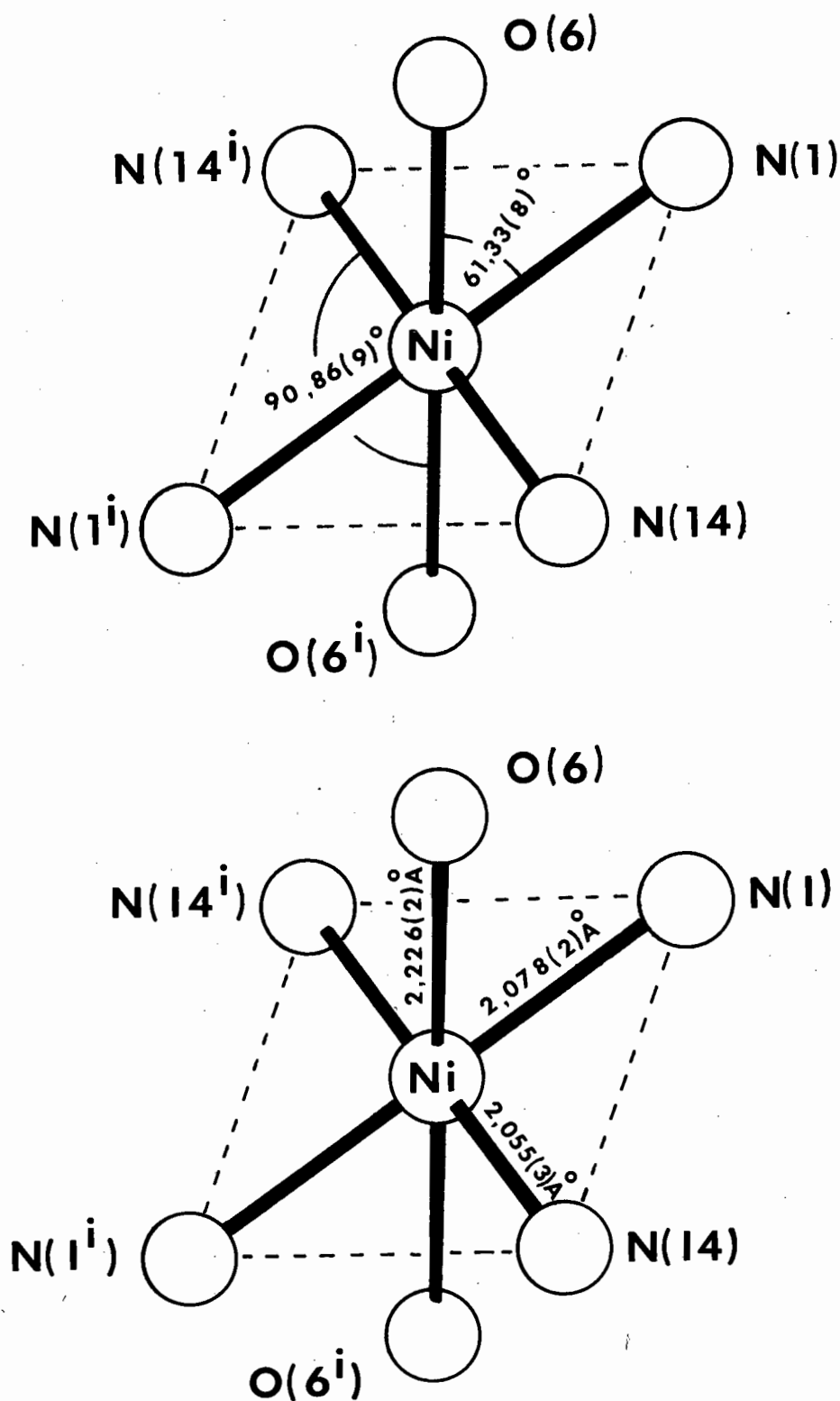
Figure VI.8 is an illustration of the nickel coordination sphere while Table VI.9 lists the relevant bond lengths and angles.

TABLE VI.9  
BOND LENGTHS (Å) AND ANGLES (DEGREES) AND THEIR E.S.D.'s  
IN THE NICKEL COORDINATION SPHERE.

Ni	- N(1)	: 2,078(2)	N(1)	- Ni	- O(6)	61,33(8)°
Ni	- N(14)	: 2,055(3)	N(14)	- Ni	- O(6)	90,86(9)
Ni	- O(6)	: 2,226(2)	N(1)	- Ni	- O(6 <sup>i</sup> )	118,67(8)
N(1)	- O(6)	: 2,199(3)	N(14)	- Ni	- O(6 <sup>i</sup> )	89,14(9)
N(14)	- O(6)	: 3,052(4)	O(6)	- N(1)	- N(14)	71,92(9)
N(14 <sup>i</sup> )	- O(6)	: 3,006(4)	O(6)	- N(1)	- N(14 <sup>i</sup> )	69,94(9)
N(1)	- N(14)	: 2,906(4)	O(6)	- N(14)	- N(1)	43,23(7)
N(1)	- N(14 <sup>i</sup> )	: 2,939(4)	O(6)	- N(14)	- N(1 <sup>i</sup> )	76,33(9)

### The imidazole ring

The bond lengths within the ring agree within experimental error with those reported by Wang and Craven<sup>23</sup> for the bis-(5,5 -diethylbarbiturato)-bisimidazole complex of Zn(II) and with those reported by Lundberg<sup>45</sup> for the complex di-imidazole-zinc(II) dichloride. The ring is planar, the greatest deviation from the least squares plane through the five atoms (plane II) being that of C(16) at a distance of 0,002Å. This plane and plane I intersect at an angle of 35,50°.



## THE NICKEL COORDINATION SPHERE

FIG. VI.8

### The barbiturate ligand structure

The bond lengths and angles in general show good agreement with those reported for two polymorphs of the parent 5-ethyl-5-isoamylbarbituric acid<sup>60</sup>.

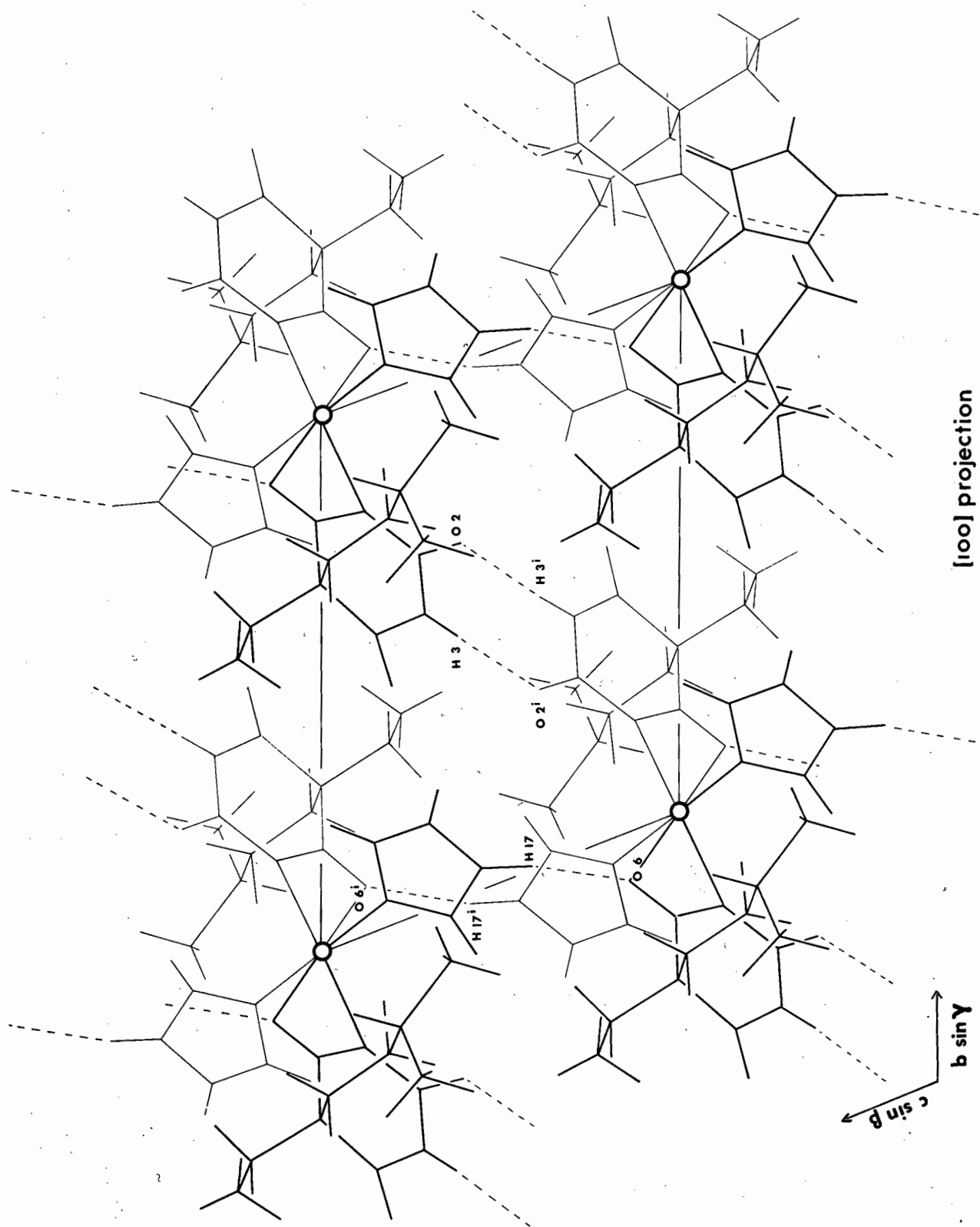
The pyrimidine ring is planar (plane III) with the largest deviation from this plane being that of atom N(3) at a distance of  $-0,009 \text{ \AA}$ . When the three exocyclic oxygen atoms are included in the calculation, it is seen that the entire trioxypyrimidine ring is planar (plane IV) the largest deviation being that of atom N(3) again, at a distance of  $-0,014 \text{ \AA}$ . The coplanarity of the exocyclic oxygen atoms and the pyrimidine ring atoms is further illustrated by the small angle of intersection of planes III and IV ( $0,25^\circ$ ). Planes I and III intersect at  $89,85^\circ$ , i.e. the plane Ni, N(1), N(14) and the pyrimidine ring plane are perpendicular. Similarly the planes through the two different moieties of the molecule, i.e. through the imidazole ring (plane II) and the pyrimidine ring (plane III) are approximately normal to each other ( $85,78^\circ$ ). The hydrocarbon chain from C(8) through C(5) to C(11) forms a plane (plane V) which is virtually normal ( $87,79^\circ$ ) to the pyrimidine ring plane (plane III). This is consistent with that observed in the parent acid.

### Hydrogen bonding

The intermolecular hydrogen bonding is shown as dotted lines in Figures VI.9 and VI.10, the  $[100]$  and  $[010]$  projections of the structure. Figure VI.11 is an illustration of the  $[001]$  projection. The geometry of the hydrogen bond interactions is shown in Figure VI.12 while all relevant bond angles are listed in Table VI.10.

Each discrete molecule of the complex is linked to four other molecules by N-H ... O hydrogen bonds arising from the interaction of the imidazole NH and barbiturate NH groups with barbiturato oxygen atoms.

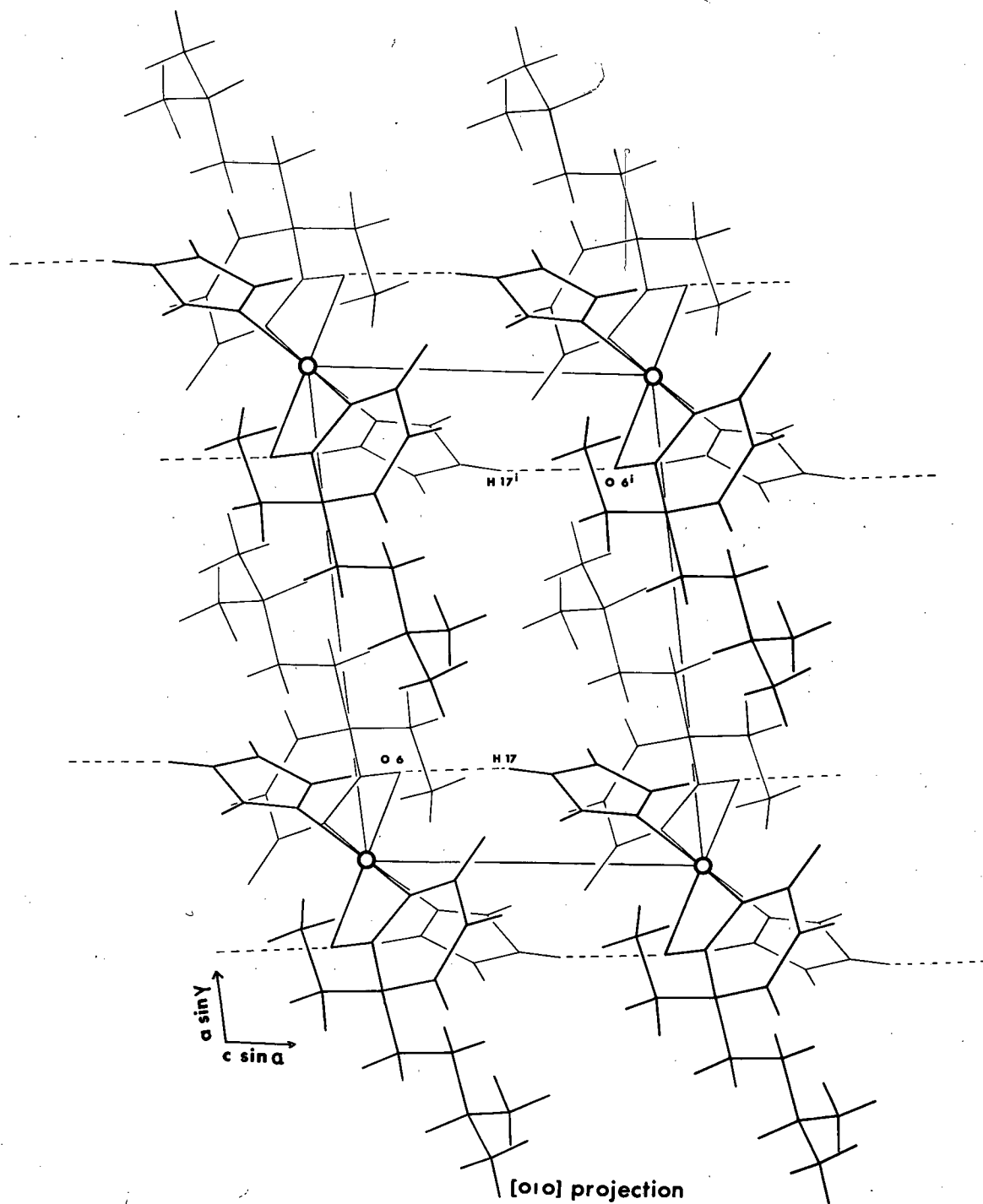
Atom H(17) of the molecule at  $x,y,z$  is hydrogen bonded to O(6) of the molecule at  $x,y,(z-1)$ . As a result of centrosymmetry, H(17<sup>i</sup>) of the molecule

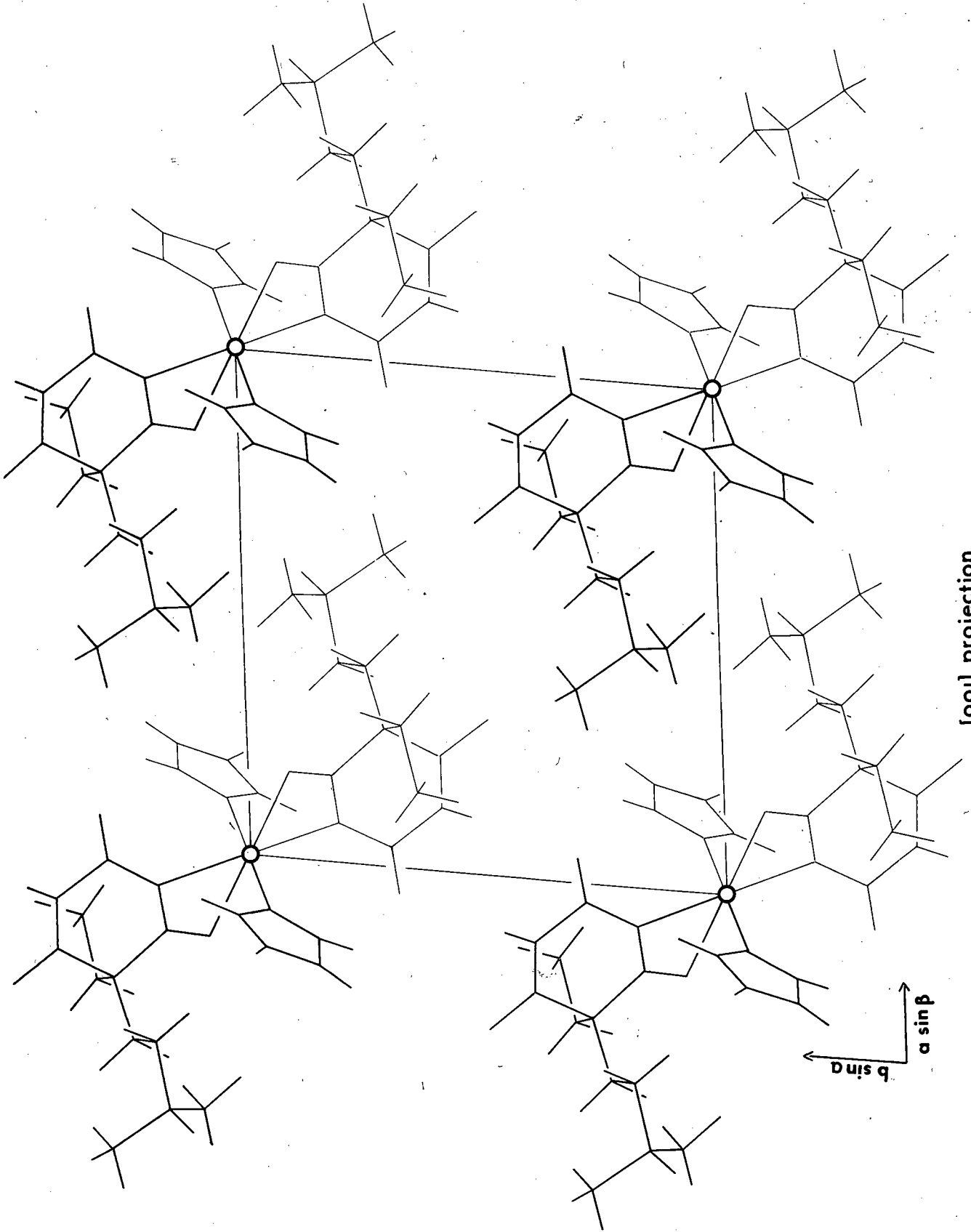


[100] projection

FIG. VI.9

FIG. VI.10





[001] projection

FIG. VI.11

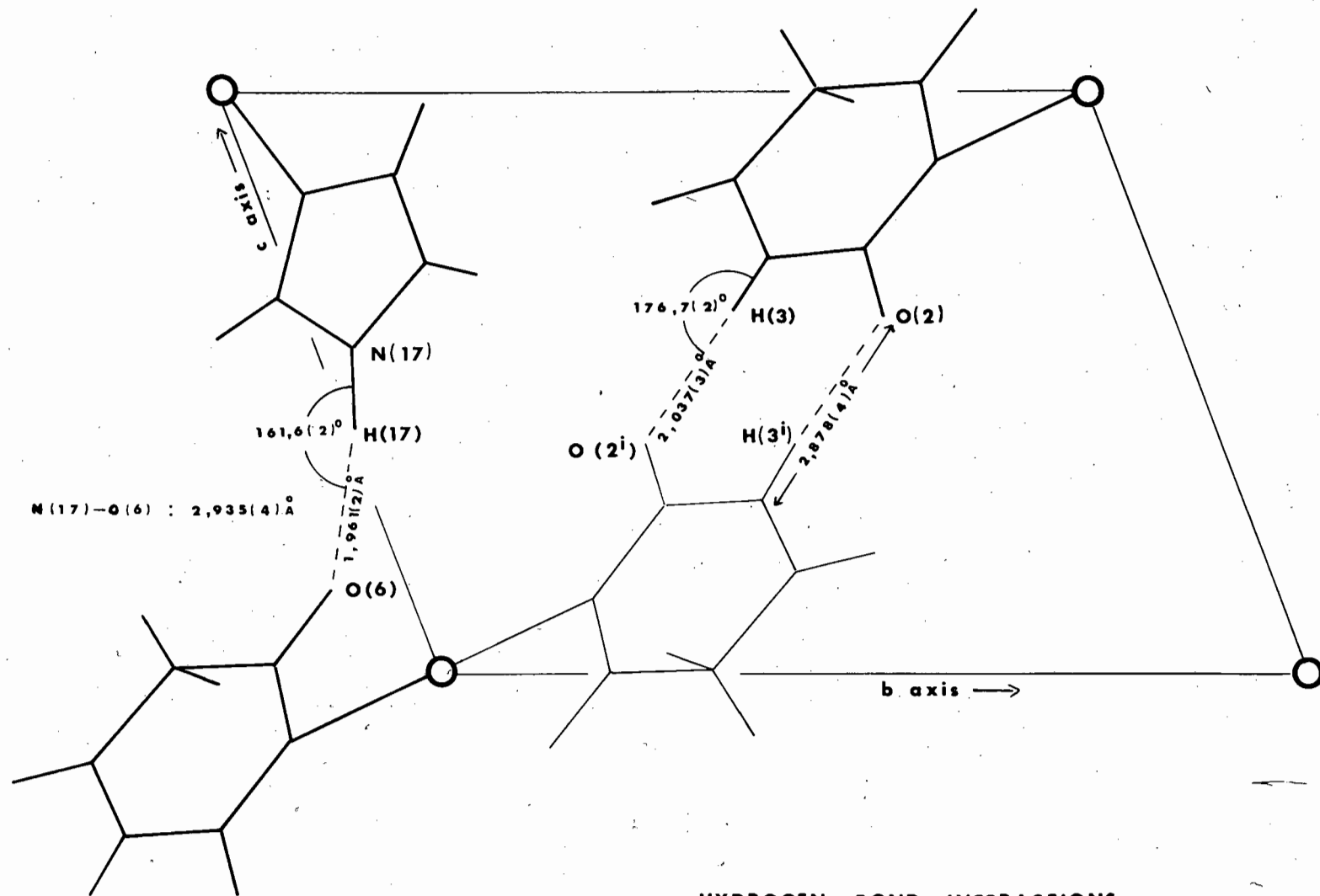
at  $x,y,z$  is hydrogen-bonded to  $O(6^i)$  of the molecule at  $x,y,(z+1)$ . These bonds form a double linkage joining adjacent molecules along the  $c$  cell axis thereby generating an infinite chain of hydrogen-bonded molecules in the  $z$  direction. The parallel chains are themselves joined by hydrogen bonds. Atoms  $H(3)$  and  $O(3)$  of the molecule at  $x,y,z$  are linked to atoms  $O(2^i)$  and  $H(3^i)$  respectively of the molecule at  $x,(y-1),(z-1)$ . These bonds occur as a double bridging linkage in the centre of the  $yz$  plane and approximately parallel to the short diagonal of the  $bc$  face.

There are thus only two crystallographically distinct hydrogen bonds,  $N(17)-H(17) \dots O(6)$  and  $N(3)-H(3) \dots O(2^i)$ . However, each molecule has associated with it a total of eight hydrogen bonds which emanate as four centrosymmetric pairs.

TABLE VI.10  
BOND LENGTHS ( $\text{\AA}$ ) AND ANGLES (DEGREES) AND THEIR  
E.S.D's INVOLVED IN THE HYDROGEN BONDING

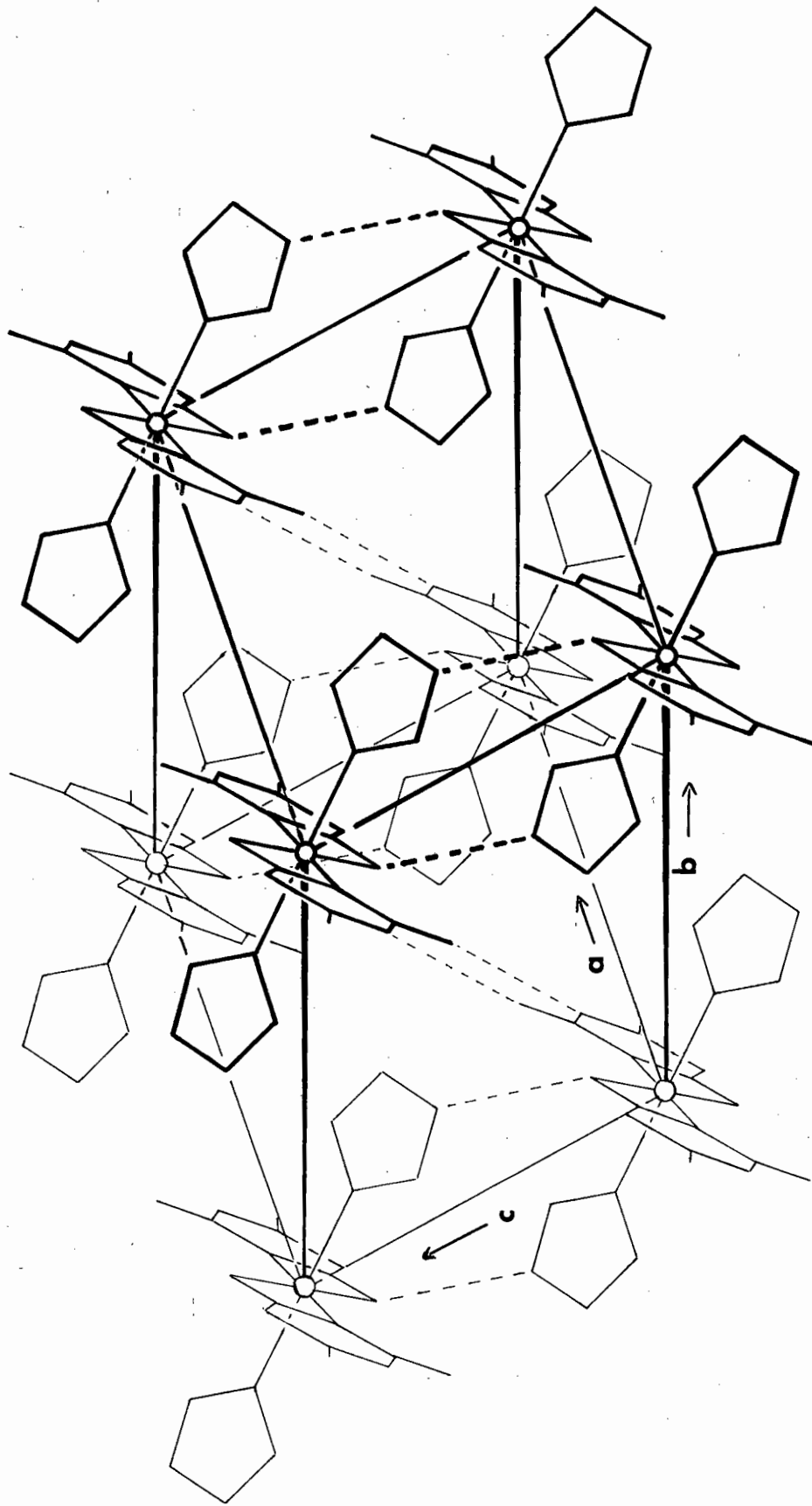
$H(3) - O(2^i)$	:	2,037(3)
$N(3) - O(2^i)$	:	2,878(4)
$N(3)-H(3)-O(2^i)$	:	176,7(2)
$H(17) - O(6)$	:	1,961(2)
$N(17) - O(6)$	:	2,935(4)
$N(17)-H(17)-O(6)$	:	161,6(2)

The packing of the molecules in the unit cell and the hydrogen bond scheme is well illustrated in Figure VI.13, in which the barbiturate side chains have been omitted for clarity.



**HYDROGEN-BOND INTERACTIONS**

FIG. VI.12



FIGS. VI.13

CHAPTER VII

DISCUSSION OF THE CRYSTAL AND  
MOLECULAR STRUCTURES OF THE COMPLEXES.

## VII.1 PREVIOUS STUDIES ON BARBITURATE COMPLEXES

Before discussing the structural features of the four complexes it is necessary to review earlier structural studies on metal-barbiturate complexes.

The first complex of the type  $M(II)(\text{barb})_2L_2$  was prepared in 1931 by the Dutch chemist Zwikker who reacted 5,5-diethyl barbituric acid with an aqueous solution of copper sulphate in pyridine. He assigned the formula  $\text{Cu}(\text{barbital})_2(\text{pyridine})_2$  to the compound.

Fialkov and Rapaport<sup>50</sup> prepared a series of  $\text{Cu}(\text{barb})_2(\text{pyridine})_2$  complexes. The components  $\text{CuSO}_4$ , barbiturate and pyridine were mixed in the molar ratio 1:2:(4 to 10) in the presence of one or two moles NaOH. Mono and bis-barbiturate complexes were obtained depending on the molar ratio of sodium hydroxide and barbiturate. In experiments with equimolar amounts of sodium hydroxide and barbiturate, bis-barbiturate complexes with the general formula  $\text{Cu}(\text{barb})_2(\text{pyridine})_2$  were obtained for luminal, amytal and pronarcone (nos. 4, 6 and 18 Table I.1). Here "barb" refers to the anion of the barbiturate in the monobasic form. These complexes were also obtained in the absence of sodium hydroxide for the barbiturates veronal (no. 1, Table I.1), luminal and amytal. In cases when two moles sodium hydroxide were used per mole barbiturate, mono-barbiturate complexes were formed with luminal, veronal and amytal. These were of the form  $\text{Cu}(\text{barb})_2(\text{pyridine})_2$  where "barb" this time is the dibasic form of the acid.

The structure of the former type, i.e.  $\text{Cu}(\text{barb})_2(\text{pyridine})_2$  was postulated as one of two possibilities in which copper has a coordination number of 6 (Figs. VII.1 and VII.2).

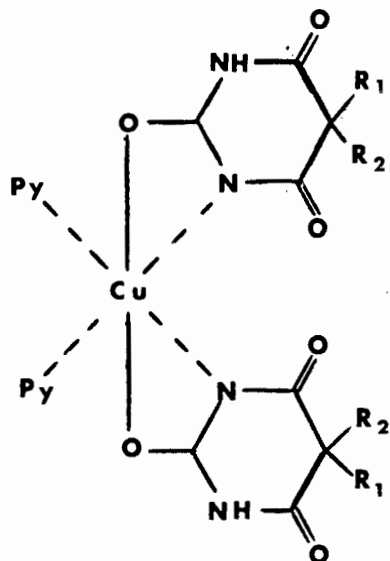


FIG. VII.1

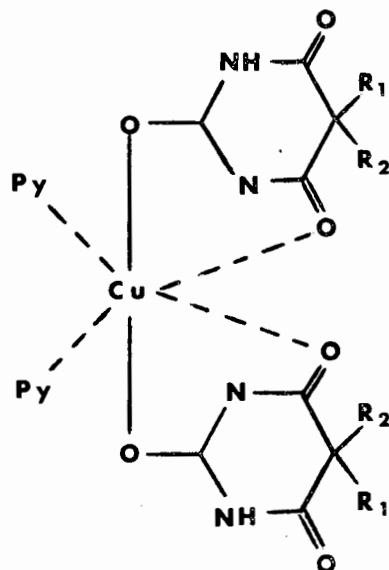


FIG. VII.2

On the other hand the mono-barbiturate complex was given the structural formulation shown in Fig. VII.3.

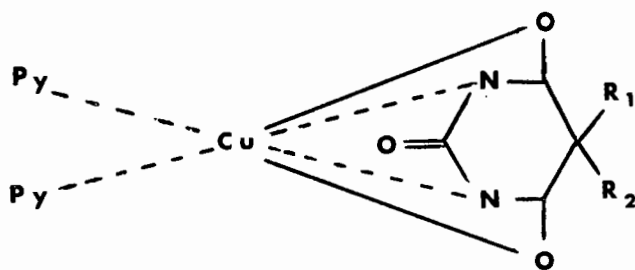
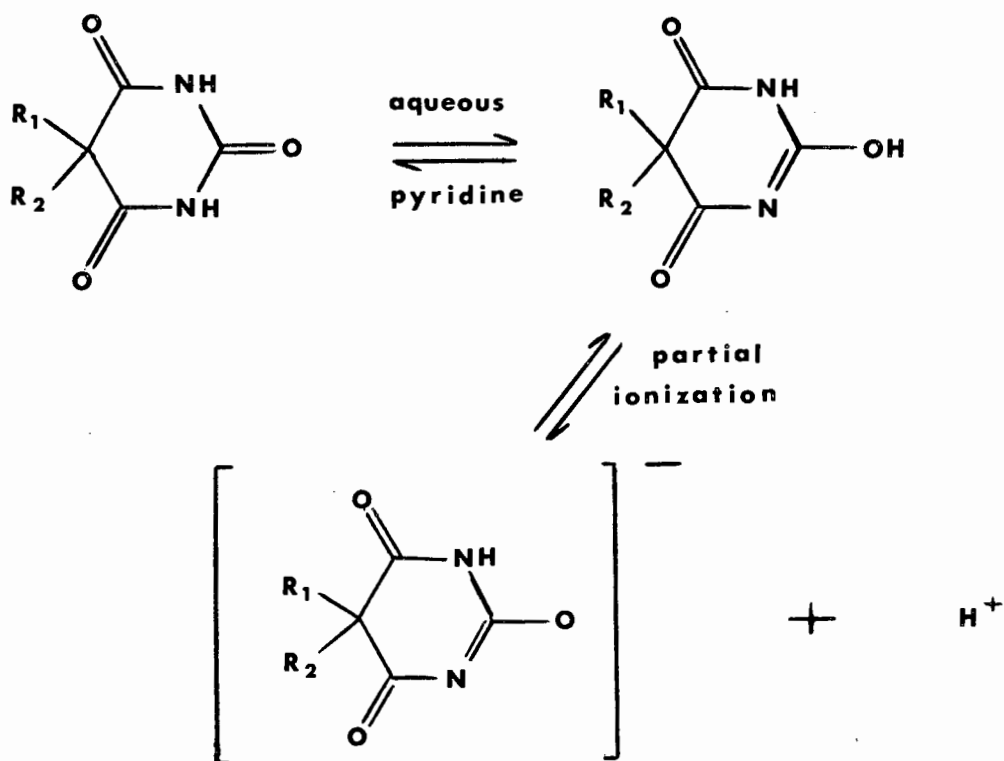


FIG. VII.3

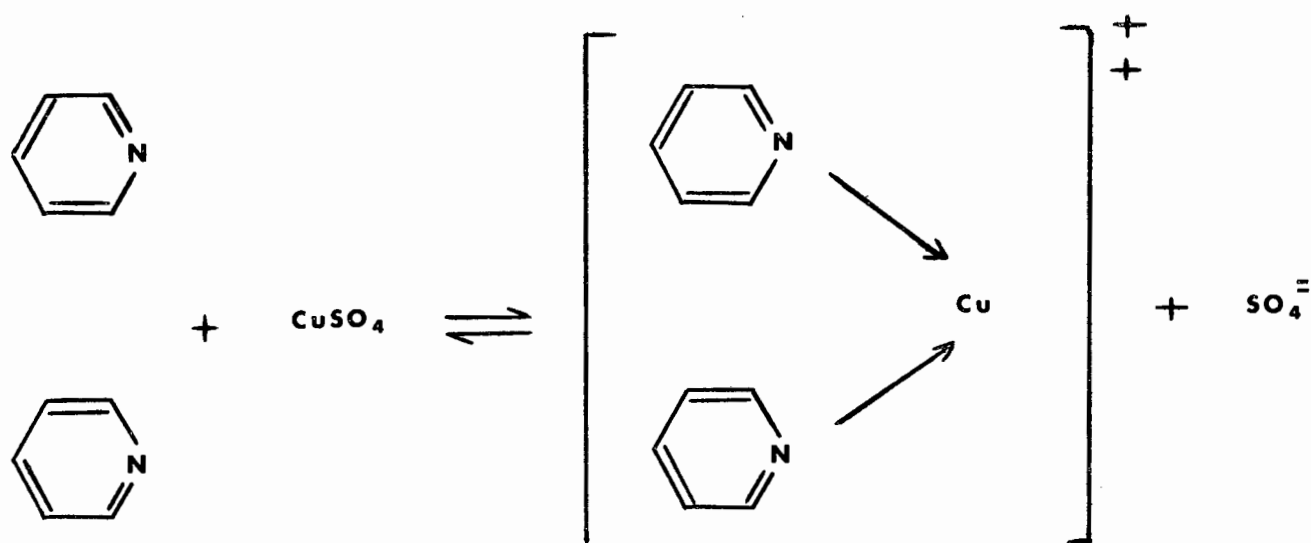
Levi and Hubley<sup>22</sup> prepared a series of 12 complexes of the same type as those of Fialkov and Rapaport, viz.  $\text{Cu(II)(barb)}_2(\text{pyridine})_2$ . They postulated the following mechanism for the formation of the complexes:

- (i) enolization followed by partial ionization of the tautomeric hydroxyl group of the barbiturate anion thereby providing a pyrimidine oxygen atom as a

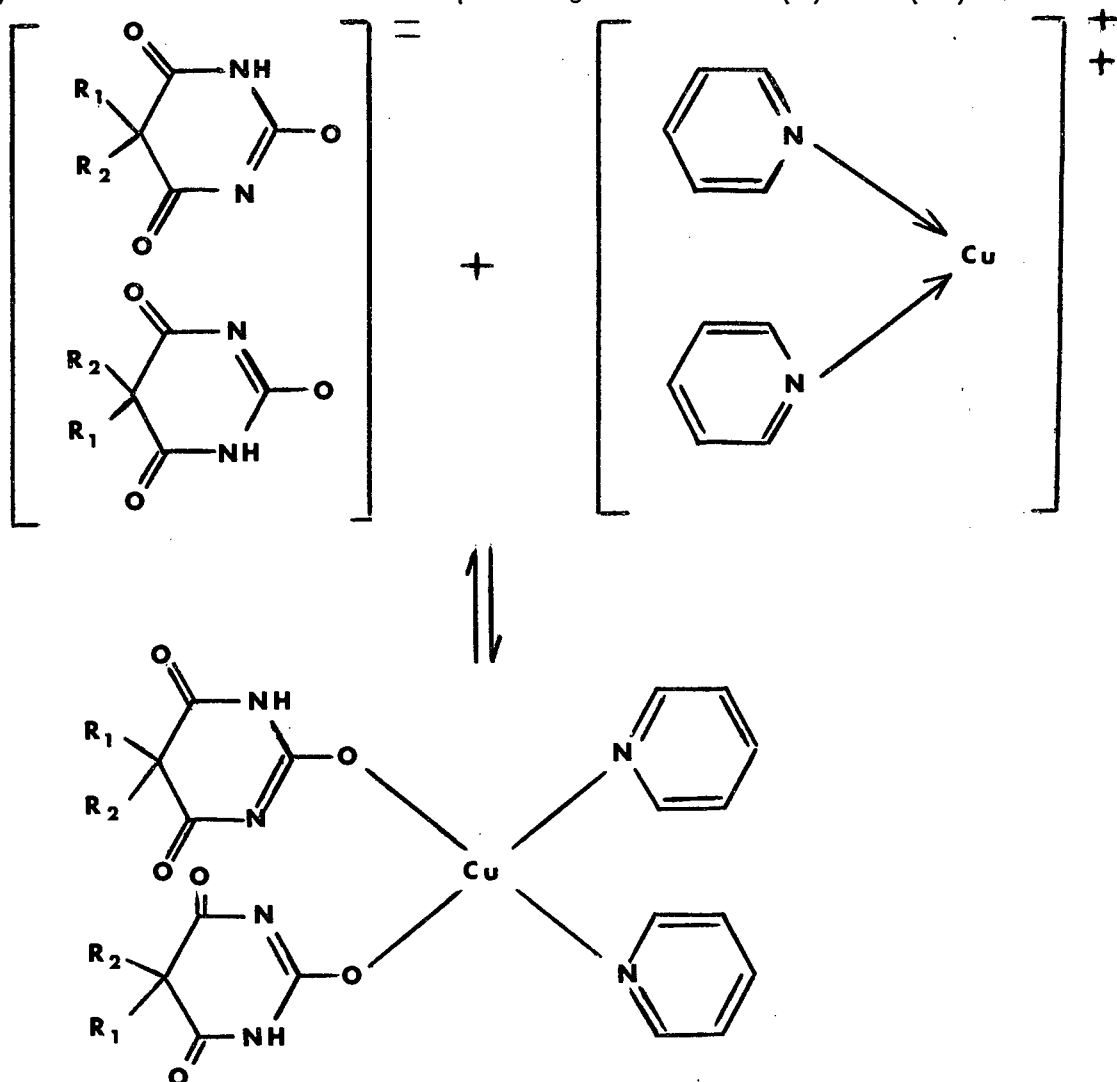
coordination site;



(ii) formation of a positively charged copper-pyridine complex ion;



(iii) interaction of the ionic species generated in (i) and (ii) above:



In accordance with this mechanism the pH of the barbituric acid solutions was found to decrease appreciably when the copper-pyridine solution was added to the barbiturate solution. This decrease in pH is due to the liberation of  $H^+$  ions in step (i) above.

Further evidence for their proposed mechanism was provided by consideration of the dissociation constants of the acids and product yields. It was observed that for those acids with relatively larger  $K$  values, the formation of their complexes occurred more rapidly. For alphenal ( $K = 4,2 \times 10^{-9}$ ), complex formation occurred instantaneously while ipral ( $K = 1,1 \times 10^{-9}$ ), formed its complex very sluggishly.

As has been mentioned earlier Levi and Hubley also carried out a study of the infra red absorption spectra of the free barbituric acids and

concluded that coordination was via the carbonyl group in the 2-position as had been predicted by their proposed mechanism. The spectra also showed that a greater degree of intermolecular hydrogen bonding occurs in the complexes than in the free barbituric acids.

Craciunescu *et al*<sup>51</sup> have reported the preparation of  $\text{Cu}(\text{barb})_2\text{L}_2$  complexes where L is  $\alpha$ ,  $\beta$ ,  $\gamma$  picoline, 2,4 lutidine, 2,6 lutidine, 2,4,6 collidine and where barb is luminal, veronal, cyclobarbital.

Wang and Craven<sup>23</sup> have reported the first crystal structure determinations of complexes involving a transition metal and a barbiturate. They have elucidated the structures of the bis-(5,5-diethylbarbiturato)-bisimidazole complexes of cobalt (II) and zinc (II). The complexes were prepared at room temperature by mixing aqueous solutions of the metal chloride, sodium barbital and imidazole in the molar ratio 1:2:2. The two structures are isomorphous. It is interesting to note that the metal atom in each case, is tetrahedrally coordinated to the nitrogen atoms of two imidazole molecules and to the deprotonated NITROGEN atoms of the two barbital anions. This is in direct contradiction to the findings of Levi and Hubley<sup>22</sup>.

The structural investigations described above provide a basis for comparison with the studies and results of this thesis. This aspect is thus considered in the next sections.

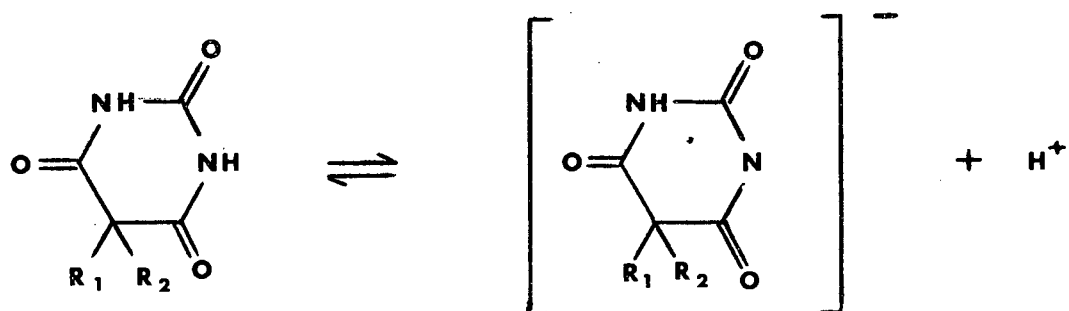
## VII.2 PROPOSED FORMATION MECHANISM OF M(II)(BARB)<sub>2</sub>L<sub>2</sub> COMPLEXES

In Chapter I.4 the principle of hard and soft acids and bases was discussed. It would now be of interest to attempt an explanation of the formation of complexes of the type M(II)(barb)<sub>2</sub>L<sub>2</sub> in terms of the HSAB theory before postulating a formation mechanism.

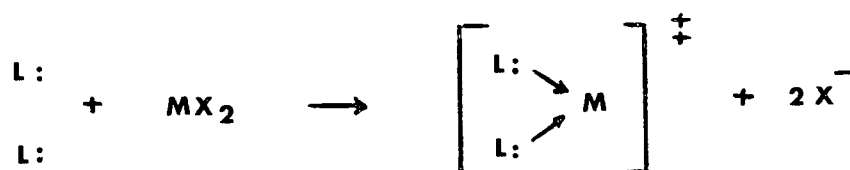
The three metals involved in the complexes, copper, zinc and nickel have all been classified as borderline cases and are neither soft nor hard acids. Similarly, the pyridines have been classified as borderline. However, examples have already been described where the process of symbiosis has rendered various borderline metal ions hard or soft depending upon the nature of the environment. All four complexes described in this thesis as well as those of Wang and Craven<sup>23</sup> and Caira *et al*<sup>27</sup> were synthesized in aqueous solution and it is therefore suggested that the hard sphere or solvation in each case symbiotically renders the metal ions hard. Since the complexes are stable it is assumed that the barbiturate and organic ligands are both behaving as hard bases and that the complex is a hard acid - hard base combination.

As far as the actual mechanism is concerned, nothing conclusive can be stated until kinetic and n.m.r. investigations are undertaken. Crystallographic studies of the parent barbiturates have shown that they exist in the keto tautomeric form. (However, this need not necessarily be the case in solution). Furthermore, this project and other studies<sup>23,27</sup> have shown that in the metal complex, coordination occurs via a deprotonated nitrogen atom. On the basis of these two experimental facts the following mechanism for the formation of M(II)(barb)<sub>2</sub>L<sub>2</sub> is proposed. It can be postulated that in solution a keto-enol tautomeric equilibrium might exist but that only the keto form complexes when the solution of the metal salt is added. This upsets the equilibrium until more of the keto form is generated.

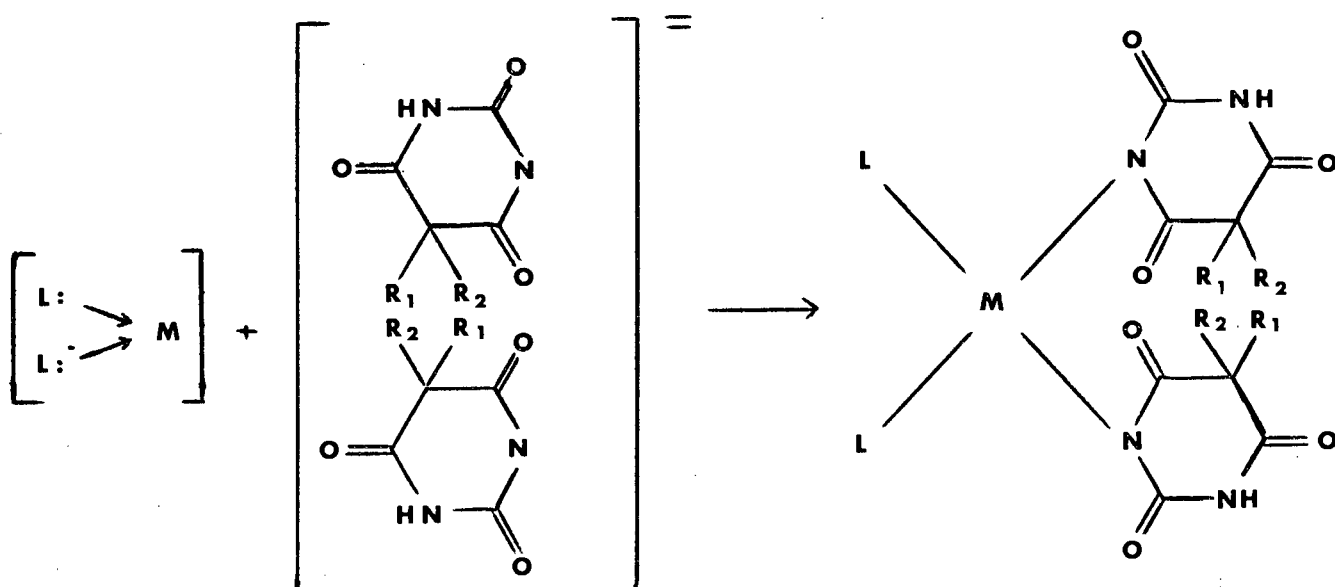
(i) partial ionization of the keto tautomer



(ii) formation of a positively charge metal-organic base complex ion. This is analagous to step (ii) in the mechanism proposed by Levi and Hubley<sup>22</sup> for  $\text{Cu}(\text{barb})_2(\text{pyridine})_2$  complexes.



(iii) interaction of the ionic species generated in (i) and (ii) above.



The above is thus offered as a possible mechanism of formation for complexes of the type  $M(II)(\text{barb})_2L_2$ . It must be appreciated however that the above treatment is merely hypothetical as no actual study of the mechanistic pathway was undertaken during the course of this project.

### VII.3 STRUCTURAL FEATURES OF THE COMPLEXES

#### Metal coordination sphere

One of the most important results of the structural investigations is the elucidation of the coordination site on the barbiturate. This has now been unequivocally established as a deprotonated nitrogen atom in all four complexes in which three different metals and three different barbiturate ligands were involved. It is thus in agreement with the observations of Wang and Craven<sup>23</sup> who also found nitrogen to be the coordination site in the isomorphous barbital-imidazole complexes of zinc and cobalt. On the other hand, the prediction of Levi and Hubley<sup>22</sup> that a barbiturate oxygen atom is involved in the coordination is now shown to be incorrect. Their postulate was based on the fact that in the IR spectra of the complexes, only two bands could be assigned to  $\nu\text{C}=\text{O}$ . However the IR spectra determined in this project (and discussed in the following Chapter (VIII)), have revealed a third band in the  $1600\text{ cm}^{-1}$  region which has been assigned to  $\nu\text{C}=\text{O}$  and this, together with other spectral evidence is consistent with the features of the metal coordination spheres observed in the X-ray analyses.

Perhaps the most interesting feature of the structures is the off-the-z-axis coordination that occurs in the two copper complexes described in Chapters III and IV. As has been mentioned earlier, this type of coordination has been observed in the complex *trans*-Bis[(chloroacetato)-( $\alpha$ -picoline)]copper(II) reported by Davey and Stephens<sup>37</sup>. In this structure the copper atom is surrounded by four ligand atoms (two oxygens and two nitrogens) in a virtually square planar arrangement. Two further oxygen atoms from the chloroacetate ligands are  $2,707\text{ \AA}$  from the copper atom and lie  $36,1^\circ$  off the normal to the square plane. A similar interaction has also been observed in the complex<sup>52</sup> diacetatodiamine copper (II) in which the Cu-O separation is  $2,77\text{ \AA}$ .

Further comparison may be obtained with the first of the structures reported by Bell, Freeman and Wood<sup>53</sup> involving copper with mixed imidazole and glycine peptide ligands. Here, carboxylate and perchlorate oxygen atoms occupy the axial positions of a distorted octahedron at Cu-O distances of 2,36(1) and 2,97(1) Å respectively. The donor ligand atoms of the equatorial plane are the imidazole nitrogens (Cu-N : 1,96(1) and 1,95(1) Å), an amino nitrogen (Cu-N : 2,02(1) Å) and a peptide oxygen atom (Cu-O : 2,01(1) Å). In the structure Cu(II)(barbital)<sub>2</sub>(pyridine)<sub>2</sub> reported by Caira<sup>27</sup> exactly the same type of off-the-z-axis coordination occurs as that found in complexes 1 and 2 of this thesis.

The copper stereochemistry of the complexes Cu(II)(barbital)<sub>2</sub>(β-picoline)<sub>2</sub>.2H<sub>2</sub>O and Cu(II)(brallobarbital)<sub>2</sub>(pyridine)<sub>2</sub>.2H<sub>2</sub>O may thus be considered as square planar or distorted octahedral depending upon whether the off-the-z-axis oxygen atoms are considered to be bonded or not bonded to the copper. Since the Cu-N bond lengths (1,980(5) and 2,018(3) Å for no. (1) and 2,06(2) and 1,97(3) Å for no. (2) are not quite as small as usually found for square planar copper complexes<sup>54</sup> (1,90 Å) it seems likely that an interaction between copper and the oxygen atoms does indeed exist. However these interactions can be regarded only as weak owing to the long Cu-O distances and the large angle between the Cu ... O directions and the z axis. As such the complexes are classified as square planar and may be said to display pseudo-octahedral geometry.

Another interesting feature is that in both complexes as well as the one reported by Caira *et al*, a similar weaker interaction seems to exist between the copper and the second of the two carbonyl oxygens adjacent to N(1). It can be seen that as either of the two interactions becomes stronger, i.e. as the structure approaches regular octahedral geometry, so the second interaction will become weaker as the particular oxygen becomes more remote relative to the copper.

It can now be seen that the structure predicted by Fialkov and Rapaport<sup>50</sup> (Fig. VII.1) for  $\text{Cu}(\text{barbiturate})_2(\text{pyridine})_2$  complexes is remarkably accurate when compared to the structures of complexes 1 and 2 and that reported by Caira *et al.*

In the structure of  $\text{Ni(II)}(\text{amylobarbital})_2(\text{imidazole})_2$  described in Chapter VI the off-the-z-axis interaction between the nickel atom and O(6) is strong enough to be considered a proper bond. In this structure, nickel is thus six-coordinate giving the molecule distorted octahedral geometry. As is expected the Ni-O(2) separation is so large ( $>5 \text{ \AA}$ ) that no interaction between these two atoms exists.

Thus, with the exception of the tetrahedral zinc complex of this thesis and the zinc and cobalt complexes of Wang and Craven, the structures of metal-barbiturate complexes are either pseudo or distorted octahedral. It would seem that the barbiturate ligands, in these cases, have a tendency to orientate themselves in the complex in such a way as to permit a metal-oxygen interaction which presumably stabilizes the structure. This feature, of course, immediately provides the necessary stimulus and incentive for investigating further complexes of the same type but with a variety of other metals such as Co, Fe, Mn, Cr and V in an attempt to correlate the metal with a particular bonding configuration.

#### The barbiturate-ligand structures

The internal ring angle C(2)-N(1)-C(6) is of interest in the structures as N(1) is the site at which the original deprotonation takes place. Berking and Craven<sup>55</sup> were first to focus attention on the environment of the deprotonation site by comparing the bond lengths and angles in barbital<sup>56</sup> with that found in its ion<sup>55</sup> (i.e. as the sodium salt). The angle C(2)-N(1)-C(6) is  $126,4^\circ$  in the barbital molecule while in the barbital ion it is  $119,2^\circ$ . This closing of the angle by  $7^\circ$  was interpreted as a consequence of deprotonation.

Furthermore, it was pointed out that the angles at the carbon atoms adjacent to N(1) open from 118,3 and 116,0° in barbital to 123,8 and 121,3° in its ion. The bond lengths too show significant differences in the two structures. The two C-N(1) bonds at the deprotonated nitrogen atom are equal and shorter (1,34 Å) than the corresponding bonds in barbital (1,36 and 1,38 Å).

Conversely the flanking carbonyl bonds C(4)-O(4) and C(2)-O(2) are significantly longer (1,24 vs. 1,21 Å). These relationships are listed in Table VII.1.

The same characteristic features for deprotonation are observed in the crystal structure of calcium barbital trihydrate<sup>57</sup>. Similarly, comparison of the relevant bond lengths and angles in metharbital<sup>58</sup> and sodium metharbital<sup>59</sup> again show the same trends (Table VII.1).

Thus on the basis of the figures shown in Table VII.1 it can be seen that as a result of deprotonation at N(1):

- (i) the angle C(2)-N(1)-C(6) closes by approximately 6°;
- (ii) the angles at the carbon atoms adjacent to N(1), viz. N(1)-C(2)-N(3) and N(1)-C(6)-C(5) open by approximately 5°;
- (iii) the bond lengths N(1)-C(2) and N(1)-C(6) are shortened ( $\sim 0,03$  Å);
- (iv) the bond lengths C(2)-O(2) and C(6)-O(6) are increased ( $\sim 0,03$  Å).

TABLE VII.1

ANGLE OR BOND LENGTH	BARBITAL		METHARBITAL	
	MOLECULE	ION	MOLECULE	ION
C(2)-N(1)-C(6)	126,4°	119,2°	127,6°	121,2°
N(1)-C(2)-N(3)	116,0°	121,3°	116,3°	121,4°
N(1)-C(6)-C(5)	118,3°	123,8°	117,5°	122,4°
N(1)-C(2)	1,380 Å	1,343 Å	1,369 Å	1,339 Å
N(1)-C(6)	1,364 Å	1,339 Å	1,363 Å	1,342 Å
C(2)-O(2)	1,209 Å	1,238 Å	1,206 Å	1,240 Å
C(6)-O(6)	1,214 Å	1,245 Å	1,211 Å	1,233 Å

It is now of interest to compare the bond lengths and angles of the barbital molecule and ion with the analogous values found in complexes 1 and 3, both of which contain barbital as a ligand. From Table VII.2 it can be seen that the bond lengths and angles of these two complexes as well as those

TABLE VII.2

ANGLE OR BOND LENGTH	COMPLEX NO. 1	COMPLEX NO. 3	WANG & CRAVEN <sup>23</sup>	CAIRA <i>ET AL.</i> <sup>27</sup>
C(2)-N(1)-C(6)	122,3°	121,9°	122,1°	124,6°
N(1)-C(2)-N(3)	120,4°	119,9°	119,1°	118,0°
N(1)-C(8)-C(5)	121,1°	120,9°	120,9°	119,2°
N(1)-C(2)	1,346	1,359 Å	1,361 Å	1,374 Å
N(1)-C(6)	1,341	1,362 Å	1,359 Å	1,345 Å
C(2)-O(2)	1,229	1,227 Å	1,223 Å	1,212 Å
C(6)-O(6)	1,239	1,225 Å	1,228 Å	1,222 Å

found in  $\text{Cu}(\text{barbital})_2(\text{pyridine})_2$  and  $\text{Zn}(\text{barbital})_2(\text{imidazole})_2$  are intermediate between those of barbital and those of its ion. However the characteristic changes that accompany deprotonation ((i) to (iv) above) seem to prevail in forming the complexes. In other words the barbital molecule undergoes similar

configurational changes in forming the metal complex as when it becomes deprotonated to form the ion. This is further illustrated by comparing the bond lengths and angles found in the structure of amylobarbital<sup>60</sup> with those found in complex (no. 4), Ni(amylobarbital)<sub>2</sub>(imidazole)<sub>2</sub>. Although the structure of the amylobarbital ion is unknown, Table VII.3 shows that complexation causes (i) the angle at N(1) to close, (ii) the adjacent angles to open, (iii) the adjacent C-N bond lengths to decrease and (iv) the adjacent carbonyl bond lengths to increase. Again, these are the expected

TABLE VII.3

ANGLE OR BOND LENGTH	AMYLOBARBITAL	
	MOLECULE	Ni-COMPLEX
C(2)-N(1)-C(6)	126,2°	122,4°
N(1)-C(2)-N(3)	116,2°	118,1°
N(1)-C(6)-C(5)	118,5°	123,6°
N(1)-C(2)	1,366 Å	1,362 Å
N(1)-C(6)	1,378 Å	1,331 Å
C(2)-O(2)	1,211 Å	1,221 Å
C(6)-O(6)	1,207 Å	1,258 Å

consequences of deprotonation.

If any valid conclusion can be drawn from this data it is that the configuration of barbiturate ligands in metal complexes seem to resemble that of its ion. Thus even though the deprotonated nitrogen atom is coordinated to the metal, the ionic character of the ligand is retained.

All other bond lengths and angles (i.e. those not affected by deprotonation and complexation) within the barbiturate ligands of structures 1, 3 and 4 agree very well with those reported for the parent barbital (structures 1 and 3) and amylobarbital (structure 4). The structure of brallobarbital is unknown.

### The conformation of the trioxypyrimidine rings

Craven et al<sup>61</sup> have compared the conformations of 14 crystallographically independent oxypyrimidine rings in 7 different barbiturate structures. They have found that in each case the ring is nearly planar with slight puckering due to deviations of up to 0,12 Å from the least squares plane through the oxypyrimidine ring. This puckering is thought to occur in one of two modes. The oxypyrimidine rings of vinbarbital<sup>62</sup> and barbital IV<sup>63</sup> for example are puckered symmetrically with respect to the line C(2) ... C(5) whereas in molecules such as barbital I<sup>56</sup>, amylobarbital IIA and IIB<sup>60</sup>,  $\gamma$  methylamylobarbital<sup>64</sup> and in the 1:1 barbital-urea complex<sup>65</sup>, the puckering is asymmetric with respect to this same direction.

The symmetric pucker can be considered as a torsion about C(2) ... C(5) whereas in the asymmetric mode this torsion is combined with a displacement ( $\sim 0,05$  Å) of C(5) from the best least squares plane through the other ring atoms.

It would appear that the rings in complexes 1 and 4 of this thesis are puckered symmetrically with respect to the C(2)...C(5) direction while in complex number 3 the two independent rings are puckered asymmetrically as C(5) is displaced by the relatively large distances of 0,048 and -0,162 Å from the calculated least squares plane through the atoms of the oxypyrimidine ring.

As has been pointed out by Craven et al<sup>61</sup>, differences in the ring puckering mode arise from differences in molecular environment from one crystal structure to another. No correlation between the nature of the substituents at C(5) and puckering exists. Thus at present there seems to be no basis for reliable prediction of molecular conformation in barbiturate crystal structures.

### The hydrocarbon side chain

In all four complexes the spine of the hydrocarbon side chain attached at C(5) defines a plane which is almost normal to the plane of the pyrimidine ring. This is not unusual and has been observed in the structures of the barbiturates, their salts and complexes.

#### VII.4 HYDROGEN BONDING IN THE COMPLEXES

As has been mentioned earlier, hydrogen bonding has been a prominent feature of the crystal structures of barbiturates, their salts and their complexes. The compounds whose structures have been described in this thesis are no exceptions. Before discussing the various hydrogen bonding schemes that have been found to prevail in barbiturates and their complexes, the meaning of the term "hydrogen bond" must be clearly defined.

A hydrogen bond is said to exist when a hydrogen atom is bonded to at least two atoms at the same time<sup>66</sup>. A hydrogen bond may thus be denoted A-H-B. In most hydrogen bond systems, the bond A-H is much stronger than the bond H-B thus allowing the interaction to be denoted as A-H ... B.

The criterion used for the existence of a hydrogen bond<sup>66</sup> is that the distance  $d(\text{H} \dots \text{B})$  shall be less than  $W_{\text{H}} + W_{\text{B}} - 0,2 \text{ \AA}$  where  $W_{\text{H}}$  and  $W_{\text{B}}$  are the van der Waals radii for atoms H and B. In most hydrogen bonds the atoms A and B are electronegative so as to ensure the presence of an acidic hydrogen atom on A and a strong Lewis base B. The atom B nearly always possesses lone-pair electrons which are largely responsible for the formation of the hydrogen bond. The atom to which the hydrogen atom is originally bound (atom A) is known as the donor while atom B is the acceptor.

The hydrogen bond angle, i.e. A-H ... B is expected to be approximately linear. Donohue<sup>39</sup> has listed O-H ... O and N-H ... O hydrogen bond data for several different compounds and concludes that a bent hydrogen bond is the rule rather than the exception with a maximum allowed deviation from linearity of 30°.

The most commonly encountered hydrogen bonds are those of the type O-H ... O and N-H ... O. The acceptor oxygen atom can be provided by a water molecule or by a carbonyl group. Donohue<sup>39</sup> has considered the geometry of

both types in a number of different hydrogen bonded compounds. Where water molecules behave as hydrogen bond acceptors, he has shown that all the atoms concerned (Fig. VII.4) are almost coplanar and that the average  $O \dots HOH \dots O$  angle is  $119^\circ$  while the average  $O \dots HO \dots N$  angle is  $120^\circ$ . He concludes therefore that the perfect tetrahedral water molecule (bond angles  $109^\circ 28'$ )

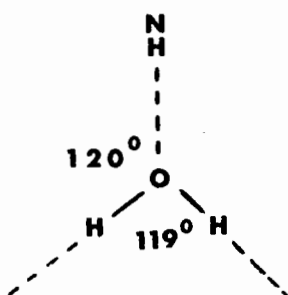
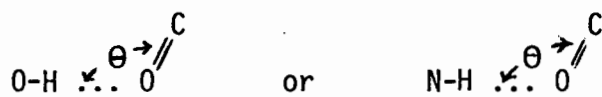


FIG. VII.4

is not a stringent structural feature in hydrogen bonded systems. In fact, the water molecule is best described as being roughly plane trigonal.

Oxygen and carbon atoms are both involved in  $sp^2$  hybridization in the formation of a carbonyl group. Thus, in hydrogen bond systems of the type



it might be expected that the angle  $\theta$  will be close to  $120^\circ$  and the OH or NH donors will lie very nearly in the plane defined by the carbon atom and its three ligands. On the basis of several experimental observations however Donohue shows that there is a wide variation of the above angle from  $120^\circ$  and that there are also large deviations of the NH (or OH) donors from the plane of the carbonyl system.

The hydrogen bonding schemes in the crystal structures of many barbiturates and their complexes have been studied. These show that in general there are two types of intermolecular hydrogen bonding linkage.

These may be termed "cyclic" if the molecules are linked by a pair of NH ... O = C hydrogen bonds giving rise to the frequently encountered doubly hydrogen bonded dimers as between barbital<sup>56</sup> molecules A1 and A2 and B1 and B2 (Fig. VII.5), or "non cyclic" if only one hydrogen bond is formed as between A1 and B1 and A2 and B2. Although there are both cyclic and non cyclic

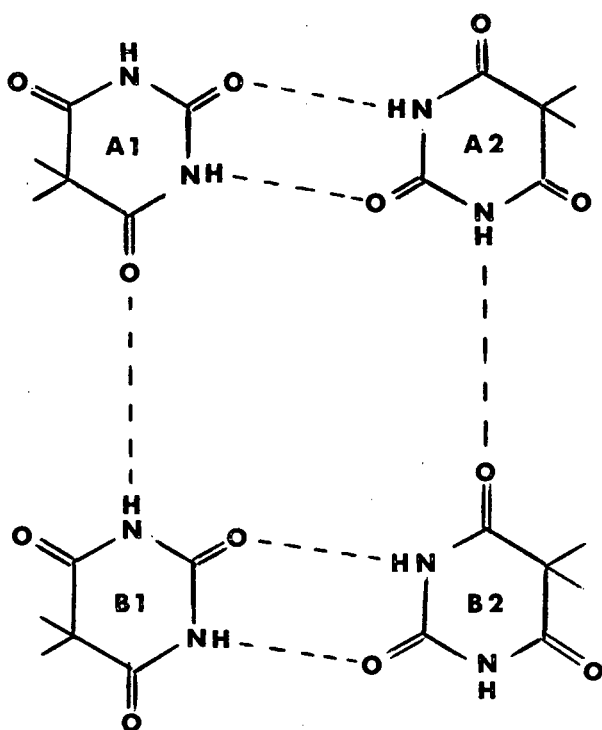


FIG. VII. 5

barbital linkages in barbital polymorph I<sup>56</sup> (Fig. VII.5) and also in the 2:1 barbital-caffeine complex<sup>67,68</sup>, there are crystal structures in which the hydrogen bonding is exclusively cyclic as in barbital polymorph II<sup>56</sup> and amylobarbital polymorphs I and II<sup>60</sup> or exclusively non cyclic as in  $\gamma$ -methylamylobarbital<sup>64</sup>.

Further possibilities for hydrogen bonding variations arise when there are insufficient NH or other donor groups to form structures in which all three barbiturate carbonyl oxygen atoms are hydrogen bonded. Under these circumstances, as we have already seen, C(2)-O(2) and C(4)-O(4) (or C(6)-O(6)) usually

accept one hydrogen bond each and C(6)-O(6) (or C(4)-O(4)) is not hydrogen bonded. (In the isolated barbiturate molecule C(4)-O(4) and C(6)-O(6) are symmetry related, each being bonded to one NH group and are thus equivalent but distinct from C(2)-O(2) which is covalently bonded to two NH groups). This occurs in the 2:1 barbital-caffeine complex<sup>67,68</sup>, the 1:2 complex of phenobarbital with 8-bromo-9-ethyladenine<sup>69</sup>, barbital I<sup>56</sup>,  $\gamma$  methylamylbarbital<sup>64</sup> and amylobarbital I and II<sup>60</sup>. In barbital II<sup>56</sup> it is C(4)-O(4) and C(6)-O(6) that are hydrogen bonded while C(2)-O(2) is not. These crystal structures all contain hydrogen bonded ribbons with different geometries. There are a few structures in which only one carbonyl (but not C(2)-O(2)) participates in two hydrogen bonds while the other two carbonyls are not involved. These include vinbarbital<sup>62</sup> (no. 10, Table I.1), heptabarbital<sup>70</sup> (no. 9, Table I.1) and barbital IV<sup>63</sup>.

The barbiturate-barbiturate hydrogen bonding observed in complexes 3 and 4 of this thesis i.e. Zn(barbital)<sub>2</sub>( $\beta$ -picoline)<sub>2</sub> and Ni(amylobarbital)<sub>2</sub>(imidazole)<sub>2</sub> thus represent the "cyclic mode" of hydrogen bonding described above. In both examples, a double hydrogen bond of the type N(3)-H(3) ... O(2) is formed while in complex no. 4 there is an additional "non cyclic" interaction involving the barbiturato O(6) atom and the imidazole NH group. In the structure Cu(barbital)<sub>2</sub>(pyridine)<sub>2</sub> reported by Caira *et al*<sup>27</sup>, the hydrogen bonding is of the non cyclic type. Here there is only one crystallographically distinct hydrogen bond and this links adjacent molecules of the complex in a zigzag pattern.

The hydrogen bonding in complex no. 1 i.e. Cu(barbital)<sub>2</sub>( $\beta$ -picoline)<sub>2</sub>. 2H<sub>2</sub>O is completely dominated by the presence of hydrate water molecules which have precluded any barbiturate-barbiturate interaction. This complex may be compared with other hydrated barbiturate crystal structures. For example, in the dihydrated form of barbituric acid<sup>9</sup> which is the parent compound of the barbiturates, intermolecular hydrogen bonding with the water molecules is

postulated despite the fact that the hydrogen atom positions were not located. Nevertheless the arrangement of the hydrogen bonds about the water oxygens is approximately trigonal and planar. Other hydrated barbiturate compounds include calcium barbital trihydrate<sup>57</sup> in which centrosymmetrically related barbital ions form doubly hydrogen bonded dimers which themselves are linked via hydrogen bonds with water molecules and guanidinium barbital dihydrate<sup>71</sup> in which hydrogen bonded dimers, similar to those found in the calcium salt of barbital, are observed.

An interesting feature in  $\gamma$ -methylamylbarbital<sup>64</sup> (or 5-ethyl-5-(3,3-dimethylbutyl) barbituric acid) is that the four atoms involved in the NH ... OC hydrogen bonding are almost collinear. This geometry is quite common in other barbiturate crystal structures. For example, the molecules of sodium barbital<sup>55</sup> are linked by hydrogen bonds involving only one carbonyl group, C(4)-O(4) and the four atoms NH ... OC are almost collinear. The collinear hydrogen bond is also found in 5-methyl-5-phenyl barbituric acid<sup>72</sup> (known as rutonal, no. 5, Table I.1) and heptabarbital<sup>70</sup> (no. 9, Table I.1). However, this mode of hydrogen bond was not observed in the structures studied in this thesis, although, as has been pointed out, the hydrogen bond angle N-H ... O, in all cases, is very close to 180°.

More recently Craven and co-workers have undertaken a series of crystal structure determinations of molecular complexes of barbital with other molecules which also contain the -NH-CO- amide grouping. These crystal structures are of interest as they provide opportunities for hydrogen bonding of the type  $A_d \dots A_a$ ,  $B_d \dots B_a$ ,  $A_d \dots B_a$  and  $B_d \dots A_a$  where A and B are the component amide and barbiturate molecules respectively and subscripts d and a refer to donor (NH) and acceptor (O=C) functions. In the isomorphous structures of the 1:1 barbital-urea<sup>65</sup> and the 1:1 barbital-acetamide<sup>73</sup> complexes there are only  $B_d \dots A_a$  and  $A_d \dots B_a$  hydrogen bonds. The  $(\text{NH})_{\text{amide}} \dots \text{O}_{\text{barb}}$  distances are significantly longer than the  $(\text{NH})_{\text{barb}} \dots \text{O}_{\text{amide}}$  hydrogen bond lengths and

in the former the  $\text{NH} \dots \text{O}$  angles are more severely bent. The  $\text{NH} \dots \text{O}=\text{C}$  hydrogen bonds in which the amide is donor ( $\text{A}_d \dots \text{B}_a$ ) are thus considerably weaker than those in which barbiturate is donor ( $\text{B}_d \dots \text{A}_a$ ). In the 1:1 crystalline complex of salicylamide and amylobarbital<sup>74</sup> it is again seen that the  $(\text{NH})_{\text{barb}} \dots \text{O}_{\text{sal}}$  distances are shorter than the corresponding  $(\text{NH})_{\text{sal}} \dots \text{O}_{\text{barb}}$  distances. The above are examples of complexes in which both types of hydrogen bond occur together i.e.  $(\text{NH})_{\text{barb}} \dots (\text{OC})_{\text{other}}$  and  $(\text{NH})_{\text{other}} \dots (\text{OC})_{\text{barb}}$ . However, Gartland and Craven<sup>65</sup> have prepared a general list of  $\text{N} \dots \text{O}$  distances including those complexes in which only one or the other of the above two types of hydrogen bond prevails. Fig. VII.6 is a histogram showing the variation in the length of these bonds. The shaded area represents those hydrogen bonds in which barbiturate is donor while the unshaded region represents those hydrogen bonds in which barbiturate is acceptor. The histogram is based on the 17 distances listed by Gartland and Craven<sup>65</sup> plus the four  $(\text{NH})_{\text{other}} \dots (\text{OC})_{\text{barb}}$  distances observed in the recently elucidated crystal structure of the 2:1 complex of 2-aminopyridine with barbital<sup>75</sup>.

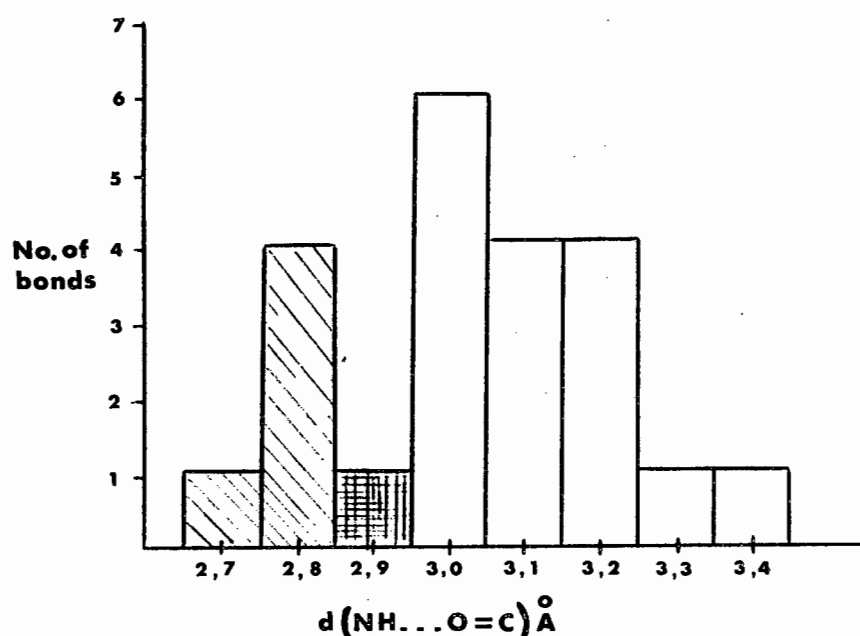


FIG. VII. 6

As might be expected, the distances fall into two distinct groups characteristic of the two types of hydrogen bond. The range of values for the  $(\text{NH})_{\text{barb}} \cdots (\text{OC})_{\text{other}}$  interactions is 2,75 to 2,82 Å while for the  $(\text{NH})_{\text{other}} \cdots (\text{OC})_{\text{barb}}$  interactions it is 2,95 to 3,39 Å. Thus it can be seen that hydrogen bonds in barbiturate crystal complexes are generally short when the barbiturate participates only as the donor and long when it participates only as acceptor. On the basis of the foregoing evidence, Gartland and Craven<sup>65</sup> have concluded that barbiturates are more effective as hydrogen bonding donors than as acceptors. Thus the urea and acetamide complexes for example may be considered essentially as the association of a hydrogen bonding acid (barbiturate) with a hydrogen bonding base (amide).

It is now of interest to consider the structure of complex no. 4,  $\text{Ni}(\text{amylobarbital})_2(\text{imidazole})_2$  of this thesis in the light of the above hypothesis. This structure is the only one of the four in which both ligands (barbiturate and imidazole) have competing hydrogen bonding donor capability. Here there are two crystallographically distinct hydrogen bonds of the type  $(\text{NH})_{\text{barb}} \cdots \text{O}_{\text{barb}}$  and  $(\text{NH})_{\text{imid}} \cdots \text{O}_{\text{barb}}$  with respective N ... O separations of 2,878(4) and 2,935(4) Å. The latter interaction (heavy shading in Fig. VII.6) is thus an example of the  $(\text{NH})_{\text{other}} \cdots (\text{OC})_{\text{barb}}$  type of hydrogen bond and it can be seen that it is slightly smaller (and hence stronger) than might be expected when compared with the values illustrated in the histogram of Fig. VII.6. Although the hydrogen bonding in complex no. 4 is not exactly analagous to that described in the urea and acetamide complexes where each component has both donor and acceptor sites, it can nevertheless be seen that the hydrogen bond involving the barbiturate NH group is stronger than that involving the NH group of imidazole. Further evidence is provided by the NH ... O angles of 176,7(2)° for  $(\text{NH})_{\text{barb}} \cdots \text{O}_{\text{barb}}$  which is less bent than the 161,6(2)° for  $(\text{NH})_{\text{imid}} \cdots \text{O}_{\text{barb}}$ . Another interesting comparison may be made with the 1:1 barbital-imidazole crystal complex<sup>76</sup>. In this structure barbital molecules bond both

with each other in cyclic dimers and with imidazole molecules. Within the barbital dimers the  $\text{NH} \dots \text{O}=\text{C}$  hydrogen bonds have  $\text{N} \dots \text{O}$  distances of 2,91 Å while the  $\text{NH} \dots \text{O}=\text{C}$  hydrogen bonds in which imidazole is donor and barbital acceptor are weak with the  $\text{N} \dots \text{O}$  distance being 3,21 Å. This lends further support to the theory of Gartland and Craven<sup>65</sup>.

That barbiturates are stronger hydrogen bonding donors than acceptors should be further borne out by examination of  $\text{NH} \dots \text{N}$  hydrogen bonds involving barbiturates as both donor and acceptor. In the barbital-imidazole complex<sup>76</sup> the  $\text{NH} \dots \text{N}$  hydrogen bond in which barbital is donor and imidazole is acceptor has a  $\text{N} \dots \text{N}$  distance of 2,78 Å. In the 2:1 crystal complex of 2-aminopyridine and barbital<sup>75</sup>, both barbital  $\text{NH}$  groups are donors in hydrogen bonds with pyridine nitrogen acceptor atoms. Here the  $\text{N} \dots \text{N}$  distances are 2,81 and 2,85 Å. The two  $\text{NH} \dots \text{N}$  hydrogen bonds observed in the phenobarbital-adenine complex<sup>69</sup> in which the barbiturate is again the donor have lengths 2,78 and 2,80 Å. All the above distances must now be compared with  $\text{NH} \dots \text{N}$  distances in which barbiturate is acceptor. Unfortunately only one such distance is available - in guanidine barbital trihydrate<sup>71</sup> the guanidinium cation is donor and the deprotonated nitrogen atom of the barbital anion is acceptor for a hydrogen bond with a  $\text{N} \dots \text{N}$  distance of 3,00 Å. Nevertheless it can be seen that the hydrogen bond distances involving barbiturate as donor are generally short and thus consistent with the view that barbiturates are strong hydrogen bonding donors.

The type of hydrogen bond just described in which nitrogen is acceptor, viz.  $(\text{NH})_{\text{barb}} \dots \text{N}_{\text{ligand}}$  was not observed in the complexes described in this thesis and thus no contribution to this aspect of the Gartland-Craven approach can be made. However future research efforts in the present program of studies on complexes of the type  $\text{M}(\text{II})(\text{barb})_2\text{L}_2$  could be directed towards including compounds such as adenine or the aminopyridines as the organic ligand in the hope of generating hydrogen bonding schemes such as that just described.

Moreover it would be of further interest to extend the study to complexes in which the organic base has both donor (NH) and acceptor (C=O) hydrogen bonding sites analogous to urea and acetamide.

With the exception of the  $(\text{NH})_{\text{imidazole}} \cdots (\text{OC})_{\text{barb}}$  hydrogen bond observed in complex no. 4, all other hydrogen bonds occurring in the complexes Nos. 3 and 4 were of the type  $(\text{NH})_{\text{barb}} \cdots (\text{OC})_{\text{barb}}$ . The N ... O distances observed in these bonds may be compared with those listed by Gartland and Craven<sup>65</sup> for barbituric acids, 1-methylbarbituric acids, barbiturate anions and barbiturate molecular complexes. These authors have considered the N ... O distances for NH ... OC hydrogen bonds in which the barbiturate provides either the NH donor, the carbonyl acceptor or both. It is interesting to note that the N ... O distances involving O(2) on the one hand and O(4) or O(6) (the latter two being equivalent) on the other, have very similar distributions with average values of 2,89 and 2,88 Å respectively. A remarkable feature (with a few minor exceptions) is the narrow range from 2,82 to 2,92 Å of the  $B_d \cdots B_a$  hydrogen bond N ... O distances for all the structures. Thus, changes in barbiturate structure, electronic charge and molecular environment appear to have little effect on the observed N ... O distances in NH ... O=C hydrogen bonds involving barbiturates as both donor and acceptor. These hydrogen bonds may thus be considered as having a N ... O distance of  $2,87 \pm 0,05$  Å. In complex no. 3,  $\text{Zn}(\text{barbital})_2(\beta\text{-picoline})_2$  there are two distinct hydrogen bonds of the type  $(\text{NH})_{\text{barb}} \cdots \text{O}_{\text{barb}}$  with N ... O distances of 2,873(4) and 2,874(4) Å. In complex no. 4,  $\text{Ni}(\text{amylobarbital})_2(\text{imidazole})_2$  there is one hydrogen bond of this type and this has a N ... O separation of 2,878(4) Å. These three distances, which agree very favourably with the value 2,87 Å mentioned above, have been combined with the 48 distances listed by Gartland and Craven and are shown as the shaded portion of the histogram in Fig. VII.7. Also included are the relevant distances reported for  $\text{Cu}(\text{barbital})_2(\text{pyridine})_2$ <sup>27</sup> and for the 1:2 complex of hexamethylphosphoramide with barbital<sup>77</sup>.

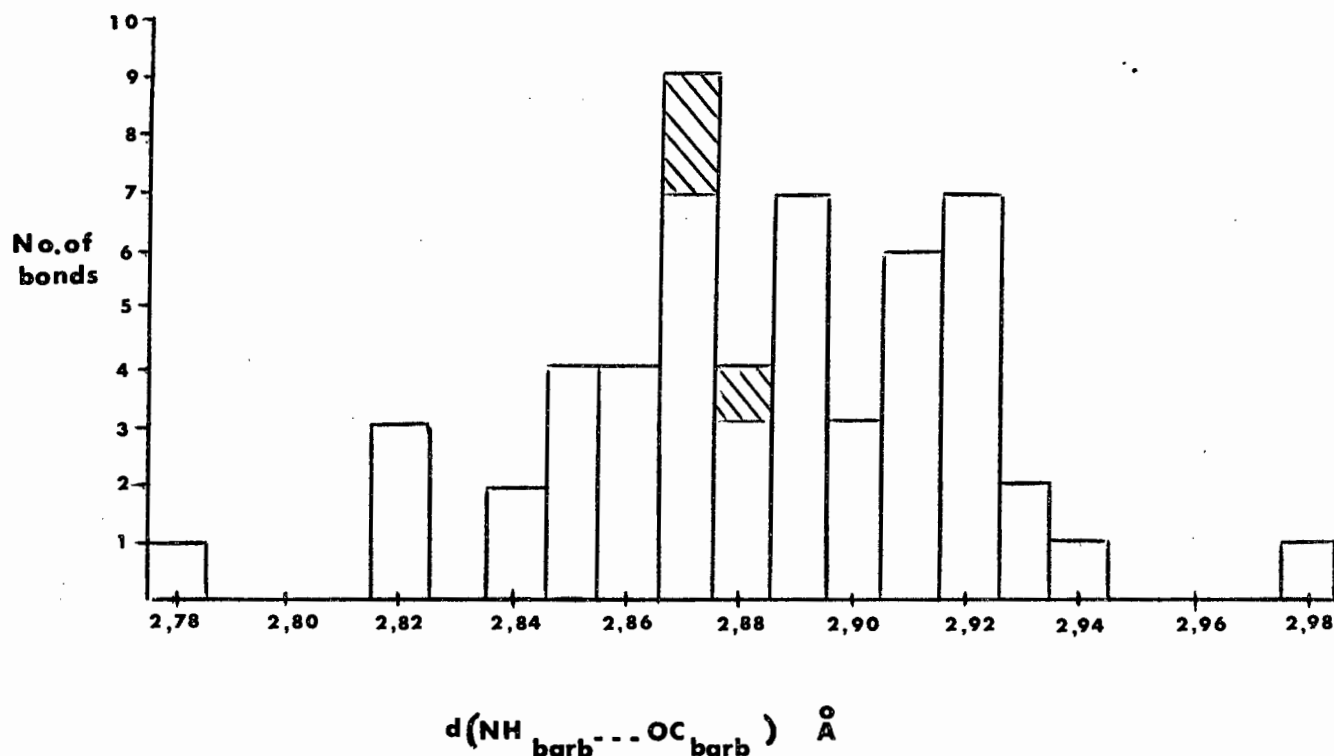


FIG. VII. 7

### The hydrogen bond angle

Mention has already been made of the fact that although the optimum hydrogen bond angle A-H ... B is in general expected to be 180°, experimental results indicate that a bent hydrogen bond is very common with deviations of up to 30° from linearity<sup>39</sup>. It is of interest to consider the hydrogen bond angles that occur in barbiturates and their complexes and to examine whether any distinct trends emerge. Gartland and Craven<sup>65</sup> do not list hydrogen bond angles and these are thus presented in Table VII.4. The values given are for the N-H ... O angles occurring in hydrogen bonds of the type NH ... OC in which barbiturate is either the donor (NH), or the acceptor (C=O), or both. The 65 bond lengths were obtained in a literature survey embracing the crystal structures of barbiturates, methylbarbiturates, barbiturate salts, barbiturate molecular complexes and barbiturate-transition metal complexes. In those cases where the N-H ... O angle was not reported, the particular angle was calculated from

the unit cell parameters and relevant atomic coordinates. These have been marked with an asterisk (\*).

The frequency distribution of the angles listed in Table VII.4 is better illustrated as a histogram (Fig. VII.8) from which it can be readily seen that the maximum frequency occurs between 170 and 175°. This is somewhat less bent than might be expected from a consideration of recent distribution studies<sup>82</sup> involving other compounds which have revealed maxima at about 165°.

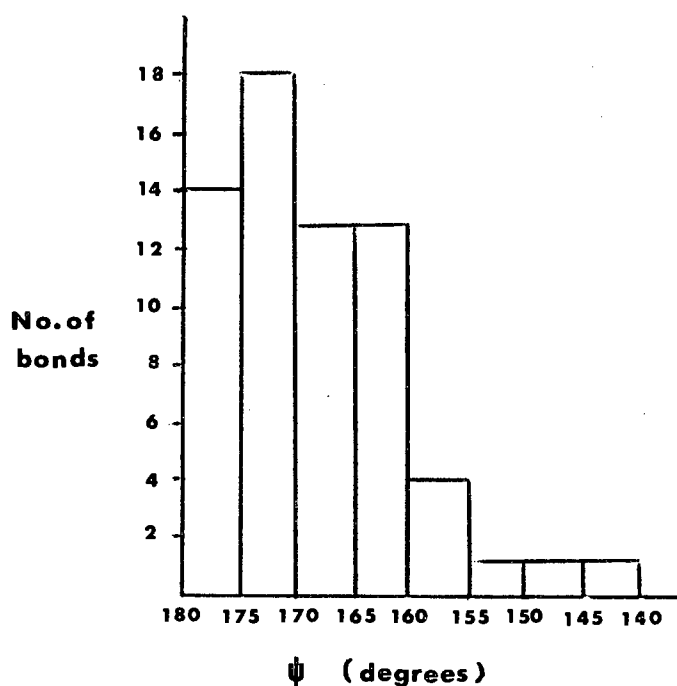


FIG. VII. 8

The above kind of treatment in which a histogram is constructed to represent the frequency distribution of hydrogen bond angles warrants some comment in the light of a recent publication by Kroon and Kanters<sup>83</sup>. They

TABLE VII.4

## N-H ... O ANGLES IN BARBITURATE STRUCTURES

CRYSTAL STRUCTURE	REF.	ANGLES (DEGREES)							
<u>(a) Barbiturates</u>									
Barbital, form I	56	173	170						
Barbital, form II	56	177							
Barbital, form IV *	63	168	155	158	163	170	174	165	169
Amylobarbitol, form I	60	172	163						
Amylobarbitol, form II	60	163	168	162	169				
$\gamma$ -Methylamylobarbitol	64	166	169						
Vinbarbitol	62	166	175						
Phenobarbitol, form III	78	163	171						
5-Ethylbarbituric acid	80	177	177						
5-Hydroxy-5-ethylbarbituric acid	80	179							
<u>(b) Methylbarbiturates</u>									
Metharbitol	58	173							
1-Methyl-5-ethyl-5-(1-cyclohexen-1-yl) barbituric acid *	84	163							
<u>(c) Barbiturate salts</u>									
Sodium barbital	55	162							
Calcium barbital trihydrate	57	174	175	176	177				
Guanidinium barbital dihydrate *	71	173							
<u>(d) Barbiturate molecular complexes</u>									
Barbital/9-ethyladenine (1:1)	79	172	176						
Barbital/caffeine (2:1) *	67	164	176	172					
Barbital/urea (1:1)	65	177	171	150	144				
Barbital/acetamide (1:1)	73	175	170	161					
Amylobarbitol/salicylamide (1:1)*	74	177	159	159					
Barbital/imidazole (1:1) *	76	161							
Barbital/hexamethylphosphoramide (2:1)	77	171	177	173	176				
Barbital/2-aminopyridine (1:2) *	75	175	168	157	170				
Barbital/N-methyl-2-pyridone (1:1)	81	164	176						
<u>(e) Barbiturate-metal complexes</u>									
Cu(II)(barbital) <sub>2</sub> (pyridine) <sub>2</sub>	27	166							
Zn(II)(barbital) <sub>2</sub> ( $\beta$ -picoline) <sub>2</sub>	this thesis	172	173						
Ni(II)(amylobarbitol) <sub>2</sub> (imidazole) <sub>2</sub>	this thesis	177	162						

point out that such frequency distributions must be adjusted by a factor, which if not taken into account influences the statistics and leads to incorrect interpretation of the histogram. This factor is of a geometric nature and depends on the N-H ... O angle,  $\psi$ . It can be seen from Fig. VII.9 that the acceptor oxygen atom at a certain N-H ... O angle can select any of the

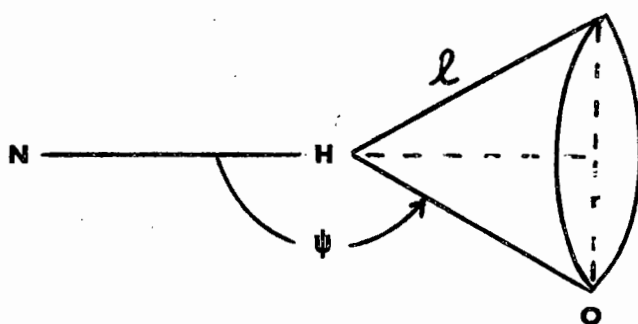


FIG. VII.9

positions that lie on the circumference of the circle whose radius,  $r = l \sin \psi$ . Thus the probability of a hydrogen bond occurring increases with increasing  $\psi$  by the factor  $2\pi l \sin \psi$ . Furthermore, as the distance  $l$  between the donor hydrogen and acceptor oxygen atoms increases the greater will be the number of possible hydrogen bonds. It is because of these geometric considerations that the above factor must be applied to the data as a correction term.

In their treatment, Kroon and Kanters assumed a constant value for  $l$  and applied the correction factor to the statistics of a series of 196 hydrogen bond angles of the type O-H ... O. They found that whereas the histogram of  $\psi$  has a maximum at  $161^\circ$ , that of  $\psi$  (corrected) has a maximum between  $175$  and  $180^\circ$ .

For the hydrogen bonds listed in Table VII.4, the variation in  $l$  is between the limits  $1,82$  and  $2,47 \text{ \AA}$  but this was found to be insignificant. \* The  $2\pi \sin \psi$  correction term was applied to the data which was then normalized to give a total of 65 hydrogen bonds. These are shown as a histogram in

Fig. VII.10. This shows the maximum in the frequency distribution as now occurring in the range 175 - 180° with a relatively small population in the 155 - 170° range. This is in contrast to that observed in the uncorrected histogram but consistent with the results of Kroon and Kanters.

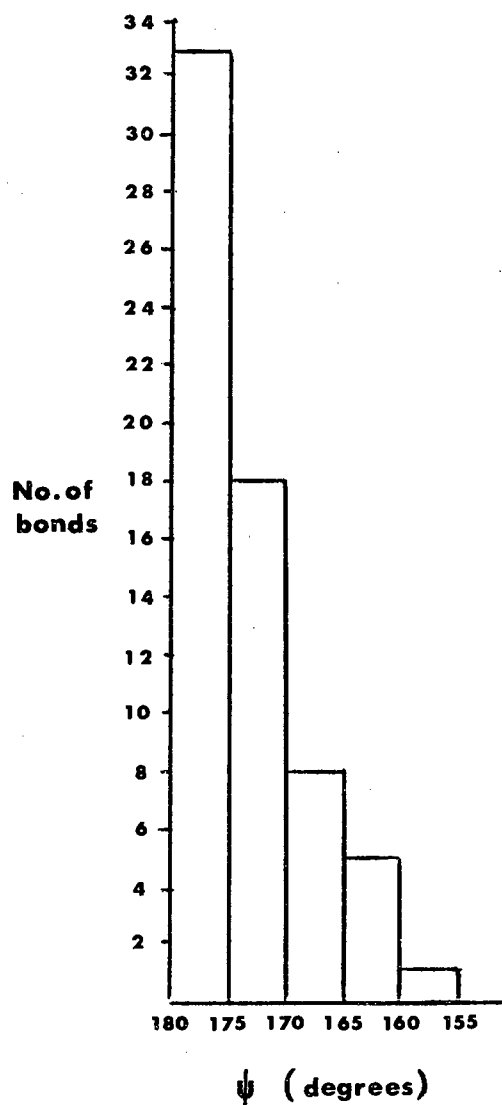


FIG. VII.10

It may thus be concluded that the experimentally observed hydrogen bond angle distributions, when properly treated, are consistent with an assumed preference for linearity.

\* The above calculation was also carried out using the correction factor  $2\pi \sin \psi$ , yielding the same bond angle distribution as shown in Fig. VII.10.

CHAPTER VIII

THE INFRARED ABSORPTION SPECTRA OF THE COMPLEXES

### VIII.1 INTRODUCTION

It has already been mentioned that the infrared spectra of a series of complexes of the type  $\text{Cu}(\text{barb})_2(\text{pyridine})_2$  has been investigated<sup>22</sup> and that on the basis of a lowering by some  $35 \text{ cm}^{-1}$  of the barbiturate carbonyl vibrations ( $\nu\text{C}=\text{O}$ ) on coordination it was concluded that coordination was via the carbonyl group in the 2-position (Fig. VIII.1). Three bands at  $1770 - 1750 \text{ cm}^{-1}$ ,  $1740 - 1710 \text{ cm}^{-1}$  and  $1710 - 1690 \text{ cm}^{-1}$  in the IR spectra of the barbiturate ligands were assigned<sup>22</sup> to  $\nu\text{C}=\text{O}$ . The higher frequency band was assigned to vibrations perpendicular to the axis of symmetry of the carbonyl groups in the 4- and 6-positions, that near  $1730 \text{ cm}^{-1}$  to a coupled vibration involving all three carbonyl groups and that in the lower frequency region to the vibration of the carbonyl group in the 2-position. This latter band was assumed to have more single bond character because of the effects of the two adjacent nitrogen atoms (Fig. VIII.1).

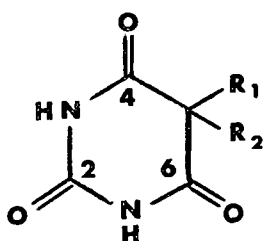


**FIG. VIII.1**

Only two  $\nu\text{C}=\text{O}$  bands were observed in the spectra of the corresponding complexes  $\text{Cu}(\text{barb})_2(\text{pyridine})_2$  from which it was concluded that coordination had occurred through the carbonyl group in the 2-position.

It was argued<sup>22</sup> that coordination through O(2) would lead to the loss of the lower band and also the coupled vibration near  $1730 \text{ cm}^{-1}$ . The

resultant C=N in the enol form of the barbiturate ligand would lead to a loss of equivalence of the remaining carbonyl groups and the appearance of two new  $\nu_{C=O}$  bands.

Since coordination is now known to occur via the nitrogen N(1) atom and not via the oxygen O(2) atom, a reinterpretation of these spectra was desirable. Figure VIII.2 is a schematic representation of the complexes  $M(\text{barb})_2L_2$ .

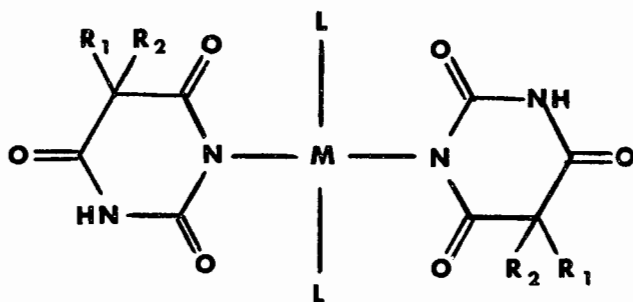


FIG. VIII. 2

### VIII.2 EXPERIMENTAL

The preparation of the complexes has already been described in the earlier chapters. The preparation of  $\text{Cu}(\text{barbital})_2(\text{pyridine})_2$  has been described by Cairn *et al*<sup>27</sup>. The anhydrous complex  $\text{Cu}(\text{barbital})_2(\beta \text{ picoline})_2$  was prepared from the corresponding hydrated complex by heating in a drying pistol at 60°C. The microanalysis figures for this complex is given in Table VIII.1 below.

TABLE VIII.1

	%C	%H	%N
calculated	54,54	6,18	13,63
experimentally found :	54,0	5,6	13,5

The IR spectra of the complexes, the free barbiturates and the individual organic ligands were determined from Nujol mulls between CsI plates on a Beckman IR-12 spectrophotometer calibrated against carbon dioxide and water vapour. (The free barbiturates were precipitated from aqueous solutions of their salts by the addition of concentrated hydrochloric acid).

### VIII.3 INTERPRETATION OF THE IR SPECTRA

#### Frequency coupling effects.

Vibrational coupling of the carbonyl vibrations was expected<sup>86</sup>. The extent to which this occurs depends on a number of factors which include the proximity of the groups and the angle between them and the degree with which the individual frequencies approach each other. Of these, the angle between the two groups is of paramount importance. Carbonyl groups at right angles to each other are unable to interact whereas those that are coplanar do so to a maximum extent. If the groups are aligned in opposite directions they will yield one band since there will be no change in dipole for the symmetric vibration.

The degree of coupling falls off as the system departs from planarity. The actual values of the individual carbonyl vibrational frequencies is another important factor in postulating the extent to which coupling occurs. The further these are apart the less interaction there will be. In many organic compounds containing more than one carbonyl group, the groups are not coplanar. This, together with the fact that the frequencies are initially different reduces the interactions so much that each band can quite properly be assigned to one of the characteristic groups alone<sup>86</sup>.

Phthalimides and succinimides (Figures VIII.3 and VIII.4 respectively) which, structurally, are closely related to the barbiturates, show two

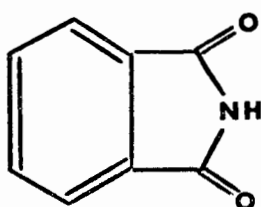


FIG. VIII.3

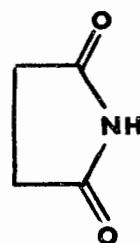


FIG. VIII.4

$\nu_{C=O}$  bands<sup>86</sup>, the higher of which has been assigned to the symmetric mode ( $\sim 1770\text{ cm}^{-1}$ ) and the lower ( $\sim 1700\text{ cm}^{-1}$ ) to the asymmetric mode. This occurs in cyclic systems in which the carbonyl groups are reasonably coplanar.

Thus some compounds show bands that may be assigned to individual carbonyl vibrations while others show bands that are coupled symmetric or asymmetric modes. These two interpretations of observed band patterns may be applied to the barbiturates.

#### IR spectra of the barbiturate ligands

The IR spectra of barbital, brallobarbital and amylobarbital reveal 3 bands in the regions 1765 - 1757, 1724 - 1720 and 1696 - 1680  $\text{cm}^{-1}$  that may be assigned to carbonyl vibrations (Table VIII.2).

TABLE VIII.2  
THE CARBONYL STRETCHING FREQUENCIES  
OF THE BARBITURATE LIGANDS

BARBITURATE	$\nu_{C=O}$		
BARBITAL	1765	1720	1680
BRALLOBARBITAL	1762	1719	1685
AMYLOBARBITAL	1757	1724	1696

Because the respective barbiturate rings are not perfectly planar, a symmetric vibration should be observed. In barbital there would also be three asymmetric modes of which two would be equivalent. A total of three bands is therefore expected. A similar situation exists in the  $\text{CCl}_4$  spectrum of 2,4,6-trioxo-1,3,5-triazine also known as cyanuric acid where two  $\nu_{C=O}$  bands are observed<sup>86</sup> (Fig. VIII.5). The higher of these bands represents the symmetric vibration (allowed because the molecule is not planar) while the lower band represents the three equivalent asymmetric vibrations.

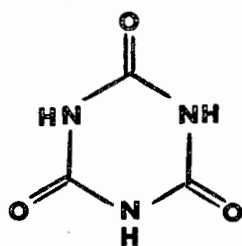


FIG. VIII. 5

Alternatively it could be proposed that because of intermolecular interactions the non-equivalence of the carbonyl groups will increase so that the observed carbonyl vibrations represent the individual vibrations coupled to some unknown degree with the other vibrations. The position of each band would depend on the degree of coupling as well as the nature and extent of the hydrogen bonding in the molecule.

In brallobarbitol and amylobarbitol the side chain substituents cause the symmetry to be lost. The result is that each of the three observed bands could represent an individual carbonyl vibration, or that additional coupling could result in extra bands. In fact, two extra weak bands are observed in the spectrum of brallobarbitol.

A combination of the above two approaches could provide a third interpretation to the observed spectra. Since the carbonyl in the 2-position is flanked on either side by a nitrogen atom, it is essentially in a different environment from the other two. This could lead to the lower band representing a purer  $\nu_{C(2)=O}$  while the upper bands represent the symmetric and asymmetric vibrations of the other two carbonyl groups. Clearly no definite assignment is possible without a detailed study of related compounds.

#### The IR spectra of the metal-barbiturate complexes

The metal complexes of the imides  $M(\text{imide})_2(\text{amine})_2$  shown in Figure VIII.6 are ideal models for the barbiturate complexes. The IR spectra of such complexes have been extensively studied<sup>87</sup>. Coordination occurs through the

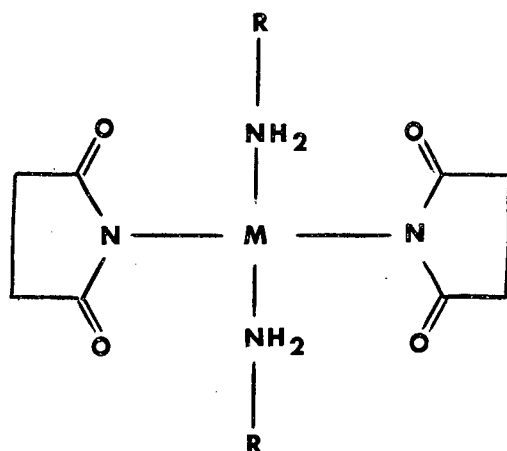


FIG. VIII. 6

nitrogen atom of succinimide and the IR spectra reveal that the two  $\nu_{C=O}$  of succinimide itself are moved by some  $70\text{ cm}^{-1}$  to lower frequency. An analogous situation exists in the  $\text{Pt(II)}^{88}$  and  $\text{Au(I)}^{89}$  complexes of  $\beta$ -diketones where coordination is via the  $\gamma$ -carbon of the keto-tautomer. For example in  $\text{K}[\text{Pt}(\text{AA})_2\text{Cl}]$  where AA = acetylacetonate,  $\nu_{C=O}$  are lowered from 1728 and  $1710\text{ cm}^{-1}$  in the ligand to 1695 and  $1653\text{ cm}^{-1}$  in the complex.

The IR spectra of the complexes  $\text{M}(\text{barb})_2\text{L}_2$  (Figure VIII.7) reveal three bands (Table VIII.3) that are assigned to  $\nu_{C=O}$ . All three bands are substantially shifted from their positions (Table VIII.2) in the free ligands.

TABLE VIII.3  
THE CARBONYL STRETCHING FREQUENCIES  
OF THE METAL-BARBITURATE COMPLEXES

COMPLEX		$\nu_{C=O}$		
A	$\text{Cu}(\text{barbital})_2(\beta\text{-pic})_2 \cdot 2\text{H}_2\text{O}$	1727	1670	1605
B	$\text{Cu}(\text{barbital})_2(\beta\text{-pic})_2$	1706	1687	1620
C	$\text{Cu}(\text{barbital})_2(\text{pyridine})_2$	1714	1679	1603
D	$\text{Zn}(\text{barbital})_2(\beta\text{-pic})_2$	1713	1689	1614
E	$\text{Cu}(\text{brallobarbital})_2(\text{pyridine})_2$	1712	1668	1618
F	$\text{Ni}(\text{amylobarbital})_2(\text{imidazole})_2$	1720	1675	1535
G	$\text{Na}^+(\text{barbital})^-$	1697	1669	1551

FIG. VIII.7

M	R <sub>1</sub>	R <sub>2</sub>	B	IR SPECTRA	
A	* Cu	C <sub>2</sub> H <sub>5</sub>	C <sub>2</sub> H <sub>5</sub>	βpic	
B	Cu	C <sub>2</sub> H <sub>5</sub>	C <sub>2</sub> H <sub>5</sub>	βpic	
C	Cu	C <sub>2</sub> H <sub>5</sub>	C <sub>2</sub> H <sub>5</sub>	py	
D	Zn	C <sub>2</sub> H <sub>5</sub>	C <sub>2</sub> H <sub>5</sub>	βpic	
E	* Cu	CH <sub>2</sub> CH=CH <sub>2</sub>	CH <sub>2</sub> C(Br)=CH <sub>2</sub>	py	
F	Ni	C <sub>2</sub> H <sub>5</sub>	CH <sub>2</sub> CH <sub>2</sub> CH(CH <sub>3</sub> ) <sub>2</sub>	imid	
G	Na	C <sub>2</sub> H <sub>5</sub>	C <sub>2</sub> H <sub>5</sub>	—	

\* Hydrated Complex

1700 1600 cm<sup>-1</sup>

THE IR SPECTRA ( 1750 - 1500 cm<sup>-1</sup> ) OF THE

METAL - BARBITURATE COMPLEXES

In the spectrum of the complex  $\text{Cu}(\text{barbital})_2(\beta\text{-picoline})_2 \cdot 2\text{H}_2\text{O}$  (referred to henceforth as A) three bands of similar intensity to those found in barbital appear at 1727, 1670 and 1605  $\text{cm}^{-1}$ . This represents a lowering of the bands from their positions in the ligand spectrum of 38, 50 and 75  $\text{cm}^{-1}$  respectively. The crystal structure of (A) (Chapter III) reveals that each carbonyl group is in a different environment as a result of weak metal-oxygen interactions and hydrogen bonding. It is therefore suggested that each carbonyl band is mainly representative of an individual carbonyl vibration although coupling to a certain degree is expected. The proposal is that the lower band (band 3) is predominantly  $\nu\text{C}(2)=\text{O}$ . This group is adjacent to the coordinated nitrogen, is hydrogen bonded to water and has a close metal-oxygen interaction. It would therefore be the most affected by coordination and hence  $\nu\text{C}(2)=\text{O}$  would be expected at lower frequency than the other vibrations. The  $\text{C}(6)=\text{O}$  group is involved in a weaker hydrogen bonding scheme and a weaker interaction with the copper atom while the  $\text{C}(4)=\text{O}$  group is involved in neither of these interactions. On this basis the middle band (band 2) is assigned to predominantly  $\nu\text{C}(6)=\text{O}$  and the upper band (band 1) to predominantly  $\nu\text{C}(4)=\text{O}$ .

Dehydration of this complex to  $\text{Cu}(\text{barbital})_2(\beta\text{-picoline})_2$  (B) causes the IR spectrum to change in the carbonyl region. Three bands are again observed at 1706, 1687 and 1620  $\text{cm}^{-1}$  representing a lowering (from  $\nu\text{C}=\text{O}$  of the ligand) of 59, 33 and 60  $\text{cm}^{-1}$  i.e. the lowering of band 1 has increased (38 to 59  $\text{cm}^{-1}$ ) while that of bands 2 and 3 has decreased (50 to 33 and 75 to 60  $\text{cm}^{-1}$  respectively). Dehydration causes a loss of the hydrogen bonding so that  $\nu\text{C}(2)=\text{O}$  and  $\nu\text{C}(6)=\text{O}$  (bands 2 and 3) would move to higher frequency. The carbonyl groups would be more equivalent and the degree of coupling would increase in consequence of which the position of band 1 would be lowered towards that of band 2.

The spectrum of (B) is similar to that of  $\text{Cu}(\text{barbital})_2(\text{pyridine})_2$  (C) whose crystal structure has also been elucidated<sup>27</sup>. In this complex  $\text{O}(6)$  is

involved in hydrogen bonding while O(2) is involved in an interaction with the copper atom which is somewhat stronger than that in (A). Comparison of the spectra of (B) and (C) reveals from the carbonyl band positions that the interactions in (C) are stronger than those in (B) and hence the  $\nu_{\text{C=O}}$ 's for (C) are more individualistic in character (band 1 is higher and bands 2 and 3 are lower). The degree of equivalence and hence coupling is higher in (B) than in (C).

Comparison of the IR spectrum of  $\text{Zn}(\text{barbital})_2(\beta\text{-picoline})_2$  (D) with the other complexes is difficult in view of the structural differences. However, band 3 has once again been lowered by hydrogen bonding. The splitting between bands 1 and 2 is indicative of the greater equivalence and coupling that exists between C(4)=O and C(6)=O as compared in the other structures.

The spectra of the anhydrous complexes (B), (C) and (D) can be interpreted according to a second approach in which band 3 is assigned to  $\nu_{\text{C(2)=O}}$  as before, while bands 1 and 2 could be considered to be the symmetric and asymmetric vibrations of the carbonyl groups in the 4- and 6-positions. Support for this hypothesis is provided by the fact that the splittings between bands 1 and 2 for (B), (C) and (D) are 19, 35 and 24  $\text{cm}^{-1}$  respectively while the difference observed for (A) is 57  $\text{cm}^{-1}$ .

To explain the presence of a large peak in the difference Fourier of  $\text{Cu}(\text{brallobarbital})_2(\text{pyridine})_2$  it was postulated (Chapter IV) that it was due to the presence of an oxygen atom of a water molecule. The complex was therefore formulated as  $\text{Cu}(\text{brallobarbital})_2(\text{pyridine})_2 \cdot 2\text{H}_2\text{O}$  (E). The IR spectrum of this complex shows a band splitting which is more closely related to that of (A) than to those of (B), (C) and (D) and on this basis is taken as adding support to the formulation proposed. There is also evidence in the 3300  $\text{cm}^{-1}$  region that water is present in the complex. The assignment of the carbonyl bands in this complex involving brallobarbital is different from the assignments made for the barbital complexes, (A) to (D). Here the closest interaction is

between Cu and O(6) and not between metal and O(2) as found in (A) and (C). Thus, band 3 is assigned to  $\nu\text{C}(6)=\text{O}$  and bands 1 and 2 to  $\nu\text{C}(4)=\text{O}$  and  $\nu\text{C}(2)=\text{O}$  respectively.

The complex  $\text{Ni}(\text{amylobarbitol})_2(\text{imidazole})_2$  (F) has been shown to have a distorted octahedral structure (Chapter VI) with the O(6) atoms occupying the fifth and sixth coordination positions. As in the case of (E) band 3 is assigned to  $\nu\text{C}(6)=\text{O}$ . Because of the strong interaction involving O(6) (it is also hydrogen bonded) this band is expected at much lower frequency. Three peaks are observed at 1720, 1675 and  $1535\text{ cm}^{-1}$ . Confusion with the imidazole bands is not expected since they are extremely weak and would be unobserved under the intense carbonyl bands. The considerable lowering of band 3 to  $1535\text{ cm}^{-1}$  is thus not unexpected in view of the fact that the comparatively weaker interactions in (A) to (D) lowered  $\nu\text{C}(2)=\text{O}$  to near  $1600\text{ cm}^{-1}$ . Furthermore the spectrum of the sodium salt of barbitol, in which  $\text{Na}^+$  is tetrahedrally surrounded by four oxygen atoms with an average Na ... O distance of  $2.33\text{ \AA}$  shows a band assignable to  $\nu\text{C}=\text{O}$  at  $1551\text{ cm}^{-1}$ .

Generally, the other bands near  $1600\text{ cm}^{-1}$  are in the region where pyridine and  $\beta$ -picoline vibrations occur<sup>90,91</sup> in complexes. These bands are usually lowered from their positions in the spectra of the free ligands by coordination. In  $\text{M}(\text{pyridine})_2\text{Cl}_2$  complexes, the band at  $1585\text{ cm}^{-1}$  is lowered to  $1570\text{ cm}^{-1}$  and that near  $1602\text{ cm}^{-1}$  is lowered to  $1590\text{ cm}^{-1}$ . These bands are found, for example, at 1594 and  $1570\text{ cm}^{-1}$  in (C).

The spectra of these barbiturate complexes exhibit several peaks below  $600\text{ cm}^{-1}$  where metal-ligand vibrations are expected to occur. However most of the peaks are observed in the spectra of the ligands. No band can reasonably be assigned to  $\nu\text{M-barb}$ . Since even the comparatively firmly bound pyridine in complexes<sup>90,92</sup>  $\text{M}(\text{pyridine})_2\text{Cl}_2$  exhibit  $\nu\text{M-N}$  in the  $250\text{ cm}^{-1}$  region and since no peaks assignable to  $\nu\text{M-N}$  were observed in the far IR spectra of the succinimide complexes<sup>87</sup>, it seems likely that in the barbiturate complexes both  $\nu\text{M-barb}$  and  $\nu\text{M-pyridine}$  have frequencies below  $200\text{ cm}^{-1}$ .

CHAPTER IX

CONCLUSION

## IX CONCLUSION

In concluding this thesis, there are two aspects to be considered:

- (i) to what extent have the objectives, outlined in Chapter I.6, been achieved and
- (ii) has the project stimulated new avenues of thought along which further research can be channelled?

The first objective - to synthesize a series of complexes of the type  $M(II)(\text{barb})_2L_2$ , has been only partially successful in that relatively few compounds were actually obtained. As has been described earlier, much difficulty was experienced in obtaining crystals of the quality required for a successful X-ray analysis. However, although only four such complexes were finally isolated they are nevertheless fairly representative of the general type since their composition includes three different metals (copper, zinc, nickel), three different barbiturates (barbital, brallobarbital, amylobarbital) and three different organic bases ( $\beta$ -picoline, pyridine, imidazole). However it had been hoped to synthesize a greater number of complexes in the series.

The crystal and molecular structures of the complexes as well as their inherent hydrogen bonding schemes have been studied in great detail in accordance with the second and third objectives. Several interesting features have emerged in the complexes themselves and in the comparisons made with other barbiturate structures.

The determination and interpretation of the infra-red spectra of the complexes have been accomplished (fourth objective) and the results of this study are consistent with the structural features observed in the X-ray analyses.

Despite the fact that the four complexes described in this thesis have been extensively investigated, the research program on  $M(II)(\text{barb})_2L_2$

complexes has by no means been exhausted. As a result of the fact that three different metals were involved in the synthesis of the complexes, it was possible to study three different metal coordination types - square planar (with off-the-z-axis coordination), tetrahedral and distorted octahedral. However before any definite correlation between coordination type and a particular metal can be made, the structures of barbiturate complexes involving other transition metals must first be investigated.

Further studies need to be concentrated on other barbiturates as well. The thiobarbiturates in particular would be of great interest in metal complexes since the presence of sulphur provides a third possible coordination site.

Careful choice of the other ligand in the  $M(II)(\text{barb})_2L_2$  complexes could generate hydrogen bonding schemes from which useful data can be determined. It has already been mentioned that ligands analagous to urea and acetamide, which have both donor and acceptor hydrogen bonding capabilities, are examples of such compounds.

A program of n.m.r. and kinetic studies on the metal barbiturate complexes needs to be undertaken so that some insight into the nature of the mechanism of their formation can be gained. Such a project would be most interesting.

Finally, the IR study can be extended as well. To establish beyond any doubt the patterns observed in the spectra, a series of complexes should be studied in which either the metal is constant and the barbiturate varied or vice versa. Furthermore  $^{18}\text{O}$ -labelling of the barbiturate would enable the various carbonyl vibrations to be identified unequivocally and the degree of coupling to be established<sup>93</sup>. On the other hand  $^{15}\text{N}$ -labelling would show the presence of the metal-barbiturate stretching frequencies if they occur in the range of the IR spectrophotometer (i.e. usually above  $200\text{ cm}^{-1}$ ).

Thus it can be seen from the above that the motivation to continue structural investigations on complexes of the type  $M(II)(\text{barb})_2L_2$  definitely exists. Such a future research program, based on the findings outlined in this thesis, promises to be most interesting and stimulating.

APPENDIX

A LOW TEMPERATURE DEVICE FOR COOLING CRYSTALS  
DURING X-RAY DIFFRACTION

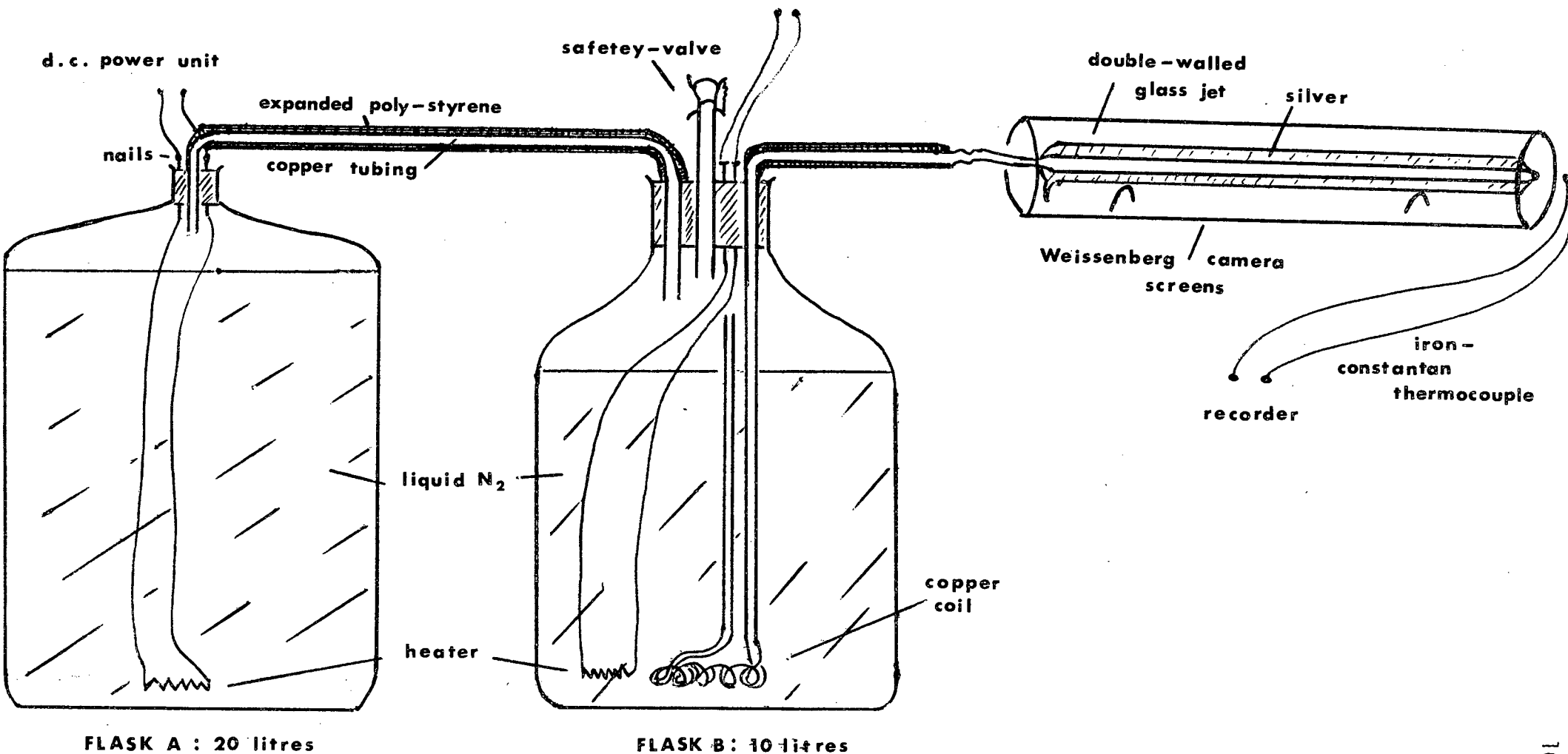
Before work began on the project described in this thesis, much time was spent on another research project involving uranyl compounds. Because the visual data collected was not of a very high quality, no progress in the x-ray structural investigation was made and the project was subsequently abandoned. During this time however a low temperature apparatus was designed, tested and developed and successfully used in the data collection process. Since it is cheap and relatively easy to construct, a description thereof is presented here.

In designing a low temperature device three essential requirements had to be considered:

- (i) the device must be capable of producing temperatures between  $-120$  and  $-130^{\circ}\text{C}$ ;
- (ii) the temperature should not fluctuate but remain constant for periods up to 10 hours;
- (iii) during this length of time the device must function without supervision or maintenance.

The apparatus system shown in Fig. A1. allowed uninterrupted runs of up to 12 hours to be effected. It consists of two large Dewar flasks, one of 20 litres capacity (flask A) and the other of 10 litres capacity (flask B). These are connected by means of a copper tube which protrudes through each rubber bung to just above the level of the liquid nitrogen. A carefully wound copper coil is positioned in the smaller flask such that its one end is situated above the level of the liquid. The other end passes through the stopper and is connected via copper and rubber tubing to a double-walled vacuum and silvered glass jet supported inside the Weissenberg camera screens.

**FIG. A1. LOW TEMPERATURE APPARATUS**



The liquid nitrogen in A is boiled by means of a heater consisting of several turns of nichrome resistance wire wound tightly on a perspex rod. The boiled off vapour passes through the copper tube into flask B where, together with the liquid nitrogen vapour in this flask, it passes through the coil and is cooled before being directed onto the crystal.

The flow rate of the vapour to the crystal and hence the temperature is easily controlled by means of a D.C power unit connected to the heater. By means of an iron-constantan thermocouple at the crystal and a pen recorder it is possible to monitor the temperature and detect any fluctuations.

A reserve heater in B can be used in the event of the one in A malfunctioning. This would enable an otherwise crippled run to continue uninterrupted.

The successful functioning of the apparatus is dependent on an absolutely air-tight system being maintained throughout. Thus, tightly fitting rubber bungs must be used to stopper both flasks and inlet and outlet tubes must be passed through small holes in these bungs. The electrical connections to the exterior can be made via two nails which pass through the stoppers.

To minimize the danger of ice forming inside the copper tubulation, dry nitrogen gas should be flushed through the coil and tubing in the hope of driving off any water vapour which might be present. Nevertheless a safety valve (pyrex glass) must be included in the apparatus so that an excess build-up of vapour pressure caused by an ice blockage can be released.

All copper and rubber tubing is carefully insulated with thick layers of expanded poly-styrene. This minimizes the required flow rate and hence extends the duration time of the runs.

One final safety device is necessary. An on-off switch is connected to the recorder and is set in such a position that, in the event of a sudden rise in temperature to a predetermined level, the movement of the pen would activate the switch thereby tripping the power supply to the X-ray generator and cooling apparatus.

REFERENCES

- 1 D.R. Williams, *Education in Chemistry*, 10, 56 (1973).
- 2 D.R. Williams, *The Metals of Life*, London: Van Nostrand (1971).
- 3 M.N. Hughes, *The Inorganic Chemistry of Biological Processes*, John Wiley and Sons (1972).
- 4 H.G. Mautner and H.C. Clemson, *Medicinal Chemistry, 3rd Edition*, Editor: A. Burger, John Wiley (1970), pp 1365 - 1385.
- 5 G. Moruzzi and H.W. Magoun, *Electroenceph. Clin. Neurophysiol.*, 1, 445 (1949).
- 6 K. Akert, W.P. Koella and R. Hess, *Amer. J. Physiol.*, 168, 260 (1952).
- 7 W.J. Doran, *Medicinal Chemistry, Vol IV*. New York. John Wiley (1959).
- 8 J.K. Wood, *J. Chem. Soc.*, 89, 1831 (1906).
- 9 G.A. Jeffrey, S. Ghose and J.O. Warwicker, *Acta Cryst.*, 14, 881 (1961).
- 10 W. Bolton, *Acta Cryst.*, 16, 166 (1963).
- 11 R.G. Pearson, *J. Amer. Chem. Soc.*, 85, 3533 (1963).
- 12 R.G. Pearson, *Chemistry in Britain*, 3, 103 (1967).
- 13 R.G. Pearson and R.S. Drago, *Chemistry in Britain*, 3, 516 (1967).
- 14 S. Ahrland, J. Chatt and N. Davies, *Chem. Soc. Quart. Rev.*, 12, 265 (1958).
- 15 R.G. Pearson, *Hard and Soft Acids and Bases*, Dowden, Hutchinson and Ross Inc., (1972).
- 16 T. Koppányi, W.S. Murphy and S. Krop, *Proc. Soc. Exptl. Biol. Med.*, 31, 373 (1933).
- 17 Büchi and Perlia, *Pharm. Acta. Helv.*, 29, 265 (1954).
- 18 Turfitt, *Quart. J. Pharm. Pharmacol.*, 21, 1 (1948).
- 19 L. Goldbaum, *Anal. Chem.*, 24, 1604 (1952).
- 20 A. Grieg, *Nature*, 170, 845 (1952).

- 21 C.J. Umberger and G. Adams, *Anal. Chem.*, *24*, 1309 (1952).
- 22 L. Levi and C.E. Hubley, *Anal. Chem.*, *28*, 1591 (1956).
- 23 B.C. Wang and B.M. Craven, *Chem. Comm.*, 290 (1971).
- 24 *The Merck Index*, Merck and Co., Inc. (U.S.A.), (1968).
- 25 B.W. Low and F.M. Richards, *J. Amer. Chem. Soc.*, *74*, 1660 (1952).
- 26 M.E. Krahl, *J. Phys. Chem.*, *44*, 449 (1940).
- 27 M.R. Caira, G.V. Fazakerley, P.W. Linder and L.R. Nassimbeni, *Acta Cryst.*, *B29*, 2898 (1973).
- 28 O. Weisz and W. Cole, *J. Sci. Instr.*, *25*, 213 (1948).
- 29 G.H. Stout and L.H. Jensen, *X-ray Structure Determination*, Macmillan (1968), p 182.
- 30 G.H. Stout and L.H. Jensen, *X-ray Structure Determination*, Macmillan (1968), p 183.
- 31 *International Tables for X-ray Crystallography*, *III*, 162 (1968).
- 32 *International Tables for X-ray Crystallography*, *II*, 295 (1967).
- 33 W.R. Busing, K.O. Martin and H.A. Levy, ORFLS : A Fortran Crystallographic Least-Squares Program. ORFFE : A Fortran Crystallographic Bond-Lengths and Angles Program. Report ORNL-TM-305, Oak Ridge National Laboratory, Oak Ridge, Tennessee. (1963).
- 34 H.P. Hanson, F. Herman, J. Lea and S. Skillman, *Acta Cryst.*, *17*, 1040 (1964).
- 35 *International Tables for X-ray Crystallography*, *III*, 215 (1968).
- 36 C.K. Johnson, ORTEP : Report ORNL-3794, Oak Ridge National Laboratory, Oak Ridge, Tennessee. (1965).
- 37 G. Davey and F. Stephens, *J. Chem. Soc. A*, 1917 (1971).
- 38 G.A. Barclay and C.H. Kennard, *J. Chem. Soc.*, 5244 (1961).
- 39 J. Donohue in *Structural Chemistry and Molecular Biology*, Editors: A. Rich and N. Davidson, San Francisco : W.H. Freeman and Co., (1968) pp 443 - 465.

- 40 X-RAY 72 SYSTEM. Technical Report TR-192 of the Computer Science Centre, University of Maryland, June 1972.
- 41 D. Cromer and J. Mann, *Acta Cryst.*, *A24*, 321 (1968).
- 42 R.F. Stewart, E. Davidson and W. Simpson, *J. Chem. Phys.*, *42*, 3175 (1968).
- 43 N. Baenziger and R. Schultz, *Inorg. Chem.*, *10*, 661 (1971).
- 44 S. Martinez-Carrera, *Acta Cryst.*, *20*, 783 (1966).
- 45 B.K. Lundberg, *Acta Cryst.*, *21*, 901 (1966).
- 46 A. Mighell, C. Reimann and F. Mauer, *Acta Cryst.*, *B25*, 60 (1969).
- 47 W.D.S. Motherwell, (Cambridge). *To be published*.
- 48 C.W. Reimann, A.D. Mighell and F.A. Mauer, *Acta Cryst.*, *23*, 135 (1967).
- 49 H. Freeman, H. Gus and R. Sinclair, *Chem. Comm.*, 485 (1968).
- 50 A. Fialkov and L. Rapaport, *J. Gen. Chem. (U.S.S.R.)*, *25*, 1855 (1955).
- 51 D. Craciunescu, E. Popa and A. Fruma, *Israel Journal of Chemistry*, *8*, 93 (1970).
- 52 Y.A. Siminov, A.V. Ablov and T.I. Malinovskii, *Z. Krist.*, *8*, 270 (1963).
- 53 J.D. Bell, H.C. Freeman and A.M. Wood, *Chem. Comm.*, 1441 (1969).
- 54 B.J. Hathaway and D.E. Billing, *Coordination Chemistry Reviews*, *5*, 143 (1970).
- 55 B. Berking and B.M. Craven, *Acta Cryst.*, *B27*, 1107 (1971).
- 56 B.M. Craven, E.A. Vizzini and M.M. Rodrigues, *Acta Cryst.*, *B25*, 1978 (1969).
- 57 B. Berking, *Acta Cryst.*, *B28*, 98 (1972).
- 58 H. Wunderlich, *Acta Cryst.*, *B29*, 168 (1973).
- 59 B. Berking, *Acta Cryst.*, *B28*, 1539 (1972).
- 60 B.M. Craven and E.A. Vizzini, *Acta Cryst.*, *B25*, 1993 (1969).

- 61 B.M. Craven, C. Cusatis, G.L. Gartland and E.A. Vizzini, *J. Mol. Struct.*, **76**, 331 (1973).
- 62 B.M. Craven and C. Cusatis, *Acta Cryst.*, **B25**, 2291 (1969).
- 63 B.M. Craven and E.A. Vizzini, *Acta Cryst.*, **B27**, 1917 (1971).
- 64 G.L. Gartland and B.M. Craven, *Acta Cryst.*, **B27**, 1909 (1971).
- 65 G.L. Gartland and B.M. Craven, *Acta Cryst.*, **B30**, 980 (1974).
- 66 W.C. Hamilton in *Structural Chemistry and Molecular Biology*, Editors : A. Rich and N. Davidson, San Francisco: W.H. Freeman and Co., (1968) pp 467 - 483.
- 67 B.M. Craven and G.L. Gartland, *J. Pharm. Sci.*, **59**, 1666 (1970).
- 68 B.M. Craven and G.L. Gartland, *Acta Cryst.*, **B30**, 1191 (1974).
- 69 S.H. Kim and A. Rich, *Proc. Nat. Acad. Sci. (U.S.A.)*, **60**, 402 (1968).
- 70 J.P. Bideau, F. Leroy and J. Housty, *C.R. Acad. Sci. Paris*, **268C**, 1590 (1969).
- 71 R.J. McClure and B.M. Craven, *Acta Cryst.*, **B29**, 1860 (1973).
- 72 G. Bravic, J. Housty and J. Bideau, *C.R. Acad. Sci., Paris*, **266C**, 969 (1968).
- 73 I-Nan Hsu and B.M. Craven, *Acta Cryst.*, **B30**, 974 (1974).
- 74 I-Nan Hsu and B.M. Craven, *Acta Cryst.*, **B30**, 843 (1974).
- 75 I-Nan Hsu and B.M. Craven, *Acta Cryst.*, **B30**, 994 (1974).
- 76 I-Nan Hsu and B.M. Craven, *Acta Cryst.*, **B30**, 988 (1974).
- 77 I-Nan Hsu and B.M. Craven, *Acta Cryst.*, **B30**, 1299 (1974).
- 78 P.P. Williams, *Acta Cryst.*, **B30**, 12 (1974).
- 79 D. Voet, *J. Amer. Chem. Soc.*, **94**, 8213 (1972).
- 80 B.M. Gatehouse and B.M. Craven, *Acta Cryst.*, **B27**, 1337 (1971).

- 81 I-Nan Hsu and B.M. Craven, *Acta Cryst.*, B30, 998 (1974).
- 82 W.C. Hamilton and J.A. Ibers in *Hydrogen Bonding in Solids*, Benjamin, New York, (1968) p 214.
- 83 J. Kroon and J.A. Kanters, *Nature*, 248, 667 (1974).
- 84 J. Bideau, F. Leroy and J. Housty, *C.R. Acad. Sci., Paris*, 271, 500 (1970).
- 85 D. Voet and A. Rich, *J. Amer. Chem. Soc.*, 94, 5888 (1972).
- 86 L.J. Bellamy, *Advances in Infrared Frequencies*, Methuen. London (1968).
- 87 N.P. Slabbert and D.A. Thornton, *J. Inorg. Nucl. Chem.*, 33, 2933 (1971).
- 88 J. Lewis, R.F. Long and C. Oldham, *J. Chem. Soc.*, 1453 (1966).
- 89 D. Gibson, B.F. Johnson and C. Oldham, *J. Chem. Soc.*, 342 (1966).
- 90 D.M. Adams, *Metal Ligand and Related Vibrations*, Arnold. London (1967).
- 91 K. Nakamoto, *Infrared Spectra of Inorganic and Coordination Compounds*, 2nd Edition, Wiley, New York (1970).
- 92 R.J.H. Clark and C.S. Williams, *Spectrochim. Acta.*, 22, 1081 (1966).
- 93 S. Pinchas, *Infrared Spectra of Labelled Compounds*, Academic Press. London (1971).